2011

# MOLECULAR TROJAN HORSES IN THE TREATMENT OF METACHROMATIC LEUKODYSTROPHY

Katherine Marie Baer

# MOLECULAR TROJAN HORSES IN THE TREATMENT OF METACHROMATIC LEUKODYSTROPHY

(Spine title: MOLECULAR TROJAN HORSES IN THE TREATMENT OF MLD)

(Thesis format: Monograph)

by

Katherine Marie Baer

Graduate Program in Biochemistry

Submitted in partial fulfillment of the

Requirements for the degree of

Master of Science

School of Graduate and Postdoctoral Studies

The University of Western Ontario

London, Ontario, Canada

THE UNIVERSITY OF WESTERN ONTARIO
SCHOOL OF GRADUATE AND POSTDOCTORAL STUDIES

**CERTIFICATE OF EXAMINATION**

| Supervisor | Examiners |
|---|---|
| Dr. Tony Rupar | Dr. Madhulika Gupta |
| Supervisory Committee | Dr. Robert Hegele |
| Dr. Jack Rip | Dr. Stephen Pasternak |
| Dr. Stan Dunn | |

The thesis by

**Katherine Marie Baer**

entitled:

**Molecular Trojan Horses in the Treatment of Metachromatic Leukodystrophy**

is accepted in partial fulfillment of the
requirements for the degree of
Master of Science

Date_____

_____
Chair of the Thesis Examination Board

**Abstract**

Metachromatic leukodystrophy (MLD) is a lysosomal storage disease caused by a mutation in the enzyme, arylsulfatase A (ASA) and is characterized by progressive and fatal demyelination in the central and peripheral nervous systems. To date, no effective treatment exists and development is hampered by the blood-brain barrier (BBB). I have successfully generated fusion proteins using an ApoE fragment as a molecular Trojan horse fused to the full-length human ASA. These proteins were expressed in eukaryotic cells transduced with lentiviral expression vectors and have been assessed for *in vitro* enzymatic activity and kinetic properties. Although preliminary studies show that these constructs did not cross an *in vitro* BBB model under these experimental conditions, there is evidence to suggest that the ApoE fragment facilitates the uptake of fusion proteins into the endothelial cells of the BBB. Recommendations for further study are encouraged to reach the goal to find treatment for MLD.

**Keywords:** MLD, ASA, molecular Trojan horse, ApoE, fusion protein, blood brain barrier

*To my father,*
*Alfred Bergelt,*
*Thank you for always keeping the home fires going.*
*I miss you.*

**Acknowledgements**

First and foremost, I would like to thank my supervisor, Dr. Rupar, for his guidance and support. Your inimitable knowledge and positive feedback have been invaluable. Also, I would like to gratefully acknowledge Dr. Gediminas Cepinskas from the Critical Illness Research Centre at the Lawson Health Research Institute for all of his help and insight into the growth and assessment of the *in vitro* blood brain barrier, for his kind gift of bEND3 cells, and also for giving me open access to his equipment and supplies. I am very appreciative of the insight and suggestions over the course of this project from the members of my advisory committee, Drs. Jack Rip and Stan Dunn. To Dr. Jiahui Liu and Ms. Cathy Regan – you were instrumental in encouraging me to think independently and making every day enjoyable. I would also like to acknowledge the contribution of Danielle Croucher for her development of the transferrin-arylsulfatase A-V5 fusion protein used in my experiments.

A big thank-you goes out to the staff members at the Biochemical and Genetics Laboratory for their willingness to answer questions and offer advice. I couldn't have asked for a better group of people to be around.

Finally, I must thank my family for putting up with a distracted wife, mother, and daughter and let them know that I so appreciate their patience and encouragement. Without your support, there was absolutely no way I could have reached this goal.

This research has been funded by the Bethanys Hope Foundation.

**Table of Contents**

**CHAPTER 2 – Materials and Methods**

**Chapter 4 – Discussion and Conclusions**

## List of Tables

**List of Figures**

## List of Abbreviations

| | |
|---|---|
| AAV5 | adeno-associated virus serotype 5 |
| AET | active-efflux transport |
| ApoE | apolipoprotein E |
| ApoTf | apo-transferrin |
| ASA | arylsulfatase A |
| BBB | blood-brain barrier |
| BP | integration reaction |
| BSA | bovine serum albumin |
| BSA488 | bovine serum albumin conjugated to Alex Fluor 488 |
| cDNA | complementary DNA |
| CHO | Chinese hamster ovary cells |
| CMT | carrier-mediated transport |
| CMV | cytomegalovirus |
| CNS | central nervous system |
| Con A | concanavalin A |
| C-terminus | carboxy-terminus |
| CV | column volumes |
| CVEC | cerebrovascular endothelial cells |
| DEAE | diethylaminoethyl cellulose |
| $dH_2O$ | deionized water |
| DHFR | dihydrofolate reductase |
| DMEM | Dulbecco's modified eage medium |
| dNTP | deoxyribonucleotide triphosphate |
| DTT | diothiothreitol |
| EDTA | ethylene diamine tetraacetic acid |
| eGFP | enhanced green fluorescent protein |
| ERT | enzyme replacement therapy |
| EtBr | ethidium bromide |
| FBS | fetal bovine serum |
| HCl | hydrochloric acid |
| HEPES | 4-(2-hydroxyethyl)-1-piperazineethanesulfonic acid |
| HIR | human insulin receptor |
| HSCT | haematopoietic stem cell transplantation |
| HT | sodium hypoxanthine and thymidine mixture |
| IgG | gamma globulin |
| IHF | integratin host factor |
| LB | Luria Bertani |
| LDL | low density lipoprotein |
| LDLR | low density lipoprotein receptor |

| | |
|---|---|
| LR | excision reaction |
| LSD | lysosomal storage disease |
| M6P | mannose-6 phosphate |
| M6PR | mannose-6 phosphate receptor |
| Mab | monoclonal antibody |
| $MgCl_2$ | magnesium chloride |
| MLD | metachromatic leukodystrophy |
| MOI | multiplicity of infection |
| NaCl | sodium chloride |
| NaOH | sodium hydroxide |
| NP40 | nonidet P 40 substitute |
| N-terminus | amino-terminus |
| PAGE | polyacrylamide gel electrophoresis |
| PBS | phosphate-buffer saline |
| PCR | polymerase chain reaction |
| pDNA | plasmid DNA |
| PEG | polyethylene glycol |
| PFA | paraformaldehyde |
| pLenti | lentiviral -based expression clones |
| pLvDNA | lentiviral plasmid DNA |
| pNCS | para-nitrocatechol sulphate |
| PNGase F | peptide-N4-(acetyl-β-glucosaminyl)-asparagine amidase N-Glycosidase F |
| PNS | peripheral nervous system |
| RFU | relative fluorescent units |
| rhASA | recombinant human arylsulfatase A |
| RMT | receptor-mediated transport |
| Rnase A | Ribonucleotide reductase A |
| S.A. | specific activity |
| SDS | sodium dodecyl sulfate |
| TE | Tris-EDTA |
| TEER | transendothelial electrical resistance |
| Tf | transferrin |
| TfR | transferrin receptor |
| TU | transforming units |

# Chapter 1 – Introduction

## 1.1 Metachromatic leukodystrophy

Metachromatic leukodystrophy (MLD; OMIM 250100) is an autosomal recessive lysosomal storage disease caused by a mutation in the gene encoding the enzyme, arylsulfatase A (ASA; EC 3.1.6.8). To date, there have been more than 100 MLD-causing mutations described with the majority of defective ASA alleles containing missense mutations. (1) Pathological hallmarks of this neurodegenerative disease include the presence of metachromatic granules in lysosomal vesicles, reduced numbers of oligodendrocytes, and the progressive demyelination of the central (CNS) and peripheral nervous systems (PNS). Clinically, there are three subtypes of disease that are distinguishable by the age of onset. Late infantile metachromatic leukodystrophy generally manifests between 1 ½ - 2 years of age; the onset of juvenile MLD occurs between the ages of 4 and16; and patients presenting after the age of 16 are diagnosed with the adult form of the disease (2, 3).

The most frequently occurring form of this disease is late infantile MLD, accounting for approximately 50% of diagnosed cases with an estimated frequency as high as 1 in 40,000 newborns (4, 5). The focus of this paper will be on the infantile form of MLD, hereafter referred to simply as MLD. Affected infants typically exhibit normal development for the first year but begin to present with a loss of age-related milestones, often beginning with gait difficulties followed by other symptoms that include mental regression, aphasia, feeding and breathing difficulties, and blindness, leading to a decerebrated state. To date, there is no

effective treatment for this disease and death generally occurs within 5 years. (2, 6)

**1.2 Arylsulfatase A**

The gene encoding ASA has been mapped to the long arm of chromosome 22 in the human genome. It is a relatively small gene (3.2 kb) composed of 8 exons(7, 8) that encode a 507 amino acid product with an 18 amino acid leader sequence and a 489 amino acid mature enzyme with a molecular weight of approximately 62kDa. (8)

As with most lysosomal enzymes, ASA follows the mannose-6 phosphate (M6P) pathway that targets enzymes to the lysosome. Translated at the rough endoplasmic reticulum, the ASA pre-protein receives several post-translational modifications including the addition of three N-linked oligosaccharide side chains and a critical conversion of a cysteine to Cα-formylglycine. These modified enzymes dimerize and move to the Golgi complex where most are recognized by mannose 6-phospate receptors (M6PR) that target them to lysosomes. Within the acidic environment of the lysosome, dimerized proteins further oligomerize into octomers and act upon their substrate, sulfatide.(9) A small percentage (10-30%) of the lysosomal enzymes bypass targeting to the lysosome and these diffuse to extracellular space (6). Here, M6PRs on the plasma membrane of neighbouring cells can recognize and endocytose the exogenous enzyme which may subsequently be targeted to lysosomal compartments. (Figure 1.1). (10, 11)

ASA catalyzes the first step in the degradation of the sphingolipid, 3-O-sulfogalactosylceramide (sulfatide). Hydrolysis by ASA breaks sulfatide down to galactocerebroside. This substrate is then enzymatically degraded by

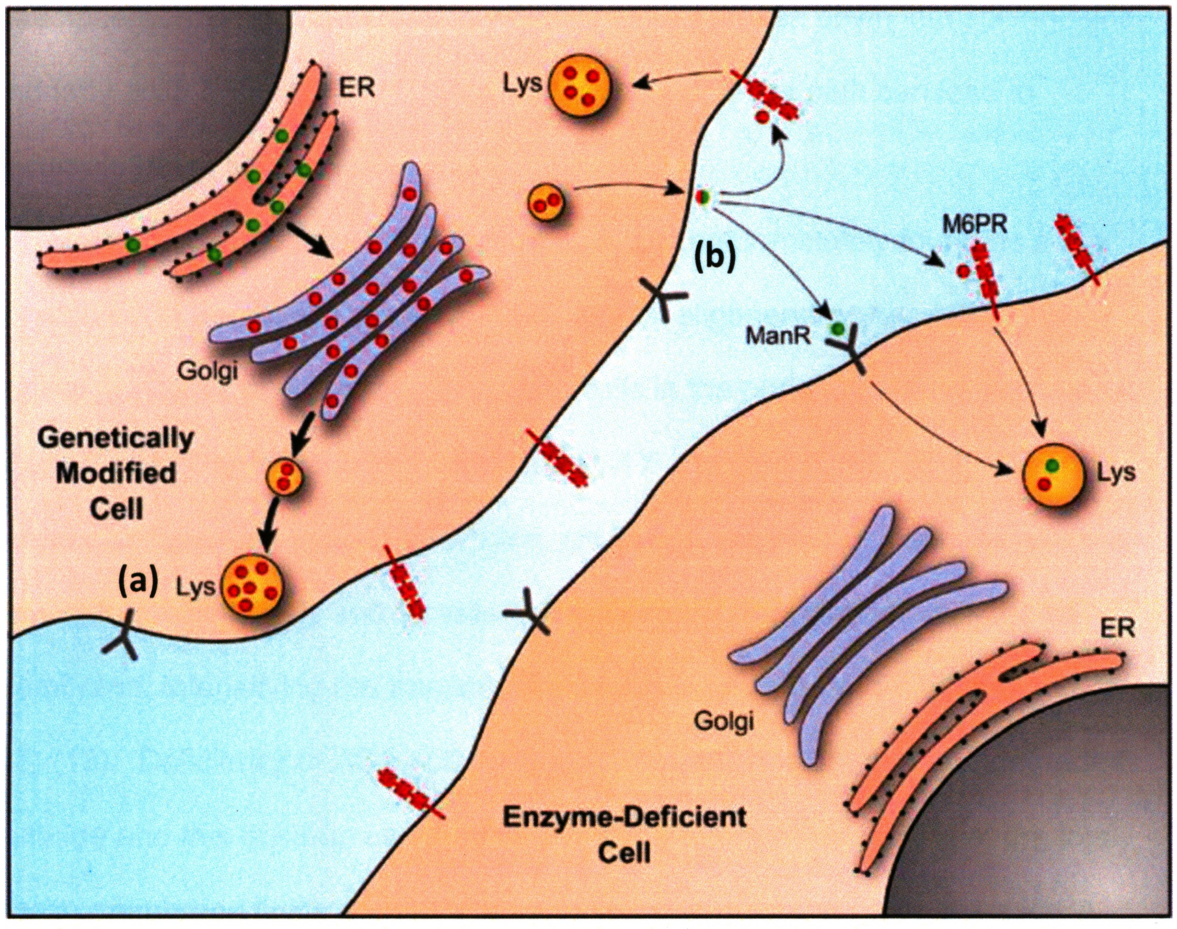


**Figure 1.1** Trafficking of lysosomal enzymes. Lysosomal enzymes are translated at the rough endoplasmic reticulum and are post-translationally modified. ASA pre-proteins dimerize and move to the Golgi complex. Most of the pro-enzymes are then targeted to the lysosomes where, under the low pH conditions, they form octomers and become active (a). A small percentage of enzyme is secreted to the extracellular space where it can be picked up by M6PR on neighbouring cells and targeted to the lysosomes of that cell to be activated (b). Illustration adapted from Sands and Davidson, 2006.

galactocerebrosidase to ceramide which is in turn broken down into sphingosine and fatty acid (Figure 1.2) (1). Any disruption along this path can lead to accumulation of substrate.

The substrate for ASA, sulfatide, is a lipid predominately found as a key constituent of the myelin sheath synthesized by oligodendrocytes within the central nervous system and by Schwann cells in the peripheral nervous systems where it normally represents approximately 4% of myelin lipids. (2, 12). Myelin wraps around axons in a spiral fashion, creating a sheath that insulates neurons from extracellular fluids and increases the electrical resistance across the cell membrane, intensifying the transmission of electrical signals in the CNS (Figure 1.3) (13). Deficiency of ASA activity leads to the accumulation of non-degraded sulfatide and this build-up can lead to levels representing up to 30% of the total myelin membrane lipids and 40% of lipids found in metachromatic granules in MLD patients. (6, 14) The increased levels of non-degraded sulfatide lead to progressive demyelination in the CNS and PNS, resulting in the eventual death of neuronal and glial cells as well as other secondary abnormalities such as the storage and misallocation of unrelated lipids and inflammatory processes (6).

A cell culture model of sulfatide storage is not available and as such, the processes leading to demyelination are not fully understood. Several mechanisms have been proposed. Resorption of sulfatide from the innermost layer of the myelin sheath is critical for its normal restructuring and is also necessary to enable axons to increase their cross-sectional diameter. The ability of myelin to undergo resorption may be compromised by sulfatide accumulations, thereby affecting the plasma membranes of CNS and PNS cells, causing their

(a)

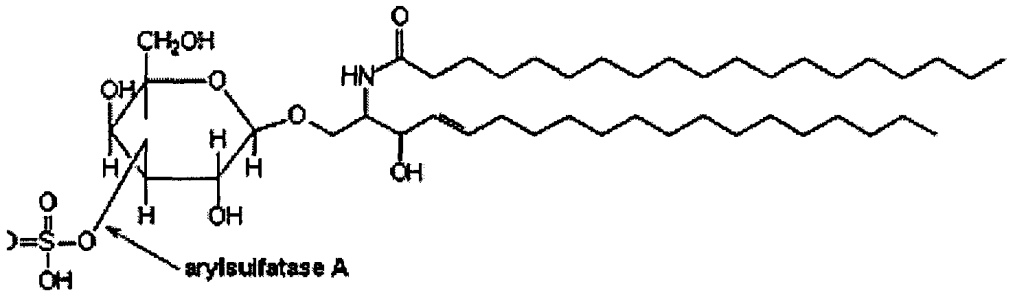


(b)

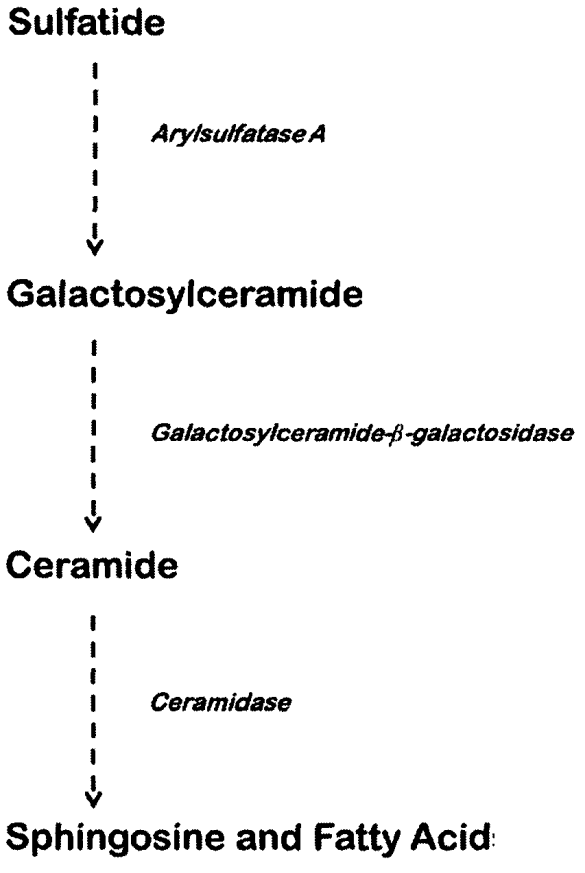


**Figure 1.2** Arylsulfatase A catalyzes the first step in the metabolism of sulfatide (a). Hydrolysis by ASA breaks sulfatide down to galactocerebroside. This substrate is then enzymatically degraded by galactocerebrosidase to ceramide which is in turn broken down into fatty acid (b) (1). Any disruption along this path can lead to accumulation of substrate.

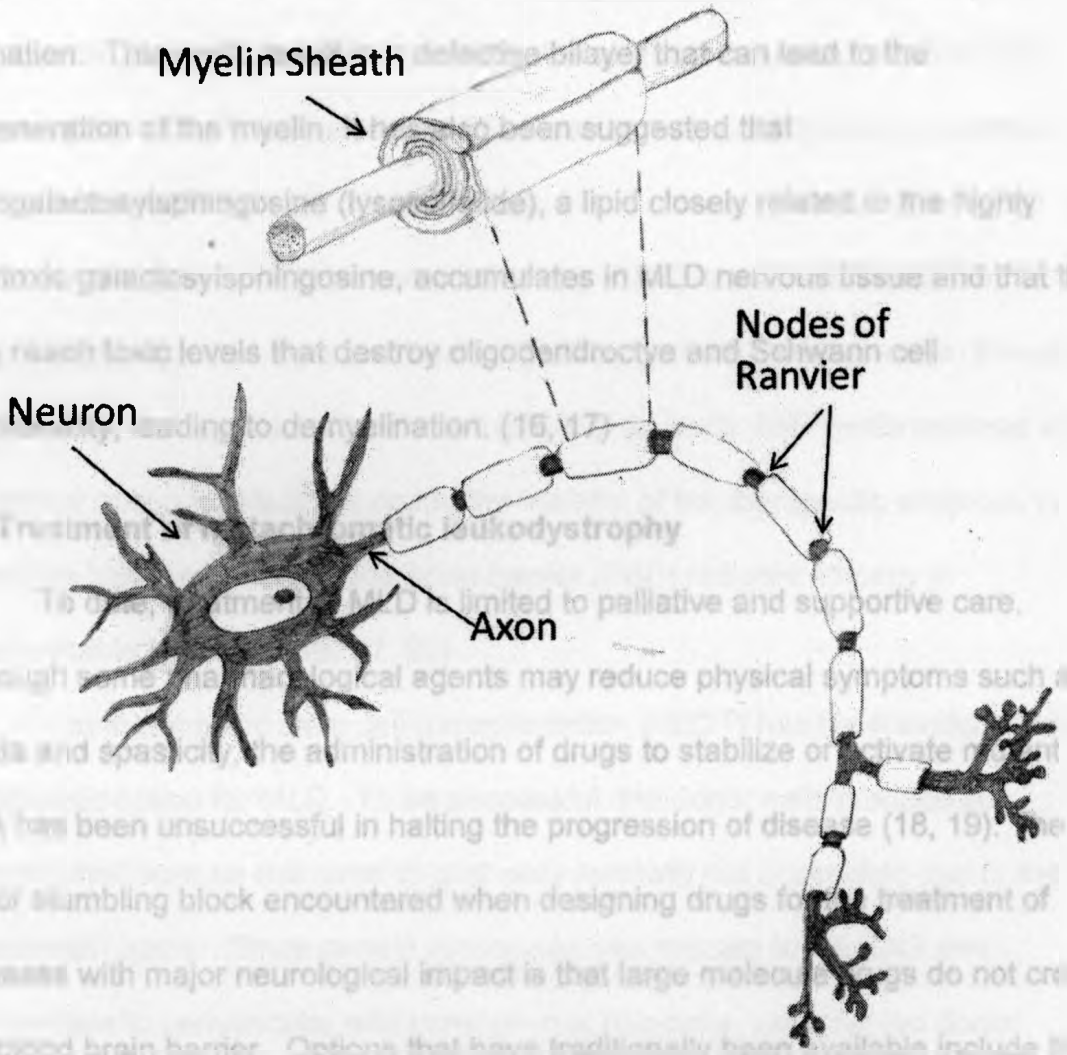


**Figure 1.3** Sulfatide is found predominately as a vital component of myelin in the CNS. Myelin sheaths wrap around axons in a spiral fashion, insulating the nerve fibres and this myelination enables rapid transmission of nerve impulses. In the CNS of patients with metachromatic leukodystrophy, axons become demyelinated and instances of neuronal death occur.

breakdown (2, 6, 8). A study conducted by Ginsberg and Gershfeld (15), indicated that myelin from MLD patients was incapable of forming normal lipid bilayers due to a shift in the in the critical temperature of membrane bilayer formation. This could result in a defective bilayer that can lead to the degeneration of the myelin. It has also been suggested that sulfogalactosylsphingosine (lysosulfatide), a lipid closely related to the highly cytotoxic galactosylsphingosine, accumulates in MLD nervous tissue and that this may reach toxic levels that destroy oligodendroctye and Schwann cell functionality, leading to demyelination. (16, 17)

### 1.3 Treatment of metachromatic leukodystrophy

To date, treatment of MLD is limited to palliative and supportive care. Although some pharmacological agents may reduce physical symptoms such as ataxia and spasticity, the administration of drugs to stabilize or activate mutant ASA has been unsuccessful in halting the progression of disease (18, 19). The major stumbling block encountered when designing drugs for the treatment of diseases with major neurological impact is that large molecule drugs do not cross the blood brain barrier. Options that have traditionally been available include the administration of a drug via peripheral or invasive, trans-cranial injection. To date, these have also met with unsatisfactory results (20).

The rationale behind many different treatments for MLD is based on cross-correction. Study designs take into account that during normal synthesis of lysosomal enzymes, a small percentage (10-30%) of enzyme produced by a cell is not directed to the lysosome but is secreted into the extra-cellular environment

slow turnover of resident tissue macrophages and microglia cells acting as functioning sources of active enzyme cannot compete with the rapid progression of the disease. (6, 18)

More recently, a phase I/II clinical trial is currently underway under the direction of Drs. A. Biffi and M. Sessa in the San Raffaele Telethon Institute for Gene Therapy (HSR-TIGET) in Milan, Italy. This study is assessing the efficacy of autologous hematopoietic stems cells that have been transduced with lentiviral vector containing the normal human ASA gene. At the time of writing, one patient had undergone treatment with favourable results but assessment of efficacy will have to wait for long-term follow up (23).

**1.4 Animal model of MLD**

The lack of a naturally occurring animal model of MLD has historically held back studies of both the pathogenesis and treatment of this disease (24). To address this issue, Hess et al., generated a mouse model with ASA-deficiency. These ASA (-/-) mice were developed using the targeted disruption of the ASA gene in embryonic stem cells resulting in mice with a complete loss of ASA activity. (3). Although ASA-deficient mice lack the widespread demyelination seen in humans, the storage pattern of sulfatide resembles the pattern seen in MLD patients (3, 24). Behavioural changes and gait disturbances are measurable by 6 months of age, correlating well with symptoms seen in human MLD patients (25). These MLD models have enabled the investigation of various treatment possibilities including gene therapy, direct injection of viral vectors into the brain, and enzyme replacement therapy. (26)

Several studies have used haematopoietic cells that have been transduced with either retroviral or lentiviral vectors to over-express enzyme and transplanted the modified cells into MLD mice. Allogenic bone marrow transplantation has been used to populate the marrow of MLD mice with cells that were retrovirally transduced to express functional human ASA to determine the ability of enzyme to enter the brain tissue and act upon sulfatide stores (27). Reduction of sulfatide in peripheral systems was noted but even though the enzyme did translocate into the brain, no reduction of sulfatide was seen (28). This is a different conclusion than that reached by Biffi *et al.*, who found that following the transplant of lentiviral transduced haematopoietic stem cells overexpressing ASA, MLD mice exhibited normalization of behavioural and gait abnormalities. It was also noted that sulfatide storage was corrected in these mice (29, 30). Caution is advised when interpreting these data. The lack of demyelination in the MLD mouse means that the reversal of damages seen cannot address the ability of these treatments to reverse demyelination seen in human patients (26).

In 2005, Matzner *et al.*, treated MLD mice with weekly intravenous injections of recombinant human ASA (rhASA). After four treatments, a reduction in brain sulfatide levels was noted (31). Further treatments beyond the four-week window, however, elicited a severe immunological response that caused high mortality. In response, an MLD mouse was successfully generated that could tolerate higher enzyme dosages for a longer period of time (32). These immunotolerant mice were treated for 26 weeks with either a low dose or high dose of enzyme and virtually none displayed apparent side effects. Those treated

with a higher dose of enzyme exhibited reduction of lipid stored in the brain but the storage reduction was similar to that seen in the previous study (31, 33).

Recombinant viral vector expressing recombinant enzyme has been directly delivered into the brain by intracerebral injection to bypass the BBB, enabling the enzyme to enter the brain where it is most needed. Injection of vector has the potential to rapidly increase concentrations of ASA and have a critical impact on the swift progression of the late-infantile form of MLD (26). Results indicate that this form of gene transfer in the MLD mouse may reverse some neurological damage in symptomatic mice as long as enzyme expression persists.(4, 18, 34, 35). Injection of late-generation lentiviral vectors encoding human ASA in 10-month old MLD mice resulted in sustained expression of enzyme throughout a large portion of the brain and appeared to convey long-term protection from developing neuropathology. In particular, lipid storage was progressively reduced over time (34). Another group injected adeno-associated virus serotype 5 (AAV5) vectors that encoded human ASA into the brains of both pre-symptomatic and early symptomatic MLD mice (3 month old and 6 month old, respectively). In the pre-symptomatic mice, delivery of the vector prevented neuropathological abnormalities and neuromotor impairment. In the 3-month old and the 6-month old mice, three months after injection of vector, reduced sulfatide storage was noted and the level of sulfatide then remained stable. In the 6-month old mice neuropathology was normalized but in contrast to the 3-month old mice, treatment did not have an effect on neuromotor disability (4, 35, 36).

Although intracranial injections may hold promise for the treatment of MLD, it is necessary for the enzyme to be distributed throughout the entire CNS. This level of diffusion may be seen with as few as five injections across a mouse brain but to cover the same relative area in a larger brain such as a human would require many more injections (37). It is therefore important to scale studies in order to appraise the efficiency of therapy in a larger brain. To this end, studies by Colle *et al.*, and Vite *et al.*, indicate that multiple intracerebral injections of enzyme-expressing vectors were well tolerated in larger animal models (38, 39). It is important to note that intracranial injections are highly invasive and ideally other forms of therapy, either alone or in conjunction with these more invasive treatments, need to be explored.

### 1.5 Blood brain barrier and implications in drug therapy

In 1885, Paul Ehrlich noted that vital dyes injected into the circulation would stain all organs except the brain and spinal cord (40, 41). Soon thereafter, scientists were further able to demonstrate that intravenous injection of acidic dyes resulted in staining throughout the body with the exception of the brain and spinal cord. Conversely they showed that injection of dye into cerebrospinal fluid led to staining of the nervous tissues and resulted in pharmolocological effects that were not seen with intravenous injections (42). These demonstrations were the first to illustrate the inability of certain molecules to cross what was termed the BBB.

Physiologically, the BBB consists of a layer of cerebrovascular endothelial cells (CVEC) – pericytes, astrocyte foot processes, and some nerve endings

(Figure 1.4). CVEC are highly specialized vascular endothelial cells fused together with high resistance tight junctions. (43, 44). They also differ from other endothelial cells in that they lack fenestrations and have very few pinocytotic vesicles (45). These adaptations create the BBB that effectively prevents the free flow of most molecules greater than 600 Da from passing from blood and entering the brain tissue (46). Although this BBB effectively creates a privileged site that has a critical protective function – this selectivity also results in an inability of many therapeutic agents to reach their targets within the brain.

If the BBB can be breached, diffusion of a drug is of lesser concern. Estimates suggest that a human brain contains approximately 100 million capillaries that cover a surface area of ~12 $m^2$. With approximately 40 μm of space between human brain capillaries, there is room available for 2 neurons between 2 capillaries. This suggests that virtually every neuron in the human brain is perfused by its own capillary. Therefore, the short intercapillary distance can enable diffusion of the drug throughout brain tissue (37, 47) resulting in a uniform and immediate increase of drug concentration through the brain. The problem then is not necessarily the CNS drug itself but rather the targeting of the drug into the CNS (20).

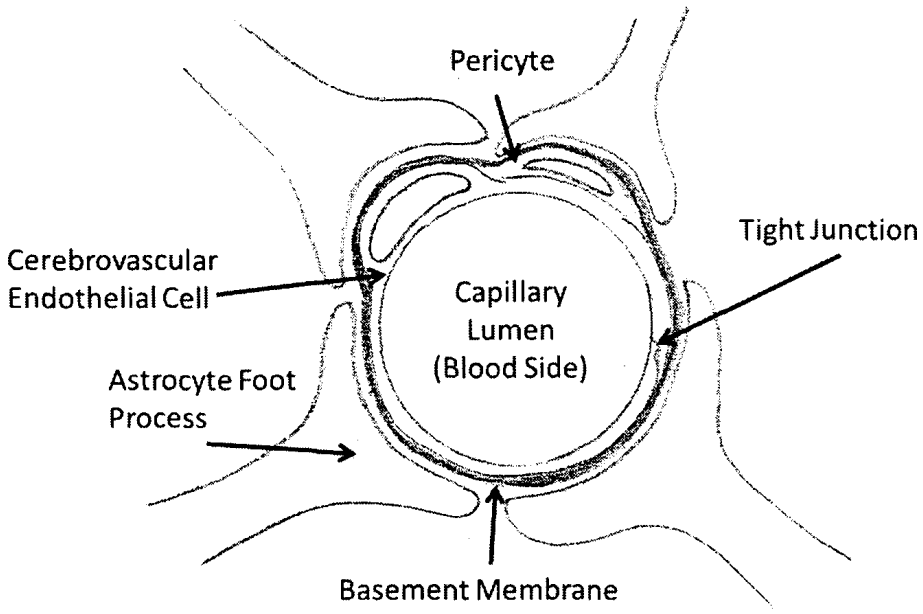


**Figure 1.4** The blood brain barrier acts to prevent the passage of solutes between the blood and brain parenchyma. It is comprised of cerebrovascular endothelial cells (CVEC), pericytes, astrocytes foot processes, and periodically, a nerve ending. CVEC are a specialized vascular endothelial cell lacking fenestrations and produce very few pinocytotic vesicles. CVEC are fused together with high resistance tight junctions. These adaptations prevent most molecules greater than 600 Da from entering the brain tissue (46).

### 1.6 Crossing the blood brain barrier

The passage of molecules into or out of the brain interstitial fluid is subject to highly regulated processes due to the high-resistance tight junctions of the blood-brain barrier. There are three methods by which solutes typically cross the BBB: carrier-mediated transport (CMT); active-efflux transport (AET); and receptor-mediated transport (RMT) (44). Carrier-mediated transport systems enable the passage of essential small polar molecules such as water-soluble vitamins, amino acids and glucose from either the blood-to-brain direction or the brain-to-blood direction (44, 48, 49). Active-efflux transport (AET) enables the efflux of low molecular mass products from the brain into the blood (44). The passage of most non-lipid solutes or those larger than 600 Da occurs by receptor-mediated transport (RMT) whereby receptors such as the insulin receptor, low-density lipoprotein receptor (LDLR), and transferrin receptor (TfR) on the cerebrovascular capillary wall recognize and bind their respective ligands such as insulin, cholesterol, and iron. These receptor-ligand complexes are endocytosed into the cerebrovascular endothelial cell. Some of the internalized solutes are then transported across the capillary wall where they can be delivered into the brain parenchyma (Figure 1.5). (50, 51).

### 1.7 Molecular Trojan horses

For several years, various groups have explored the possibility of using receptor-mediated transport to deliver various agents into the brain (37, 52-56). A developing interest in the protein or peptide ligands that bind receptors on the blood brain barrier has led to their use as molecular "Trojan horses". These

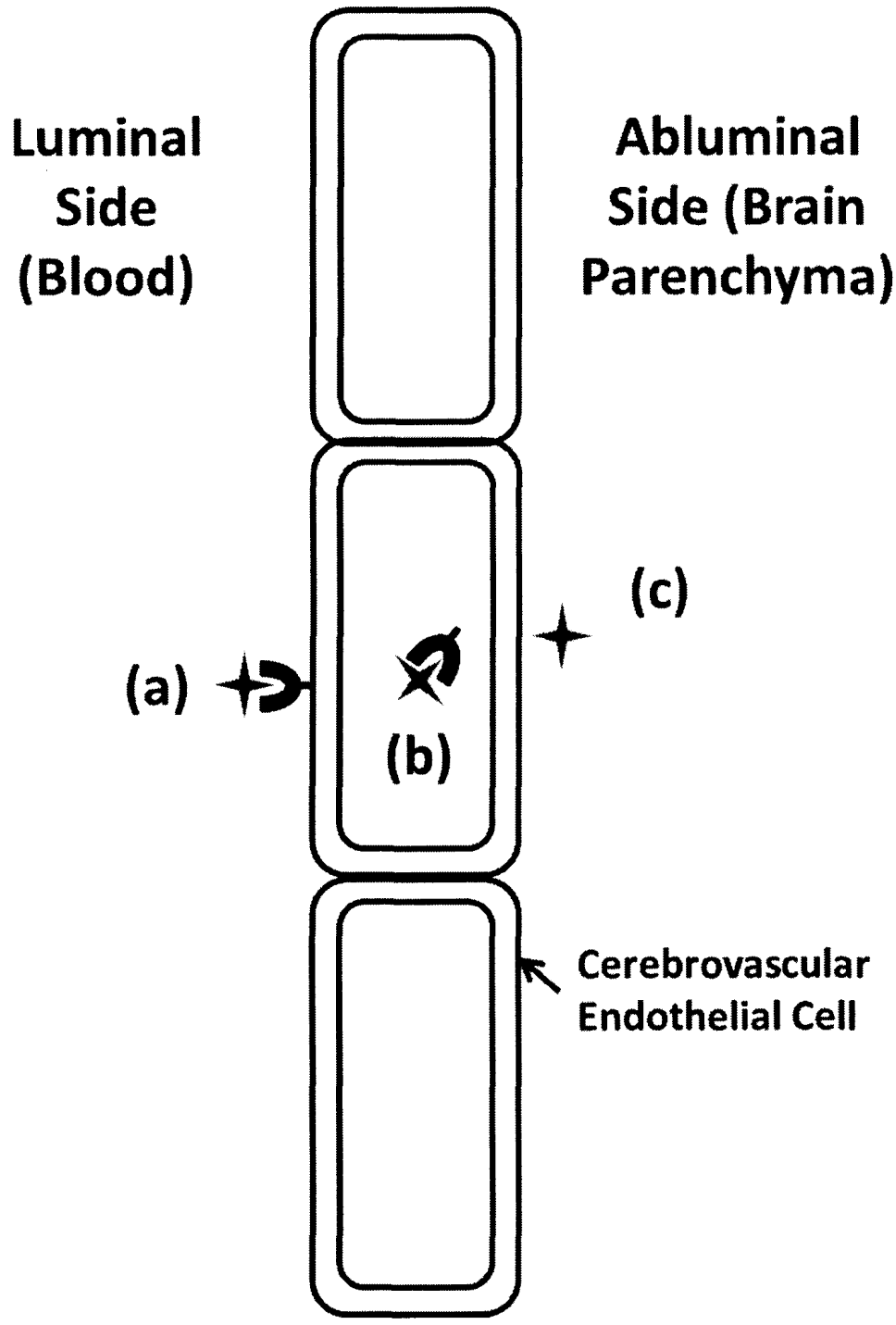


**Figure 1.5** Receptor-mediated transcytosis of protein across the blood brain barrier. Circulating protein is recognized as ligand by specific cell-surface receptors (a) and endocytosed by cerebrovascular endothelial cells (CVEC) (b). This protein can be transported across the blood-brain barrier and delivered to the abluminal side of the CVEC for entry into the brain parenchyma (c). Adapted from Pardridge, 1999.

Trojan horses are fused to various therapeutic agents to generate recombinant fusion protein that bind endogenous receptors on the blood brain barrier, shuttling the fused product from the bloodstream across the BBB and into the brain where they can deliver the therapeutic payload into the brain tissue. In order to be effective, Trojan horses must target an endocytotic BBB system; maintain high affinity for the receptor as a Trojan horse-drug fusion product; there must be high uptake of the fusion protein; and following uptake, the system must exhibit a therapeutic effect in the CNS (20) .

A variety of different proteins or peptides have been used as Trojan horses including monoclonal antibodies to the human insulin receptor (HIR) (52, 53, 57-59); monoclonal antibodies to mouse transferrin receptor (MAbTfR) (56); and apolipoproteins that bind low-density lipoproteins receptors(LDLR)(37). Molecular Trojan Horses offer a new approach for targeting therapy across the BBB into the brain to treat diseases with neurodegenerative effects.

### 1.8 Thesis introduction

In principle ASA delivery into the nervous system would correct the enzyme deficiency in MLD but the blood brain barrier (BBB) prevents the enzyme from entry. With the current lack of successful treatment for metachromatic leukodystrophy, there is a need to push forward with new therapeutic options and develop biopharmaceutical drugs that could help ameliorate symptoms of this devastating disease. The recent use of Trojan horse technology offers such an approach to treating this neurodegenerative disease.

The LDL receptor (LDLR) can enable protein transport across the BBB via receptor-mediated transcytosis. LDLR is expressed on the apical (blood) side of the BBB and transcytoses lipids bound to apolipoproteins to the basolateral (brain) side (84).

Normally, apolipoprotein E combines with circulating lipids and targets them for catabolism. The ApoE-lipid complex is endocytosed by cells after binding to cell-surface LDL receptors and these complexes are typically targeted to lysosomes and with the receptor released to be recycled to the cell surface (60). At the BBB, however, ApoE complexes bound to the LDLR are transcytosed to the abluminal face of the BBB and exported into the brain parenchyma (60, 61). This transfer of ApoE is critical for the delivery of cholesterol in both the development and repair of axons (12).

In 2007, Spencer and Verma fused apolipoprotein B to glucocerebrosidase. The apolipoprotein portion of the fusion protein was able to bind LDLR, crossed the BBB and successfully delivered active glucocerebrosidase into the brain of mice. Following the delivery of enzyme across the BBB with Trojan horse technology, active glucocerebrosidase was determined to have located to the lysosomes of neurons and astrocytes of the CNS (37).

In this thesis, I hypothesize that the LDLR-binding site of Apolipoprotein E can be fused to full-length ASA. This fusion protein will bind to the low density lipoprotein receptors expressed on the vascular side of endothelial cells of the blood brain barrier leading to the transport of arylsulfatase A to endothelial cell

lysosomes, retaining enzyme activity. Furthermore, ASA will pass through the blood brain barrier by exocytosis and enter into the CNS.

Following the Spencer and Verma model, the purpose of this research project was to construct a fusion protein containing V5-epitope-tagged arylsulfatase A fused to the LDLR binding region of ApoE. The retention of bifunctionality of this fusion protein was assessed for both the ability of the ApoE fragment to facilitate protein endocytosis as well as the ability of the fused arylsulfatase A to exhibit enzymatic activity. Constructs were built with the ApoE peptide at the C-terminus of ASA-V5 and they were assessed for *in vitro* enzymatic activity and kinetic properties. A second fusion protein was constructed using the ApoE peptide at the C-terminus eGFP to enable visual confirmation of the ability of the ApoE fragment to be taken up by cell cultures. A third fusion protein, concurrently developed in the laboratory, was similarly constructed with the full-length murine transferrin protein at the N-terminus of V5-epitope-tagged ASA. These fusion proteins were expressed in Chinese Hamster Ovary (CHO) cells transduced with lentiviral expression vectors using the Invitrogen MultiSite Gateway® Pro kit. Expressed proteins were isolated and delivery of active enzymes through an *in vitro* blood-brain barrier developed by the Cepinskas lab at the Lawson Health Research Institute was assessed.

## Chapter 2 – Materials and Methods

### Generating fusion proteins

To generate the desired fusion products, MultiSite Gateway® Pro Kit (Invitrogen) was used. This technology ensured that both DNA elements of the fusion proteins were inserted into destination vectors in the correct order and orientation. To accomplish this, forward and reverse primers for each construct were designed that incorporate specific *att*-sites flanking the PCR products (Table I). The *att*-flanked PCR products underwent a recombination event to insert the sequence of interest into donor vectors to generate entry clones. Entry clones were then used in a second recombination event with destination vectors to generate expression clones expressing the fusion protein (Figure 2.1).

### 2.1 Polymerase chain reaction (PCR)

Amino acids, RARLSTHLRKMRKRLMR, encompassing the LDLR-binding region of murine ApoE (87, 88, UniProtKB/Swiss-Prot P08226.2) were PCR-amplified from genomic DNA of C57B16 mice (supplied by this laboratory) using forward and reverse primers C-ApoE-F and C-ApoE-R (Table I) to generate DNA element C-ApoE.

The full-length eGFP sequence, including the Kozak consensus sequence *cgccacc* upstream of the start codon, was PCR-amplified from peGFP-N1 (GenBank Accession #U55762, Figure 2.2) using primers N-eGFP-F and N-eGFP-R (Table I) to generate DNA element N-eGFP.

Full-length human arylsulfatase A with a C-terminus V5 epitope tag was

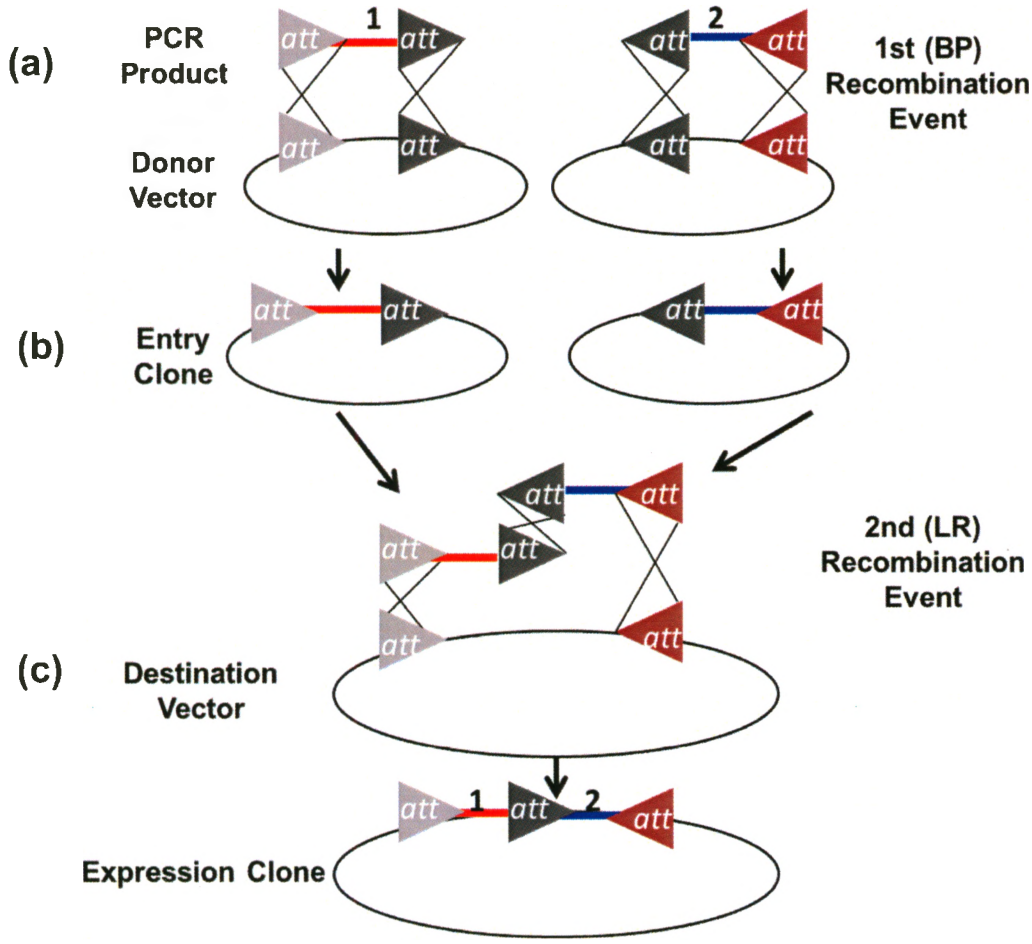


**Figure 2.1** Target DNA is amplified in PCR reactions with primers containing specific *att* sites to generate *att*-flanked amplicons (a). Two PCR products undergo separate recombination events with two donor vectors to generate entry clones (b). These two entry clones undergo a second recombination event together with a destination vector to create an expression clone containing both original DNA elements in correct orientation (c).

| Entry Clone | Primer Set | Sequence (5' – 3') |
|---|---|---|
| **N-ASA** | N-ASA-F | GGGGACAAGTTTGTACAAAAAAGCAGGCTGGATGGGGGCACCGCGGTCCCTCCTC |
| | N-ASA-R | GGGGACAACTTTTGTATACAAAGTTGTCGTAGAATCGAGACCGAGGAG |
| **N-eGFP** | N-eGFP-F | GGGGACAAGTTTGTACAAAAAAGCAGGCTGGCGCCACCATGGTGAGCAAGGGCGAGGAGCTG |
| | N-eGFP-R | GGGGACAACTTTTGTATACAAAGTTGTCTTGTACAGCTCGTCCATGCCGAGAGT |
| **C-ApoE** | C-ApoE-F | GGGGACAACTTTGTATACAAAAGTTGAAATGCGGGCGCGGCTCTCCACACAC |
| | C-ApoE-R | GGGGACCACTTTGTACAAGAAAGCTGGGTACTACCGCATCAAGCGCTTGCGCAT |

**Table I** To generate entry clones, forward and reverse primers were designed to incorporate specific *att* sites into PCR products for insertion in specific pDONR™ entry vectors using Invitrogen's MultiSite Gateway® Pro kit. The nucleotide sequences that constitute the *att* sites are underlined.

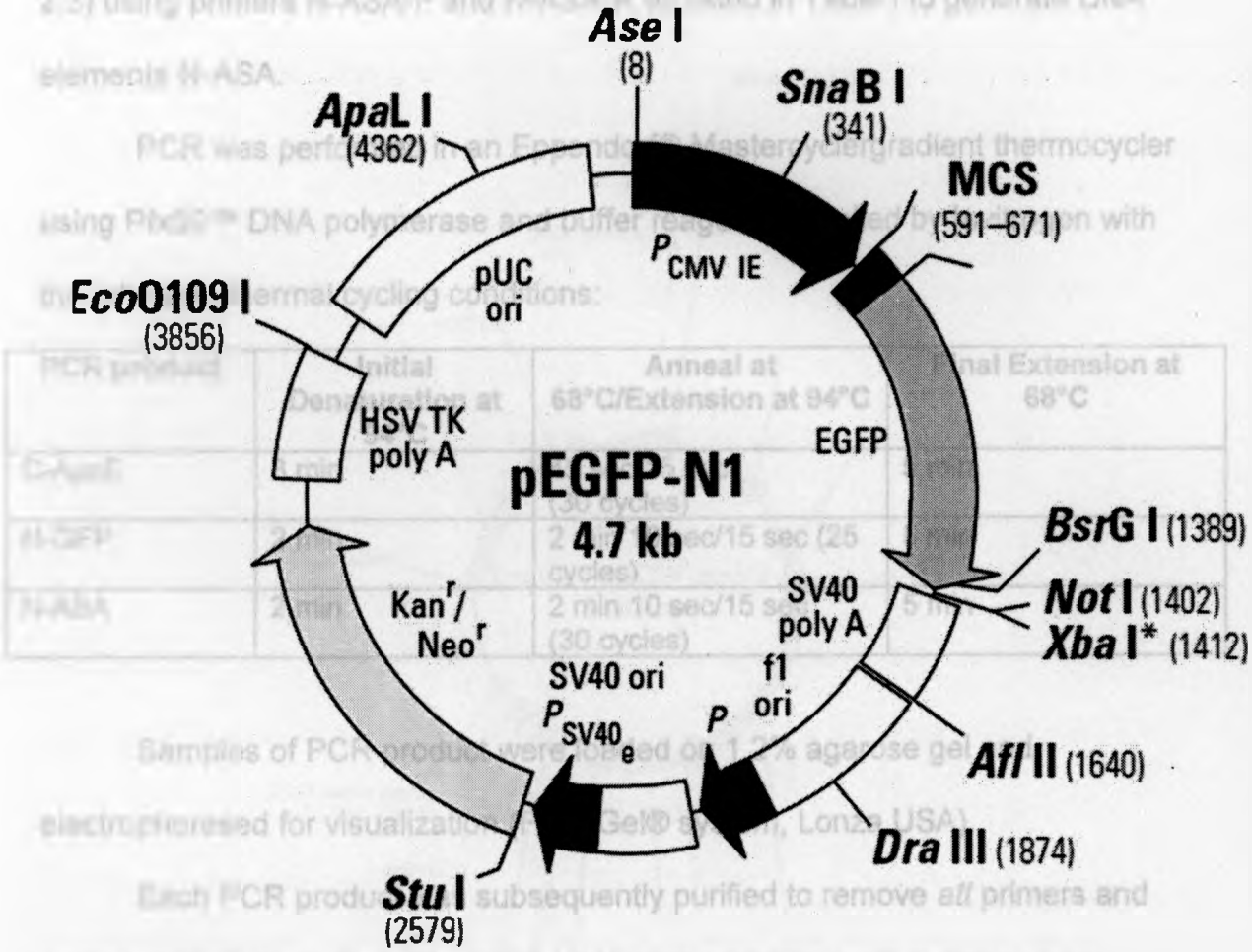


**Figure 2.2** Full length eGFP was PCR-amplified from the plasmid, peGFP-N1 (GenBank Accession #U55762) with primers containing specific flanking *att*-sites. Amplicons were used in downstream events to generate fusion proteins designated GFP-ApoE.Illustration from Clontech Laboratories (http://www.clontech.com).

PCR-amplified from pLenti6.3-v5GW-asaV5 (supplied by this laboratory, Figure 2.3) using primers N-ASA-F and N-ASA-R as listed in Table I to generate DNA elements N-ASA.

PCR was performed in an Eppendorf® Mastercyclergradient thermocycler using Pfx50™ DNA polymerase and buffer reagents supplied by Invitrogen with the following thermal cycling conditions:

| **PCR product** | **Initial Denaturation at 94°C** | **Anneal at 68°C/Extension at 94°C** | **Final Extension at 68°C** |
|---|---|---|---|
| C-ApoE | 3 min | 45 sec/15 sec (30 cycles) | 5 min |
| N-GFP | 2 min | 2 min 10 sec/15 sec (25 cycles) | 5 min |
| N-ASA | 2 min | 2 min 10 sec/15 sec (30 cycles) | 5 min |

Samples of PCR product were loaded on 1.2% agarose gel and electrophoresed for visualization (FlashGel® system, Lonza USA).

Each PCR product was subsequently purified to remove *att* primers and primer-dimers. Both N-eGFP and N-ASA PCR products were purified using polyethylene glycol (PEG) purification. Briefly, 75 µl 1X TE buffer (Tris-EDTA, pH 8.0) was added to 25 µl of amplification reaction mixture containing *att*-flanked PCR product followed by the addition of 50 µl 30% PEG 8000/30 mM $MgCl_2$ (supplied with MultiSite Gateway® Pro, Invitrogen). The mixtures were mixed thoroughly and centrifuged at 10,000 x g for 15 min at room temperature. The supernatant was removed and the remaining pellet was dissolved in 25 µl 1X TE buffer and stored at -20°C for downstream applications.

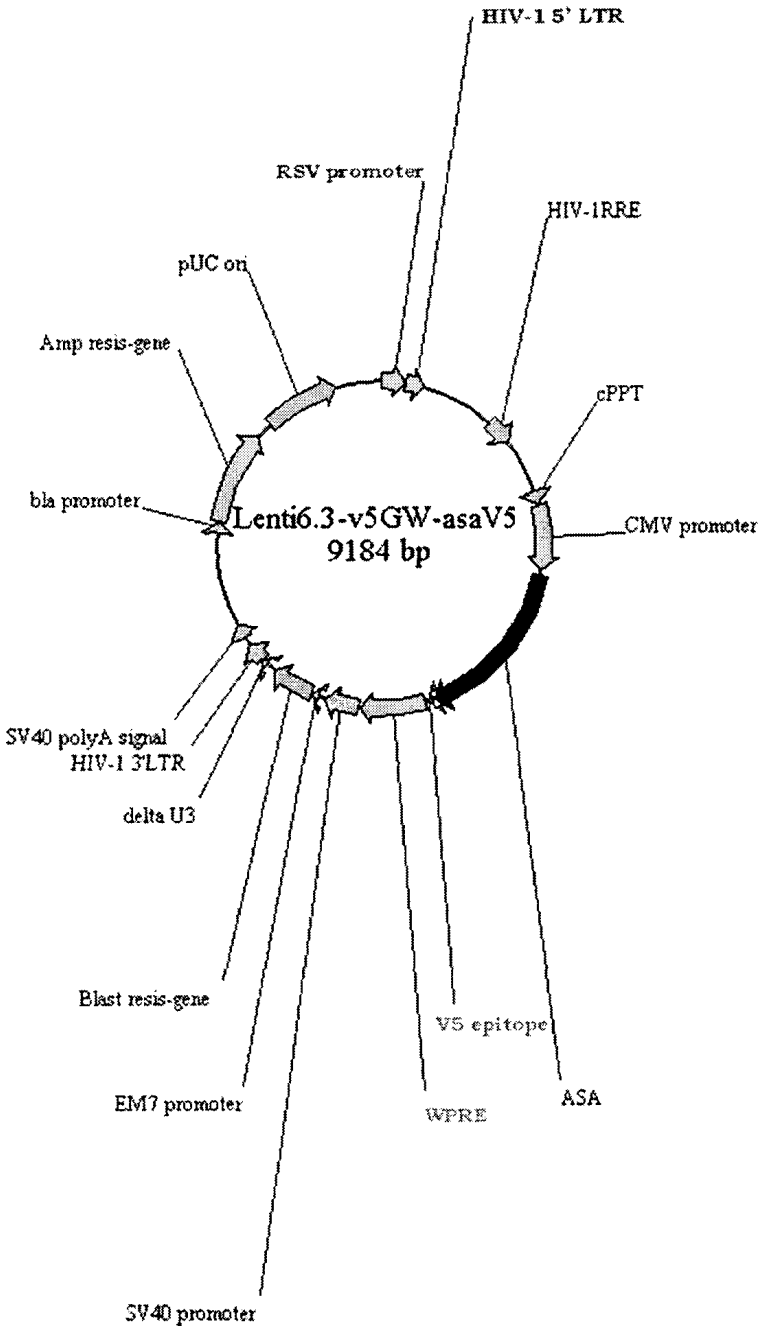


**Figure 2.3** Full length ASA with a C-terminus V5 epitope tag was PCR-amplified with primers containing specific flanking *att*-sites from the plasmid, pLenti6.3-v5GW-asaV5. Amplicons were used in downstream events to generate fusion proteins designated ASAApoE. Control expression clones were also generated using this plasmid.

C-ApoE PCR products were gel purified from 4% agarose using the PureLink™ Quick Gel Extraction kit (Invitrogen) according to the manufacturer's instructions. Briefly, the area of the gel containing C-ApoE was excised and dissolved in 2 volumes of gel solubilization buffer in a 50°C water bath for 30 min. Following the addition of isopropanol, all product was transferred onto an extraction column. Samples were centrifuged and washed with wash buffer containing ethanol. The samples were incubated for 1 min with elution buffer and purified PCR products were pelleted by centrifugation and stored at -20°C for downstream applications.

The quality and quantity of all purified DNA products were measured by spectrophotometry (NanoDrop™ 1000 Spectrophotometer, Thermo Scientific) and were visualized using either 1.2% or 2.2% agarose gel electrophoresed for 5-7 min at 275V (FlashGel® system, Lonza USA).

**2. 2 Creating entry clones with pDONR™ vectors**

Entry clones were generated using a BP recombination event that inserted purified PCR amplicons into specific pDONR™ vectors to generate entry clones that would be used in downstream second recombination events (Figure 2.1).

**2.2.1 BP reaction**

PCR elements N-ASAV5 and N-eGFP were inserted into pDONR 221 P1-P5r and element C-ApoE was inserted into pDONR 221 P5-P2 (Figure 2.4) as a result of a BP recombination event. Gateway BP Clonase™, an enzyme mixture containing Integration Host Factor (IHF) and Integrase proteins catalyzed the insertion of the PCR product into donor vectors. Briefly, 15-150 ng of each *att*-

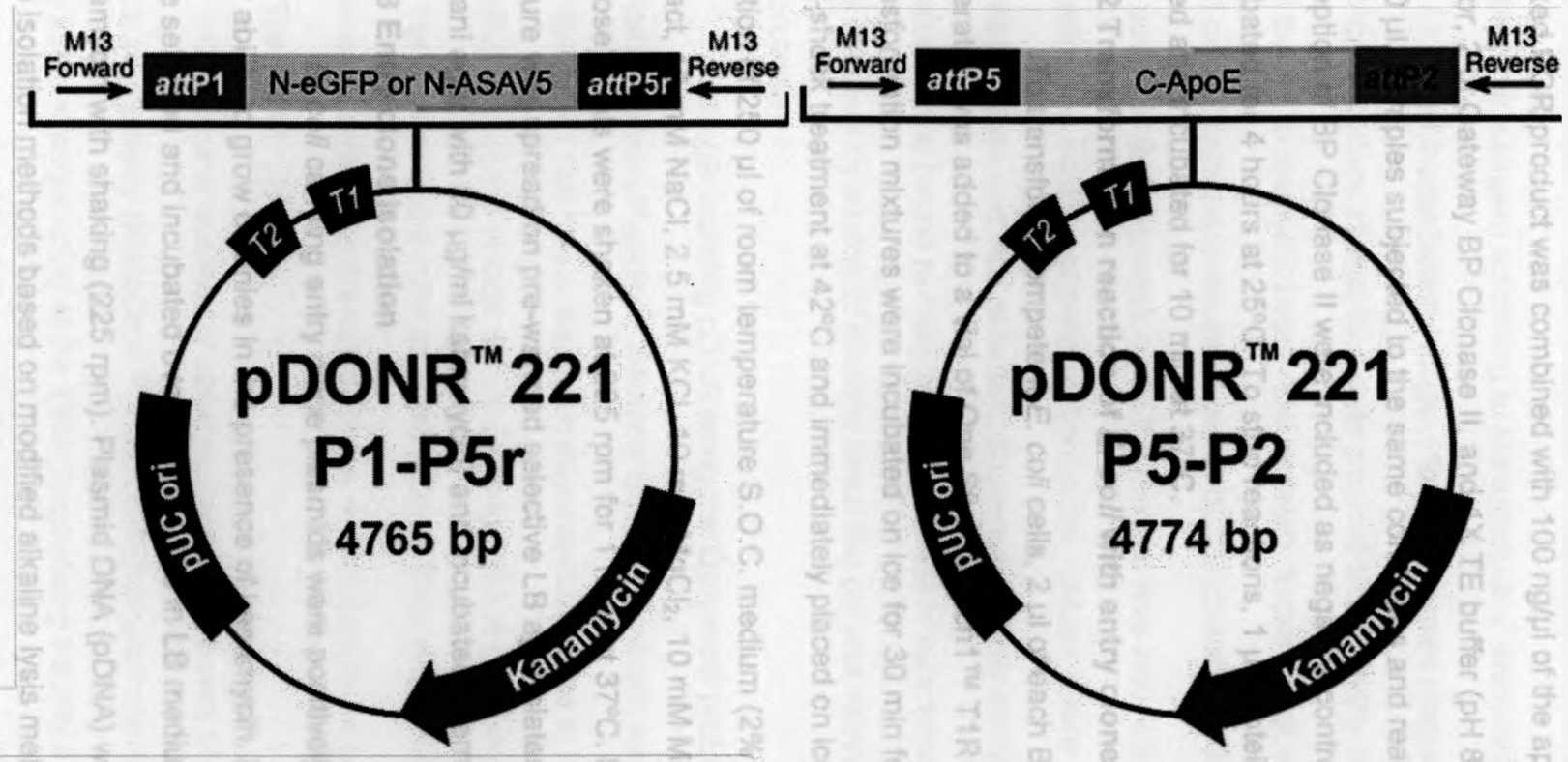


**Figure 2.4** *att*-flanked PCR amplicons were used in BP recombination events along with pDONR entry vectors from Invitrogen's MultiSite Gateway® Pro kit to generate entry clones. DNA elements containing either the full-length hASAV5 or full-length eGFP were inserted into pDONR™ 221 P1-P5r. The LDLR-binding region of murine ApoE was inserted into pDONR™ 221 P5-P2. Figure adapted from Invitrogen.

flanked PCR product was combined with 100 ng/µl of the appropriate pDONR vector, 2 µl Gateway BP Clonase II, and 1X TE buffer (pH 8.0) for a total volume of 10 µl. Samples subjected to the same conditions and reagents with the exception of BP Clonase II were included as negative controls. All mixtures were incubated for 4 hours at 25°C. To stop reactions, 1 µl Proteinase K (2 µg/µl) was added and incubated for 10 min at 37°C.

### 2.2.2 Transformation reaction of *E. coli* with entry clones

To transform competent *E. coli* cells, 2 µl of each BP reaction mixture generated was added to a vial of One Shot® Mach1™ T1R Competent *E.coli*. Transformation mixtures were incubated on ice for 30 min followed by a 30 sec. heat-shock treatment at 42°C and immediately placed on ice for 2 min. After the addition of 250 µl of room temperature S.O.C. medium (2% tryptone, 0.5% yeast extract, 10 mM NaCl, 2.5 mM KCl, 10 mM $MgCl_2$, 10 mM $MgSO_4$, 20 mM glucose), vials were shaken at 225 rpm for 1 hour at 37°C. Each transformation mixture was spread on pre-warmed selective LB agar plates (37.0 g/L Luria Bertani agar with 50 µg/ml kanamycin) and incubated overnight at 37°C.

### 2.2.3 Entry clone isolation

*E. coli* carrying entry clone plasmids were positively selected based on their ability to grow colonies in the presence of kanamycin. Discrete colonies were selected and incubated overnight at 37°C in LB medium containing 50 µg/ml kanamycin with shaking (225 rpm). Plasmid DNA (pDNA) was isolated by mini-prep isolation methods based on modified alkaline lysis methods (62) using either

the ChargeSwitch® NoSpin Plasmid Kit (Invitrogen) or the QIAprep® Spin Miniprep Kit (Qiagen) according to manufacturers' instructions.

The ChargeSwitch NoSpin Plasmid Kit uses magnetic beads with a switchable surface charge to isolate plasmid DNA. Briefly, transformed bacteria were bound to magnetic beads and pelleted. Supernatant was removed and the bead-bound cells were resuspended in buffer containing RNase A. Lysis buffer was added to the suspension and the mixture was incubated for up to 5 min. Following the addition of precipitation buffer, cellular debris became bound to the magnetic beads and was pelleted. Supernatant, now containing pDNA, was transferred and bound to fresh magnetic beads in new tubes. pDNA was washed twice followed by elution of plasmid when the pH was raised using the supplied elution buffer.

To begin isolating pDNA using the QIAprep® protocol, cell cultures were harvested by centrifugation. Bacteria carrying plasmids were lysed in lysis buffer with RNase A. The lysate was neutralized and adjusted to high-salt followed by centrifugation to precipitate debris, leaving DNA in suspension. The suspension was transferred to columns for adsorption of DNA and washed twice. Elution buffer was added, and the solution was centrifuged, eluting entry clone plasmids into Tris buffer.

Quality and quantity of isolated plasmid DNA was analyzed by spectrophotometry (NanoDrop™ 1000 Spectrophotometer). Candidate samples were sent for sequencing at the DNA Sequencing Facility at Robarts Research Institute using M13F (-20) and M13R sequencing primers (Table II).

Transformed colonies containing complete and accurate sequences were incubated overnight at 37°C with shaking in LB medium with 50 µg/ml kanamycin. Plasmid DNA (pDNA) was isolated using midi-prep isolation using the PureLink™ HiPure Midiprep kit (Invitrogen) following manufacturer's instructions. This isolation method uses anion-exchange chromatography whereby bacteria is harvested and resuspended in resuspension buffer with RNase A. Cells were lysed in lysis buffer, precipitation buffer was added and debris was pelleted using centrifugation. Supernatant containing plasmid DNA was passed through anion exchange columns, binding DNA to the column. The column was washed to remove impurities and the DNA was eluted with supplied elution buffer. The eluted DNA was desalted and concentrated using an alcohol precipitation and subsequently resuspended in Tris buffer.

Quality and quantity of pDNA was analyzed by spectrophotometry (NanoDrop™ 1000 Spectrophotometer). Entry clones were designated: pNASAV5, pCApoE, and pNeGFP.

**2.3 Creating expression clones using pcDNA 6.2/V5-DEST vectors**

To generate expression vectors encoding the desired fusion proteins, two entry clones and the pcDNA 6.2/V5-DEST Gateway® vector (Figure 2.5) were used in an LR recombination event. This reaction simultaneously transferred both DNA fragments into the destination vector. Reaction mixtures were transformed into competent *E. coli* and expression clones were selected for.

| Primer | Sequence (5' – 3') |
|---|---|
| M13F (-20) | 5'-GTAAAACGACGGCCAG-3' |
| M13R | 5'-CAGGAAACAGCTATGAC-3' |
| P1F | 5'-AGTGCGCGAGCAAAATTTAAG-3' |
| P2F | 5'-GTTCGGATGGGCATGTACCCT-3' |
| P3F | 5'-CTCCCTGATGGAGCTGGATGC-3' |
| P4F | 5'-ACTGCTCATGAGCCCCCGCTG-3' |
| T7 Promoter | 5'-TAATACGACTCACTATAGGG-3' |
| V5R | 5'-ACCGAGGAGAGGGTTAGGGAT-3' |
| CMV | 5'-CGCAAATGGGCGGTAGGCGTG-3' |

**Table II** Entry and expression clones were sent to the DNA Sequencing Facility at the Robarts Research Institute for sequencing. Entry clones pN-ASAV5, pN-eGFP, and C-ApoE were sequenced using M13F (-20) and M13R primers. Expression clones used the following sequencing primers: pASAV5ApoE expression clones used P1F, P2F, P3F, P4F; pGFPApoE expression clones used T7 promoter and V5R; pLvASAApoE used CMV, P2F, P3F, P4F; and pLvGFPApoE used CMV and V5R.

### 2.3.1 LR *reaction*

Each entry clone was used in a LR recombination reaction (Figure 2.1) to insert DNA elements into destination vectors to generate expression clones. Entry clones were paired up to include both N-terminus targeted DNA elements and C-terminus targeted DNA elements: pNASAV5 and pCApoE; pNeGFP and pCApoE. These reactions required the use of Gateway® LR Clonase® Plus, an enzyme mixture containing Integrase, IIHF, and Excisionase enzymes to catalyze recombination between entry clones and pcDNA 6.2/V5-DEST (Figure 2.5). Briefly, 10 fmoles of each appropriate entry clone was combined with 20 fmoles of destination vector, 1X TE Buffer, and 7µl of LR Clonase™ Plus enzyme. Mixtures were vortexed briefly and incubated at room temperature for 16 hr. To stop the reaction, 1 µl of Proteinase K solution (2 µg/µl) was added and tubes were incubated for 10 min at 37°C. Negative controls were subjected to the same conditions and reagents with the exception of LR Clonase™ Plus which was omitted.

### 2.3.2 Transformation reaction of *E. coli* with pcDNA 6.2/V5-DEST

To transform competent *E. coli* cells, 2 µl of each LR reaction mixture generated was added to a vial of One Shot® Mach1™ T1R Competent *E.coli* (Invitrogen). To generate control expression clones encoding ASAV5 (pLvASAV5), a vial of One Shot® Mach1™ Competent *E.coli* was transformed with 100 ng of pLenti6.3-v5GW-asaV5 (Figure 2.3, supplied by this laboratory). The same protocol for the transformation reaction was used in section 2.2.2 with the exception of the selective agar: each transformation mixture was spread on

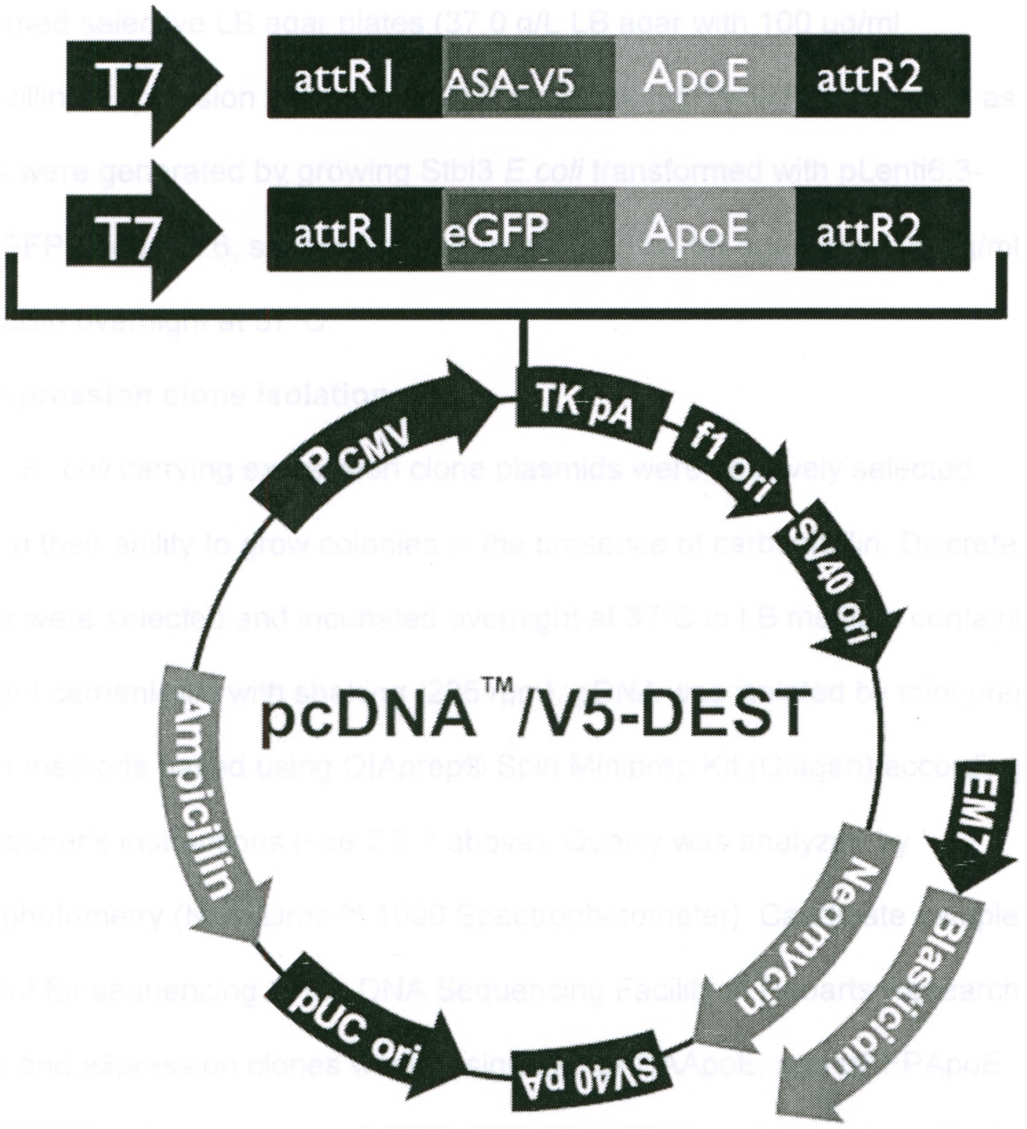


**Figure 2.5** Entry clone pCApoE and either pNASAV5 or pNeGFP were used in LR recombination events along with the pcDNA™/V5-DEST expression vector from Invitrogen to generate expression plasmids pASAApoE and pGFPApoE. Figure adapted from Invitrogen.

pre-warmed selective LB agar plates (37.0 g/L LB agar with 100 µg/ml carbenicillin). Expression clones for eGFP expression (pLvGFP) to be used as controls were generated by growing Stbl3 *E.coli* transformed with pLenti6.3-v5GW-GFP (Figure 2.6, supplied by this laboratory) on LB agar with 100 µg/ml carbenicillin overnight at 37°C.

**2.3.3 Expression clone isolation**

*E. coli* carrying expression clone plasmids were positively selected based on their ability to grow colonies in the presence of carbenicillin. Discrete colonies were selected and incubated overnight at 37°C in LB medium containing 100 µg/ml carbenicillin with shaking (225 rpm). pDNA was isolated by mini-prep isolation methods based using QIAprep® Spin Miniprep Kit (Qiagen) according to manufacturer's instructions (see 2.2.3 above). Quality was analyzed by spectrophotometry (NanoDrop™ 1000 Spectrophotometer). Candidate samples were sent for sequencing at the DNA Sequencing Facility at Robarts Research Institute and expression clones were designated pASAApoE, and pGFPApoE. A nested set of sequencing primers (P1F, P2F, P3F, P4F) were used to sequence pASAApoE. To sequence pGFPApoE, T7 promoter primer and V5 reverse primer were used (Table II). Transformed colonies containing complete and accurate sequences were grown and pDNA purified by midi-prep isolation methods listed previously. Quality and quantity of pDNA was analyzed by spectrophotometry (NanoDrop™ 1000 Spectrophotometer).

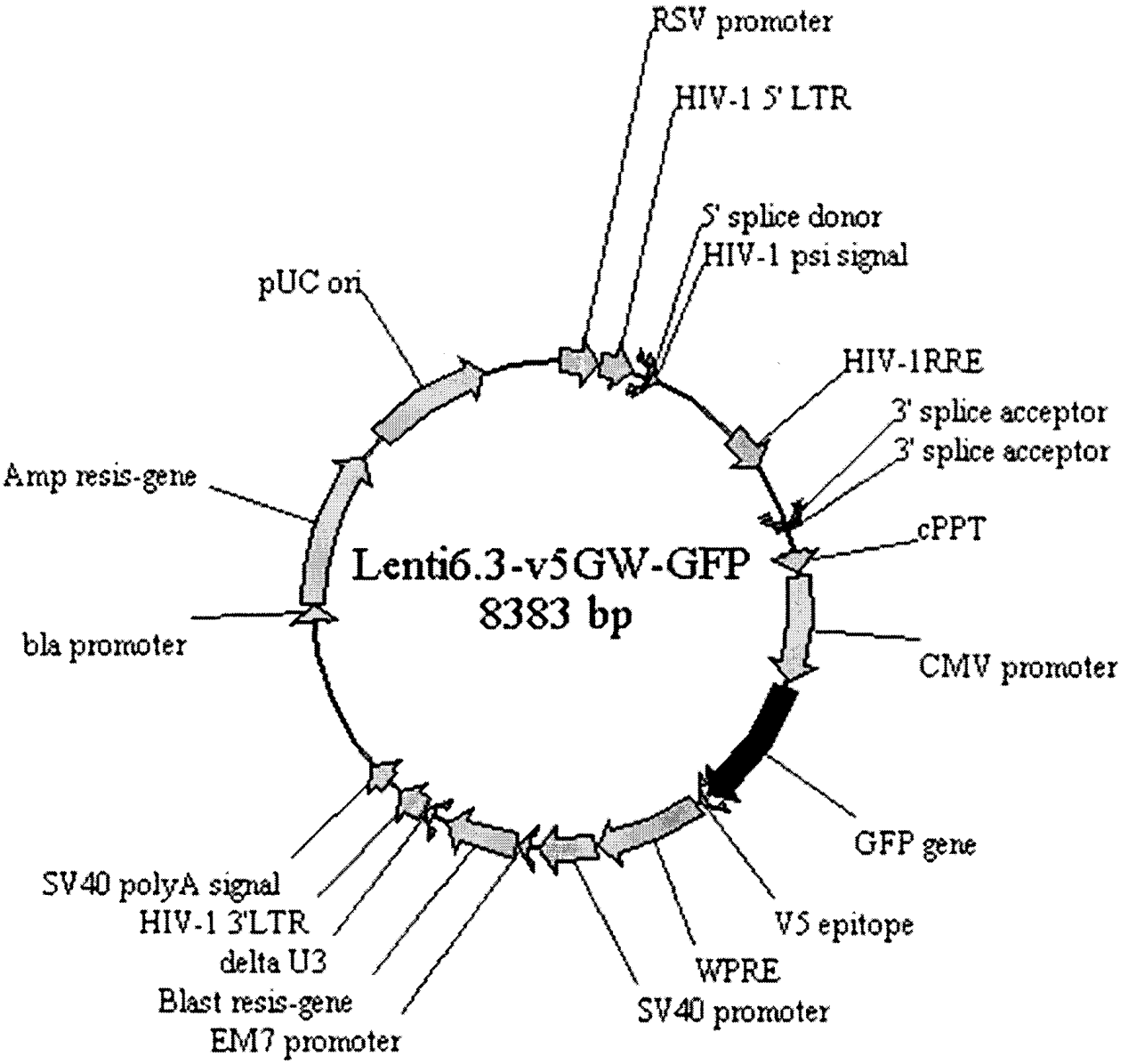


**Figure 2.6** Full length eGFP was PCR-amplified from the plasmid, pLenti6.3-v5GW-GFP with primers containing specific flanking *att*-sites. Amplicons were used in downstream events to generate fusion proteins designated GFPApoE. This plasmid was also used to transform competent *E.coli* and used to generate control expression clones

## 2.4 Transfection of CHO cell lines with pASAApoE and pGFPApoE

### 2.4.1 Cell culture

Chinese hamster ovary cells (CHO DG44) that were used for experiments were dihydrofolate reductase (DHFR)-deficient cells adapted to be an adherent cell line by this laboratory. Cells were maintained in complete CHO medium composed of HyClone DMEM/F-12 (Dulbecco's Modified Eagle Medium/Nutrient Mixture F-12, Thermo Scientific), 10% fetal bovine serum (FBS, Gibco by Invitrogen), and 1X antibiotic-antimycotic (Gibco) at 37°C in 5% $CO_2$. Cells were passaged when confluent using TrypLE™ Express (Gibco) to dissociate CHO cells from cultureware and transferred into T-75 $cm^2$ flasks (BD Biosciences).

### 2.4.2 Plasmid transfection

To increase likelihood of expression in transfected cells, plasmids were linearized using restriction endonucleases to cleave plasmids in a location outside of any critical elements and outside of the recombinant gene sequence. Plasmids carrying the fusion constructs (pASAApoE, pGFPApoE) were linearized using *SapI* (New England BioLabs) and plasmids carrying controls (pLvASAV5, pLvGFP) were linearized using *SspI* (New England BioLabs). Briefly, 2 µg of plasmid were combined with 5 µl 10x buffer (supplied) and $dH_2O$ to a final volume of 50 µl. Restriction enzyme was added (3 µl *SapI* or 1.5 µl *SspI*) and mixtures were incubated at 37°C for 3 hr and heat-inactivated at 65°C for 20 min. Aliquots were electrophoresed on 0.8% agarose gel and visualized with ethidium bromide to assess linearization. Images of gels were captured using BioRad Gel Doc UV-

Transilluminator Imaging System and annotated and analyzed using Quantity One® 4.6.1 quantitation software.

Plasmids were ethanol precipitated. Briefly, 1/10 of a volume of 3 M sodium acetate buffer (pH 5.2) and 2-½ volumes of ice cold 100% ethanol were added to samples and stored at -20°C for a minimum of 1 hr. pDNA was pelleted by centrifugation at 10,000 x g for 15 min at 4°C and the supernatant was discarded. The pDNA pellet was washed with cold 70% ethanol and centrifuged for 10,000 x g for 5 min at 4°C. The pelleted plasmid was air dried for 10 min and resuspended in Tris-EDTA buffer. Quality and quantity of linearized plasmids were analyzed by spectrophotometry (NanoDrop™ 1000 Spectrophotometer).

Transfection of plasmid DNA into CHO cells was performed in duplicate using Lipofectamine™ LTX and PLUS™ reagents (Invitrogen). One day before transfection, CHO cells were seeded with complete CHO medium into 24-well plates and incubated at 37°C with 5% $CO_2$. When cells reached 70-80% confluence, media was removed and replaced with 0.5 ml fresh DMEM/F-12 medium containing 10% FBS (Gibco). For each transfection reaction, 0.5 µg of plasmid was diluted into 100 µl Opti-MEM® I reduced-serum medium (Invitrogen) and 0.5 µl of PLUS™ reagent was added. These mixtures were incubated for 5 min at room temperature and 1.7 µl of Lipofectamine™ LTX was added. The DNA-lipid mixture was incubated for 30 min at room temperature and DNA-lipid complexes were added. Mock transfections were set up using naïve CHO cells without the addition of lipofectamine as well as naïve CHO cells incubated with lipofectamine but without pDNA. Plates were then incubated at 37°C in 5% $CO_2$

for 4-6 hr. Any unattached complexes were removed, replaced with DMEM/F-12 medium containing 10% FBS (Gibco), and returned for incubation. After 48 hr, the medium was replaced with CHO complete medium containing 3 µg/ml blasticidin to select for stable transfectants. Medium was replaced with fresh blasticidin-containing medium every 48-72 hr for 11 days until stable transfectants were firmly established.

### 2.5 Detecting recombinant fusion proteins expressed by stable transfectants

#### 2.5.1 Detection of eGFP expression

To detect eGFP expression, live CHO cells transfected with pGFPApoE and pLvGFP were visualized using fluorescence microscopy. All images were obtained using a Leica DMIRB fluorescence microscope equipped with a QImaging Retiga 1300 camera and processed with Improvision Openlab software.

Fluorescence in collected cell lysate and cell media (see section 2.5.2) was measured with excitation/emission wavelengths of 471/508 nm using a multimode microplate reader (Varioskan™, Thermo Electron Corp.) controlled by SkanIt® software, version 2.2.

#### 2.5.2 Collection of cell lysate and media

Each stable transfected cell line (transfected with pASAApoE, pGFPApoE,pLvGFP, and pLvASAV5) and naive CHO cells were grown to confluence and harvested. Briefly, cells were washed four times with chilled DMEM/F-12. Cells were gently scraped, suspended in cold DMEM/F-12 medium, and then pelleted by centrifugation at 1,000 x g for 5 min at 4°C. Cells were

resuspended in 3 ml chilled 20mM Tris (pH 8.0) and lysed by sonication. Lysate was cleared of cellular debris by centrifugation at 20,000 x g for 15 min at 4°C and supernatant was carefully removed.

Conditioned medium was collected from CHO cells expressing ASAV5 and ASAApoE every 48-72 hr, centrifuged at 12,000 x g for 5 min at 4°C to pellet cellular debris, and filter-sterilized through 0.2 µm sterile syringe filters (VWR).

**2.5.3 Assessing enzyme activity**

The cell homogenate and/or supernatant from CHO cells transfected with pApoEASA, pASAApoE, and pLvASAV5 were analyzed for arylsulfatase A activity using p-nitrocatechol sulfate (pNCS) as substrate according to Gordon and Rip (63). Samples of media or cell homogenate (50 µl) were incubated in standard 96-well plates with 50 µl p-NCS solution in sodium acetate buffer (10 mM, pH 5.0) at 4°C. Blanks containing 50 µl sample only were incubated under the same conditions. After 48-72 hours, all assays were terminated with the addition of 150 µl of 1M NaOH and 50 µl of pNCS solution was added to blanks. All samples were analyzed spectrophotometrically at 516 nm using a multimode microplate reader (Varioskan™, Thermo Electron Corp.) controlled by SkanIt® software, version 2.2 and absorbance values converted to nanomoles (nmol) activity of ASA. Numbers were standardized by dividing the nmol of pNCS cleaved by the number of hours the assays were run (nmol/hr).

**2.6 Generating lentiviral expression plasmid**

To increase the stability and expression levels of fusion proteins, lentiviral expression plasmids were generated using entry clones pNASAV5, pCApoE, and pNeGFP previously produced (see Chapter 2.2). Two entry clones

and the pLenti6.3/V5–DEST expression vector (Figure 2.7) were used in an LR recombination event. Following recombination, mixtures were transformed into competent *E.coli* and expression clones were selected based on growth in the presence of antibiotic.

### 2.6.1 LR reaction

Following the LR reaction method detailed in Chapter 2.3.1, pLenti6.3/V5-DEST vectors were used in conjunction with entry clones listed above to generate lentiviral-based expression clones (pLenti). pNASAV5 and pCApoE were paired together to generate expression clone, pLvASAApoE. pNeGFP and pCApoE were used to generate expression clone pLvGFPApoE.

### 2.6.2 Transformation reaction of *E. coli* with pLenti

To transform competent *E. coli* cells, 3 µl of each LR reaction mixture was added to a vial of One ShotR Stbl3™ Chemically Competent *E. coli* (Invitrogen). Transformation mixtures were incubated on ice for 30 min followed by a 30 sec. heat-shock treatment at 42°C and immediately placed on ice for 2 min. Mixtures were transferred to conical tubes containing 1 ml of pre-warmed S.O.C. medium and were shaken at 225 rpm for 1 hour at 37°C. Each transformation mixture was spread on pre-warmed selective LB agar plates (37.0 g/L Luria Bertani agar with 100 µg/ml carbenicillin) and incubated overnight at 37°C.

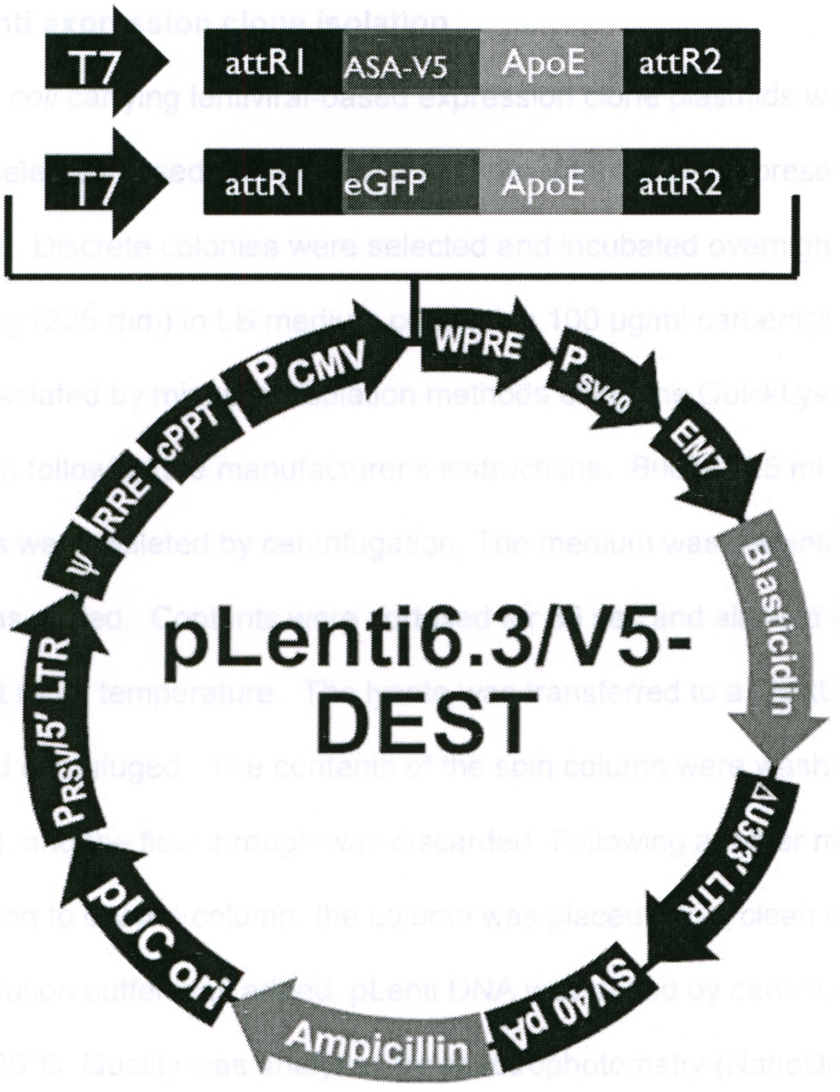


**Figure 2.7** Entry clone pCApoE and either pNASAV5 or pNeGFP were used in LR recombination events along with the pLenti6.3/V5-DEST expression vector from Invitrogen to generate expression plasmids pLvASAApoE and pLvGFPApoE. Figure adapted from Invitrogen.

### 2.6.3 pLenti expression clone isolation

*E. coli* carrying lentiviral-based expression clone plasmids were positively selected based on their ability to grow colonies in the presence of carbenicillin. Discrete colonies were selected and incubated overnight at 37°C with shaking (225 rpm) in LB medium containing 100 µg/ml carbenicillin. pLenti DNA was isolated by mini-prep isolation methods using the QuickLyse Miniprep Kit (Qiagen) following the manufacturer's instructions. Briefly, 1.5 ml transformed *E. coli* cells were pelleted by centrifugation. The medium was decanted and lysis solution was added. Contents were vortexed for 30 sec and allowed to incubate for 3 min at room temperature. The lysate was transferred to a QuikLyse spin column and centrifuged. The contents of the spin column were washed, centrifuged, and the flow through was discarded. Following another round of centrifugation to dry the column, the column was placed into a clean collection tube and elution buffer was added. pLenti DNA was eluted by centrifugation and stored at -20°C. Quality was analyzed by spectrophotometry (NanoDrop™ 1000 Spectrophotometer). Samples were sequenced at the DNA Sequencing Facility at Robarts Research Institute using the CMV forward primer and P2F, P3F, and P4F for sequencing pLvASAApoE expression clones. The CMV forward primer and V5R reverse primer were used to sequence pLvGFPApoE clones (Table II).

### 2.7 Restriction enzyme analysis of pLenti

pLenti DNA was analyzed by restriction digestion to confirm rearrangement in the LTR regions of the plasmid had not occurred using a combination of endonucleases *Afl*II and *Xho*I. All reagents were supplied by New England BioLabs. Briefly, 1 µg of each expression clone was diluted to 17 µl in

deionized water and mixed gently with 2 µl of 10X Buffer and 0.2 µl bovine serum albumin (BSA). *AflII* and *XhoI* (10 U each) were added and mixtures were incubated at 37°C for 3hr. Enzyme activity was heat-inactivated for 20 min at 65°C. Aliquots were electrophoresed on 0.8% agarose gel and visualized with ethidium bromide to assess fragment sizes. Images of gels were captured using BioRad Gel Doc UV-Transilluminator Imaging System and annotated and analyzed using Quantity One® 4.6.1 quantitation software.

Transformed colonies containing complete and accurate sequences were grown and pLenti was isolated by midi-prep isolation methods based on modified alkaline lysis methods (62) using a QIAfilter Plasmid Purification Kit (Qiagen) following manufacturer's instructions. Briefly, transformed *E.coli* cells were pelleted by centrifugation. The pellet was resuspended in the supplied resuspension buffer and lysis buffer was added, and the mixture incubated for 5 min at room temperature. Precipitation buffer was added and contents were immediately transferred to the barrel of a Qiafilter cartridge followed by incubation at room temperature for 10 min to allow precipitates to float to the top on the cartridge. The lysate was then filtered into an equilibrated Qiagen tip containing an anion-exchange resin, binding pLenti DNA. The Qiagen tip was washed twice with supplied buffer and pLenti DNA was eluted using supplied elution buffer. The pLenti DNA was precipitated with room-temperature isopropanol and pelleted by centrifugation. The supernatant was discarded and the pellet was washed with 70% ethanol, followed by centrifugation. The pellet was air dried and pLenti DNA was redissolved in a 100 µl TE buffer (pH 8.0). Quality and

quantity of pDNA was analyzed by spectrophotometry (NanoDrop™ 1000 Spectrophotometer).

### 2.8 Lentivirus production

ViraPower™ Packaging Mix (Invitrogen) and the pLenti expression clones, LvASAApoE and LvGFPApoE, were co-transfected into a 293FT producer line to produce two different replication incompetent lentiviral stocks following the manufacturer's instructions. The titer of each virus was measured and lentiviral stocks were used to transduce CHO-DG44 cell lines.

#### 2.8.1 Propagating 293FT producer cell lines

The initial 293FT cell lines were provided by this laboratory and maintained in 293FT complete DMEM media (high glucose Dulbecco's Modified Eagle Medium, 10% FBS, 0.1 mM MEM Non-Essential Amino Acids, 2 mM L-glutamine, and 1X Anti-Anti) supplemented with 500 µg/ml Geneticin. Cells were incubated at 37°C in 5% $CO_2$ and passaged when confluent. All cell culture reagents were supplied by Gibco.

#### 2.8.2 Co-transfection of 293FT cells with ViraPower™ and pLenti expression clones

One day prior to co-transfection, 293FT cells were seeded in 293FT complete media without antibiotic in T-75 $cm^2$ flasks (BD Biosciences) at a density to ensure that cells would be ~90-95% confluent for transfection. Cells were incubated overnight at 37°C in 5% $CO_2$.

On the day of transfections, 293FT culture medium was discarded and replaced with 5 ml of 293FT complete medium supplemented with 1mM sodium pyruvate (Gibco) without antibiotic. For each transfection reaction, 9 µg of pLenti

and 3 µg of ViraPower™ packaging mix were diluted into 1.5 ml OptiMEM I Medium. Thirty-six µl of Lipofectamine™ 2000 was diluted in 1.5 ml of OptiMEM I Medium and incubated for 5 min at room temperature. Following incubation, diluted lipofectamine was added to pLenti mixture, mixed gently, and incubated for 20 min at room temperature to allow DNA-lipofectamine complexes to form. Complexes were added drop wise to 293FT cells in flasks, mixed gently, and incubated overnight at 37°C in 5% $CO_2$. The following day, 293FT medium containing DNA-lipofectamine complexes was replaced with 10 ml of 293FT complete medium without antibiotics and incubated for 48 hr at 37°C in 5% $CO_2$.

**2.8.3 Harvesting lentivirus**

Virus-containing medium was removed, transferred to sterile tubes, and centrifuged at 3000 rpm for 15 min at 4°C to pellet debris. Cleared supernatant was filtered through a Millex-HV 0.45 µm PVDF filter (Millipore) and stored at -70°C.

In order to titer lentiviral stocks, CHO-DG44 cells in CHO complete medium were plated in 6-well plates and incubated at 37°C in 5% $CO_2$ until ~50% confluent. Serial dilutions from $10^{-2}$ to $10^{-6}$ of lentiviral stocks (LvASAApoE and LvGFPApoE) were prepared by diluting stock in CHO complete medium. Medium was removed from wells and diluted lentivirus was added to wells containing CHO cells. A mock transfection was also set up with the omission of lentivirus. Hexadimethrine bromide (Polybrene®, Sigma) was added to each well to a final concentration of 6 µg/ml and plates were gently swirled to combine. Plates were incubated overnight at 37°C in 5% $CO_2$.

The following day, medium containing virus was removed and replaced with fresh, complete CHO medium containing 3 µg/ml blasticidin. Cells were kept under selective pressure until all cells in mock transfected wells had died.

Cells were fixed with the addition of 4% paraformaldehyde (PFA) and incubated for 5-10 min at room temperature. PFA was removed and cells were washed with phosphate-buffer saline (PBS). PBS was removed and 100 µl of crystal violet solution was added to each well, incubated for 10 min at room temperature, and removed. Cells were washed twice with PBS. Colonies were counted and titer was determined.

**2.9 Transducing CHO cells with lentivirus**

CHO cells were seeded into 6-well plates with complete CHO medium and incubated at 37°C in 5% $CO_2$ until ~70% confluent. Medium was removed and replaced with 1 ml of 1/10 dilute lentivirus in complete medium. A mock transfection was included with the addition of medium only. Hexadimethrine bromide (Polybrene®, Sigma) was added to each well to a final concentration of 6 µg/ml and plates were gently swirled to combine. Plates were incubated overnight at 37°C in 5% $CO_2$. Medium was replaced every 48-72 hr with fresh complete CHO medium supplemented with 3 µg/ml Blasticidin until antibiotic-resistant colonies were firmly established.

Control cell lines expressing either ASAV5 or GFP were used in the assessment of protein expression and uptake experiments. These CHO-DG44 cell lines, supplied by this laboratory, were transduced with lentiviral stock derived from either pLenti6.3-v5GW-asaV5 or pLenti6.3-v5GW-GFP.

## 2.10 Collection of fusion proteins

To decrease the amount of interference encountered by the presence of albumin while purifying protein, all transduced CHO cell lines (transduced cell lines expressing ASAV5, GFP, ASAApoE, and GFPApoE) were weaned into serum-free medium (HyClone® SFM4CHO-A™, ThermoScientific) supplemented with 4 mM L-glutamine (Gibco), 1 X Anti-Anti (Gibco), and 10 X HT media supplement (Sigma Aldrich). Ammonium chloride (5 μM) and 1X Insulin-Transferrin-Selenium-A Supplement (Gibco) were added to serum-free medium in order to maximize GFP-ApoE secretion and inhibit its degradation (64-66).

Media was collected from transduced CHO cell lines every 48-72 hr. Upon collection, media was centrifuged at 1,000 x g for 5 min at 4°C and filter-sterilized through either 0.2 μm sterile syringe filters (VWR) or Nalgene® filter units. Media was pooled and stored at -20°C. Concentration of proteins was performed at 4°C using Amicon® Centrifugal Filter Devices (Millpore Corp.). Proteins were kept on ice between steps. Analysis of enzyme activity was done with each step of purification using the protocol as listed in Section 2.5.3.

ASAV5, ASAApoE, TfASAV5 proteins were purified using fast performance liquid chromatography (FPLC) with the ÄKTApurifier™ system (GE Healthcare) at 4°C controlled by UNICORN™ software.

### 2.10.1 Desalting

Media containing ASAV5, ASAApoE, or TfASAV5 was concentrated ~25 fold as noted previously and loaded directly onto a Sephadex-packed desalting column (HiPrep 26/10 Desalting, Amersham Biosciences) for buffer exchange into 20 mM Tris-HCl, pH 8.0 (Invitrogen) unless otherwise noted. The column

was equilibrated with 2 column volumes (CV) of 20 mM TrisHCl, pH 8.0, and proteins eluted with 3 CV of the same buffer. Flow rate was 7.5 ml/min.

**2.10.2 Blue sepharose chromatography**

As per 2.10.1, medium containing ASAV5, ASAApoE, or TfASAV5 was desalted into buffer with the following change: the buffer used for the exchange was 20 mM sodium phosphate, pH 7.0.

Following buffer exchange, up to 10 ml of desalted solution was applied to a blue sepharose column (HiTrap™ Blue HP, Amersham Biosciences) equilibrated with 5CV of Buffer A (20 mM sodium phosphate, pH 7.0). This column contains Cibacron Blue F3G-A, an aromatic anionic ligand that binds albumin by electrostatic and/or hydrophobic interactions. The column was washed with 5 CV of Buffer A and the flow-through was collected. Bound proteins were eluted with 5 CV of elution buffer (Buffer A with 2M NaCl, pH 7.0). The flow-through fractions were then applied to the desalting column (2.10.1) for buffer exchange to 20 mM Tris-HCl for further purification. The flow rate was 2.5 ml/min. The collected solutions were measured for enzyme activity and protein (absorbance 280 nm).

**2.10.3 ConA sepharose 4B chromatography**

As per 2.10.1, medium containing ASAV5, ASAApoE, or TfASAV5 was desalted into buffer with the following change: the buffer used for the exchange contained 20 mM Tris-HCl, 0.5 M NaCl, 1 mM $MnCl_2$, 1 mM $CaCl_2$, pH 7.4.

Up to 10 ml of the desalted solution was loaded onto a ConA sepharose 4B column (HiTrap™ ConA 4B, Amersham Biosciences) equilibrated with 5 CV of Buffer A (20 mM Tris-HCl, 0.5 M NaCl, 1 mM $MnCl_2$, 1 mM $CaCl_2$, pH 7.4.) The

desalted solution was applied 1 ml at a time with a flow rate of 0.25 ml/min with a 5 min pause between each ml applied to allow proteins to bind. The column was washed with 2 CV of Buffer A and the flow-through was collected. Bound proteins were eluted at a flow rate of 0.25 ml/min with 10 CV of elution buffer (Buffer A with 0.4 M methyl-α-D-mannoside, pH 7.4) by applying the first 2 CV of elution buffer followed by incubation for 30-60 min to allow the elution buffer to displace bound proteins. The remaining 8 CV of elution buffer was applied to displace proteins. Proteins that were tightly bound and would not elute under these conditions were stripped off of the column with 15 CV of 0.1 M borate buffer (pH 6.5) followed by regeneration of the ConA column with 10 CV of regeneration buffer (20 mM TrisHCl, 0.5 M NaCl, pH 8.5).

**2.10.4 DEAE-cellulose chromatography**

Up to 10 ml of desalted solution was loaded onto a DEAE column (HiPrep DEAE FF 16/10 column, Amersham Biosciences) equilibrated with 5 CV of Buffer A (20 mM TrisHCl, pH 8.0) and washed with 3 CV of the same buffer. Proteins were eluted via a linear gradient of NaCl (0.1 M to 0.46 M in Buffer A) over 5.75 CV. Any proteins still bound to the column were flushed with 3 CV of 1.0 M NaCl in Buffer A and the column was re-equilibrated with 3 CV of Buffer A. The flow rate was 2.5 ml/min. Fractions were collected and measured for enzyme activity and absorbance (280 nm) using the method outlined in Section 2.5.3.

**2.10.5 Gel filtration chromatography**

DEAE fractions having enzyme activity were pooled and concentrated (~ 15 fold). Up to 250 µl of concentrated protein was loaded onto a sizing column

(Superdex® 200 10/300 GL, Amersham Biosciences) equilibrated with 3 column volumes of 20 mM Tris-HCl, pH 8.0, and eluted for 2 column volumes in the same buffer using a flow rate of 0.200 ml/min. Fractions were collected and measured for enzyme activity and protein (absorbance 280 nm). Fractions with enzyme activity were pooled and specific activity was calculated following the outline in Section 2.5.3.

**2.11 Analyzing fusion proteins**

**2.11.1 Enzyme activity**

The enzyme activity of ASAApoE, TfASAV5, and ASAV5 was calculated using the protocol listed in section 2.5.3. Protein concentration was determined using the Bradford method (67) (Bio-Rad) using bovine IgG standards. The amount of specific activity was expressed as nmol p-NCS cleaved/hr/µg protein.

**2.11.2 Gel electrophoresis**

SDS-PAGE was performed according to Laemmli, 1970 (68). Briefly, samples containing 10 µg of protein were diluted in $dH_20$ to 20 µl and added to non-reducing lane marker sample buffer (5X, Pierce) containing 0.125 M dithiothreitol (DTT). After heating for 5 min at 95°C, samples were subjected to electrophoresis in 12% Precise™ precast polyacrylamide gel (Pierce) using BupH™ Tris-HEPES-SDS running buffer. Proteins were silver-stained using GelCode™ SilverSNAP® Stain Kit (Pierce) following manufacturer's protocol. Using reagents supplied with this kit, the gel was rinsed with deionized water ($dH_2O$) after electrophoresis and fixed for 30 min in 30% ethanol, 10% glacial acetic acid. Following fixing, the gel was washed in 10% ethanol and then washed in $dH_2O$. The gel was exposed to a sensitizing solution, rinsed in $dH_2O$

and transferred for 30 min to stain solution. After a brief wash step in $dH_20$, developer solution was added and removed once protein bands appeared (2-3 min). To stop the developer, the gel was incubated in 5% acetic acid. Images of gels were captured using the BioRad Gel Doc UV-Transilluminator Imaging System and annotated and analyzed using Quantity One® 4.6.1 quantitation software.

**2.11.3 Analyzing fluorescence**

To detect eGFP expression, live transduced CHO cells expressing GFPApoE and GFP were assessed using fluorescence microscopy. All images were obtained using a Leica DMIRB fluorescence microscope equipped with a QImaging Retiga 1300 camera and processed with ImprovisionOpenlab software.

**2.11.4 Glycosylation**

To assess glycosylation of TfASAV5 and ASAApoE fusion proteins and ASAV5 proteins, proteins were incubated with peptide-N4-(acetyl-β-glucosaminyl)-asparagine amidase N-Glycosidase F (PNGase F, New England Biolabs), an amidase that cleaves the link between asparagine residues and N-acetylglucosamine of N-linked glycoproteins. Apo-transferrin was used as a positive control. Briefly, 15 µg samples of each fusion protein and apo-transferrin were denatured with1X denaturing buffer (New England Biolabs) for 10 min at 100°C. After the addition of 1% NP40 and 1X reaction buffer (50 mM sodium phosphate, pH 7.5), 1000 units of PNGase F were added and the mixture incubated at 37°C for 1 hr. Samples were loaded onto 12% polyacrylamide precast gels (Precise, Pierce) and electrophoresed, silver-stained, and visualized as outlined in 2.11.1.

## 2.12 Generating an *in vitro* blood brain barrier

### 2.12.1 Propagation of bEND3 cells

An immortalized murine brain endothelial cell line, bEND3 cells (ATCC#CRL-2299), was a generous gift from Dr. Gediminas Cepinskas at the Centre for Critical Illness Research, Lawson Health Research Institute. bEND3 cells were maintained in modified DMEM (Dulbecco's Modified Eagle's Medium, 10% FBS, 1X Pen-Strep). To prepare flask surfaces for cells, T-75 cm2 flasks were incubated for at least 20 min with a 1/20 dilution of rat tail collagen, type I (Sigma) at room temperature which was subsequently removed prior to seeding bEND3 cells. Medium was replaced every 48-72 hr.

### 2.12.2 Growth of bEND3 monolayers

bEND3 cells were grown in monolayers on cell culture inserts to form an *in vitro* blood brain barrier. These monolayers have polarity with the top of the surface representing the apical side and the bottom surface representing the basolateral side (69). To assess the effectiveness of these barriers, the transendothelial electrical resistance (TEER) across monolayers was measured and used in conjunction with permeability studies performed using bovine serum albumin conjugated to Alexa Fluor® 488 (BSA488, Invitrogen) to determine paracellular passage across the confluent bEND3 monolayers.

bEND3 cells monolayers were grown on cell culture inserts with 3.0 µm pores (BD Falcon, BD Biosciences) that were coated with collagen as noted previously. Pre-warmed modified DMEM (600 µl) was added to each well of a 24-well tissue culture plate (BD Biosciences). Collagen-coated inserts were aseptically placed into wells and bEND3 cells diluted in 200 µl pre-warmed

modified DMEM were added to each insert. Cells were incubated at 37°C in 5% $CO_2$ until confluent.

### 2.12.3 Measuring transendothelial electrical resistance across the monolayer

To determine the resistance across confluent bEND3 monolayers grown on permeable supports, TEER measurements in ohms (Ω) were taken using an epithelial voltohmmeter (EVOM2, World Precision Instruments) using an EndOhm-6 chamber. Prior to measuring resistance, the resistance across the tissue culture membranes without the presence of cells was measured to establish the blank reading. The value of this blank was subtracted from resistance readings across monolayers to determine true tissue resistance. TEER readings were taken prior to any manipulations ($T_0$) as well as after incubation was completed ($T_{16}$) to evaluate any significant changes in resistance, indicating changes in permeability (70).

### 2.12.4 Assessing paracellular transport of BSA

Prior to assessing the passage of BSA across a monolayer, a system was set up to ensure that BSA488 was able to move through an insert without any cells. Modified DMEM (600 µl) was added to each well of a 24-well plate and a cell culture insert was aseptically added. BSA488 diluted in modified DMEM (200 µl total volume) was added to the culture insert and the system was incubated at 37°C in 5% $CO_2$. Samples were taken from both the insert and well at different time points and were fluorometrically scanned with an excitation/emission wavelength of 497/520 nm using a multimode microplate reader (Varioskan™,

Thermo Electron Corp.) controlled by SkanIt® software, version 2.2. to assess the diffusion of BSA488 over time.

To ascertain if the bEND3 monolayers represent relatively impermeable barriers, medium from the apical side of confluent cells was replaced with 50 µl of 1.0 µg/µl BSA488 in 150 µl modified DMEM and incubated for 16hr at 37°C in 5% $CO_2$. Following incubation, media from both apical and basolateral sides of monolayers were collected and fluorometrically scanned. Any background fluorescence was subtracted and the percentage of BSA488 passing through the barrier was calculated.

**2.13 Uptake of LDLR-binding fragment of ApoE**

The ability of the LDLR-binding fragment of ApoE to be taken up by bEND3 cells was assessed by comparing the fluorescence of bEND3 cells incubated with either GFP or GFPApoE for 23 hr. Lysate from CHO cells expressing either GFP or GFPApoE was assessed as was medium collected from GFPApoE-expressing CHO cells. The GFPApoE-expressing CHO cells had been incubated with or without ammonium chloride (5 µM) and 1X Insulin-Transferrin-Selenium-A Supplement (Gibco). Briefly, 1 µ-Slide VI $^{0.4}$ ibiTreat cell microscopy chambers (ibidi, Germany) were incubated with collagen for 20 min to prepare the surface for bEND3 cells. Excess collagen was removed and bEND3 cells suspended in pre-warmed modified DMEM were added. The chambers were incubated at 37°C in 5% $CO_2$ for 90 min and modified DMEM medium was added to fill chamber halfway and cells were incubated until confluent.

When cells reached confluence, the medium was removed and 60 µl each of protein and modified DMEM were added. Cells were incubated at 37°C in

5% $CO_2$ overnight and assessed for fluorescence. Representative images were collected in a Zeiss Axiovert 200M fluorescence microscope using AxioVision 4.6 software with the appropriate filter sets.

**2.14 Passage of fusion proteins through *in vitro* blood brain barrier**

To assess the passage of fusion proteins, ASAApoE and TfASAV5, across *in vitro* blood brain barriers, bEND3 cells were grown to confluence on cell culture inserts in a 24-well plate as noted previously. TEER readings were taken across each insert ($T_0$) prior to manipulations. The fusion proteins, TfASAV5 and ASAApoE, as well as the control protein, ASAV5, were diluted in modified DMEM and matched for enzyme activity. The existing medium was removed from each insert (apical side), the diluted proteins were applied to the apical side of the monolayers, and cells were incubated for 16hr at 37°C in 5% $CO_2$. Following incubation, the media from both the apical and basolateral sides of the monolayers were collected and assessed for arylsulfatase A activity and the percentage of enzyme activity passing through the monolayer was calculated.

# Chapter 3 – Results

## PART 1 LENTIVIRAL VECTOR PREPARATION

### 3.1.1 Polymerase chain reaction

The first step in the construction of fusion proteins was the generation of *att*-flanked PCR products by amplifying target DNA with primers containing *att* sites. The 17-amino acid sequence of murine cDNA from C57B16 mice corresponding to the LDLR-binding region of ApoE was amplified and yielded PCR fragments corresponding to the expected length of 115 bp. Amplification of V5-epitope tagged full-length ASA from pLenti6.3-v5GW-asaV5 and of eGFP from peGFP-N1 yielded fragments corresponding to the expected lengths of 1654 bp and 781 bp, respectively (Figure 3.1).

### 3.1.2 Creating entry clones

Purified PCR products were used in BP recombination events that inserted the DNA of interest into donor vectors to generate entry clones. These clones were subsequently used to transform One Shot® Mach1™ T1R Competent *E.coli*. Transformed cells grew in the presence of kanamycin, indicating successful uptake of target DNA in conjunction with the displacement of the *ccd*B gene that inhibits cell growth (see Chapter 2, Figure 2.4). Entry clone DNA (pDNA) was miniprep isolated from transformed colonies and sequenced to verify accuracy in BP recombination.

Following sequencing, pDNA was midiprep isolated from colonies and the quality and quantity of the entry clones were analyzed by spectrophotometry. For all midiprep-isolated pDNA, the absorbance ratio 260/280 was 1.91-1.94 and the absorbance ratio 260/230 was 2.2-2.3, indicating relatively pure DNA. The

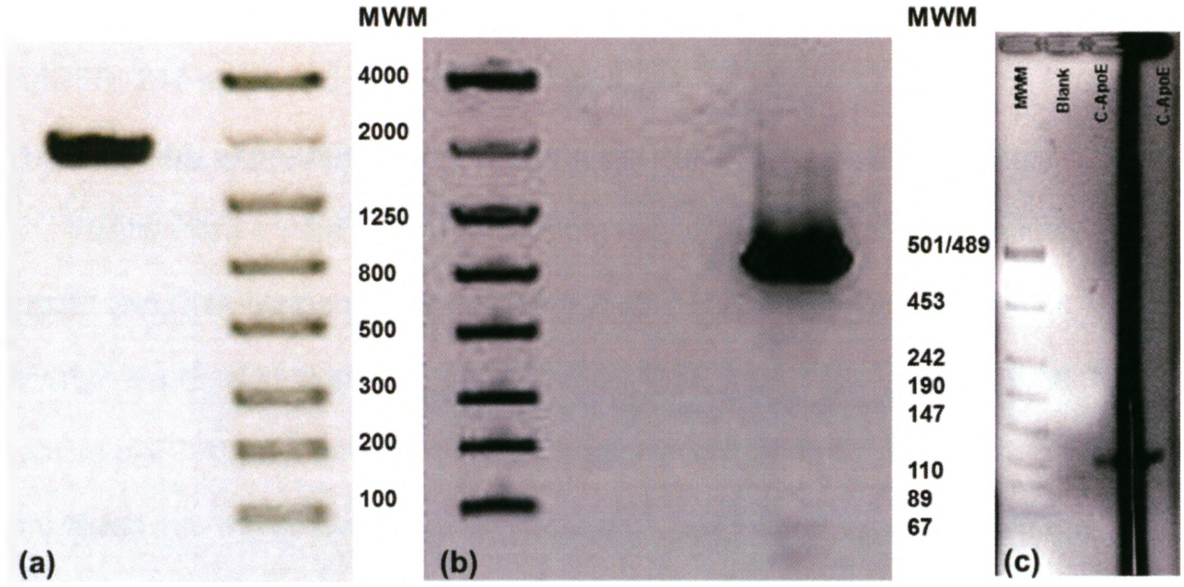


**Figure 3.1** Gel electrophoresis of PCR amplicons. DNA was PCR-amplified with primers designed with specific *att*-sites and purified for use in downstream recombination events. N-ASAV5 and N-eGFP PCR products were PEG-purified and C-ApoE amplicons were gel purified from 4% agarose. Analysis of N-ASAV5 amplicons yielded fragments with expected size of 1654 bp (a), N-eGFP amplicons returned fragments with the expected size of 781 bp (b) and C-ApoE amplicons generated fragments of 115 bp (c). N-ASAV5 and N-eGFP products were visualized on 1.2% agarose (FlashGel® system, Lonza). C-ApoE amplicons were visualized on 4% agarose stained with ethidium bromide.

concentration of entry clones was determined as follows: pNASA, 330 ng/µl; pNeGFP, 247 ng/µl; and pCApoE, 121 ng/µl.

### 3.1.3 Creating expression clones using pcDNA 6.2/V5-DEST vectors

Entry clones were used in LR recombination events to simultaneously transfer two DNA elements into pcDNA 6.2/V5-DEST destination vectors to generate expression clones. pNASA and pCApoE were transferred together to produce pASAApoE expression clones and pNeGFP and pCApoE were transferred into the destination vector to create pGFPApoE expression clones. Following the LR reaction, expression clones were transformed into One Shot® Mach1™ T1R Competent *E. coli.* Plasmid DNA was miniprep-isolated and sequenced to verify each DNA element was inserted accurately (Figure 3.2). Transformed cells were positively selected in the presence of carbenicillin and pDNA was midiprep-isolated. The quality and quantity of the entry clones were analyzed by spectrophotometry. For midiprep-isolated pDNA, the absorbance ratio 260/280 was 1.88-1.91 and the absorbance ratio 260/230 was 2.19-2.25. The concentration of expression clones was determined to be 802 ng/µl for pASAApoE and 478 ng/µl for pGFPApoE.

### 3.1.4 Transfection of CHO cell lines with pASAApoE and pGFPApoE

Prior to transfection, pASAApoE and pGFPApoE and control vectors, pLvASAV5 and pLvGFP were linearized using restriction enzymes and yielded the expected fragments of ~8.5 kb for pLvGFP, ~9.0 kb for pLvASAV5, ~6.0 kb for pGFPApoE, and ~7.0 kb for pASAApoE (Figure 3.3).

Linearized plasmids were ethanol precipitated and analyzed for quality and quantity by spectrophotometry. The ratio of absorbance 260/280 (nm) ranged

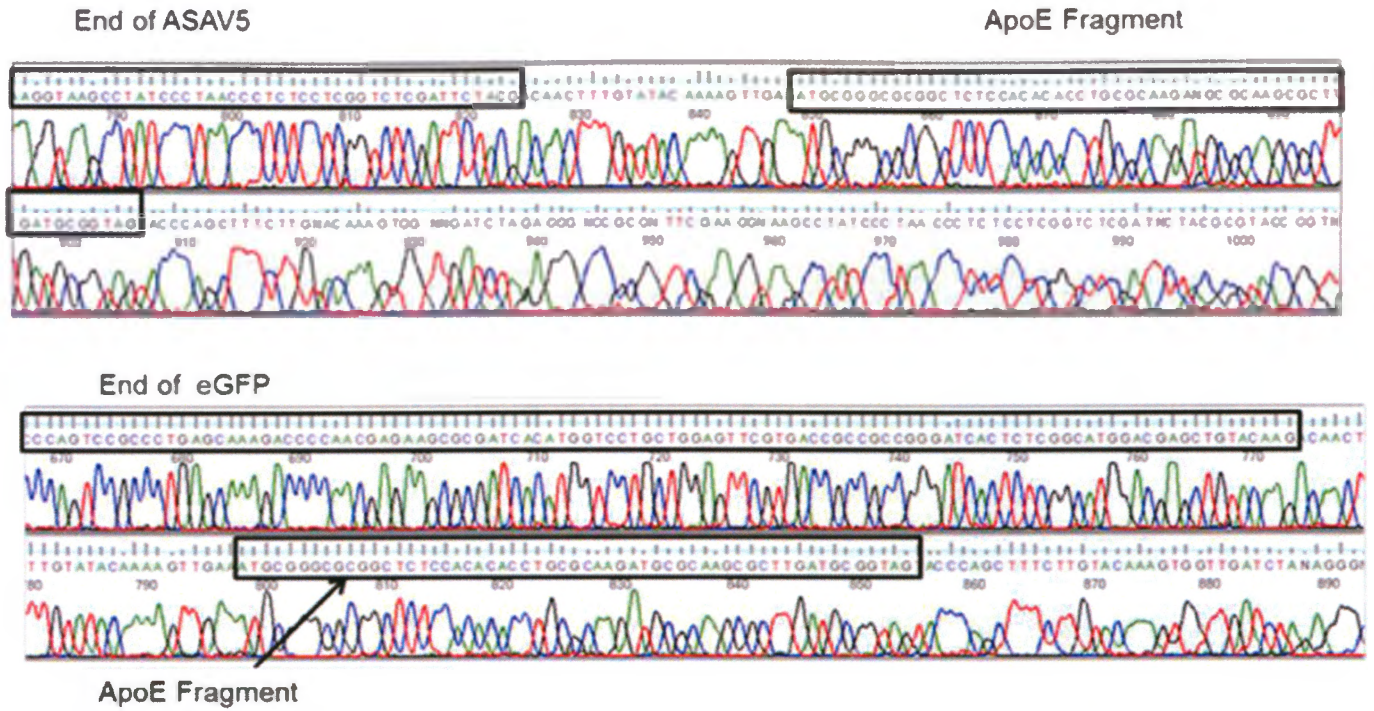


**Figure 3.2** DNA sequences of pcDNA6.2V5-DEST expression clones generated. DNA from two entry clones were simultaneously inserted into the destination vector, pcDNA6.2/V5-DEST. Tracings indicate proper insertion of DNA elements in the pASAApoE (top) and pGFPApoE (bottom) expression vectors. Boxes on tracings enclose the end of either the ASAV5 or eGFP sequences as well as the entire ApoE fragment.

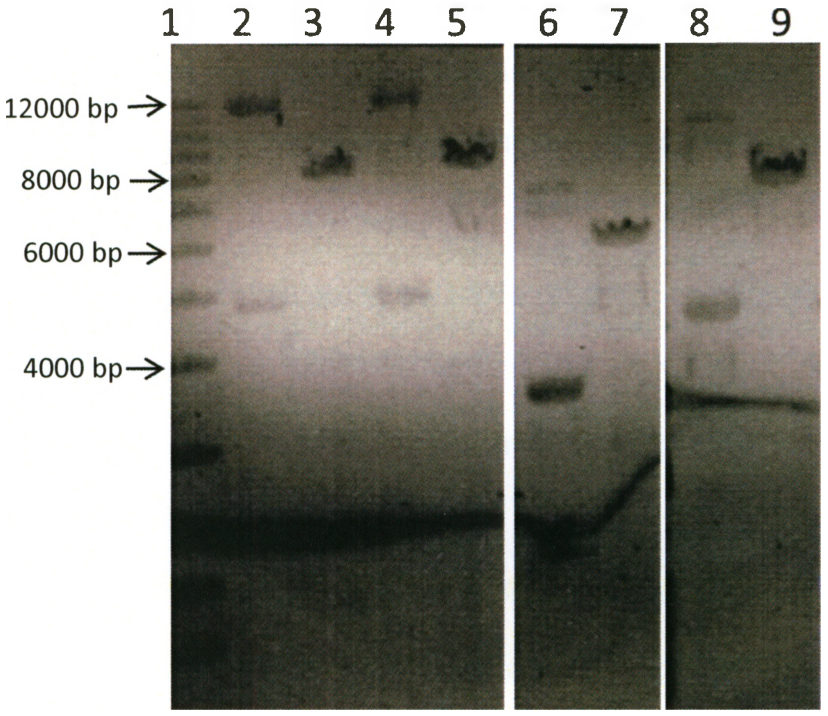


**Figure 3.3** Linearization of fusion constructs and control plasmids. Plasmids to be used in transfection experiments were linearized using restriction enzymes. Control plasmids pLvGFP (lane 3) and pLvASAV5 (lane 5) were cleaved with *Ssp*I to yield approximately 8.5 kb and 9.0 kb fragments, respectively. pGFPApoE (lane 7) and pASAApoE (lane 9) were cut with *Sap*I to generate approximately 6 kb and 7 kb fragments, respectively. Lane 1 contains molecular weight markers. Lanes 2,4,7,8 contain uncut plasmids pLvGFP, pLvASAV5, pGFPApoE, and pASAApoE, respectively. Fragments were electrophoresed on 0.8% agarose gel and visualized with ethidium bromide.

between 1.91-1.97 and absorbance 260/230 (nm) ranged between 1.00-1.48. The concentration of linearized plasmid was as follows: pLvGFP, 126 ng/µl ; pLvASAV5, 154 ng/µl; pGFPApoE 84 ng/µl; and pASAApoE, 148 ng/µl.

CHO cells were transfected with linearized plasmids using lipofectamine and after 48 hr, were placed under selective pressure using 3 µg/ml blasticidin in medium. After 11 days, no non-transfected (mock transfected) cells were viable.

### 3.1.5 Detection of recombinant fusion proteins expressed in transfectants

#### 3.1.5.1 Transient transfectants

Within 48 hr of performing the transfections, medium was collected for enzyme assays and cells expressing GFP and GFPApoE were assessed via fluorescence microscopy. GFP was distributed throughout the entire cell but GFPApoE appeared to be localized in more discrete areas of the cells (Figure 3.4). Also, fewer cells expressed GFPApoE compared to the number of cells expressing GFP and the cells were morphologically different with more rounding of the GFPApoE cell line (data not shown).

Enzyme activity in medium collected from transiently transfected CHO cells was compared to the endogenous enzyme activity in naïve CHO cell medium. Assays were performed in duplicate for 48 hr at 4°C. Enzyme activity was calculated by dividing Abs516 reading by the nanomolar extinction coefficient for pNCS (0.012) and expressed in nmol/hr/ml. There was a 7.6-fold increase in enzyme activity expressed as nmol/hr measured in medium collected from cells transfected with pLvASAV5 and greater than a 5.5-fold increase in enzyme activity (nmol/hr) in medium from cells transfected with pASAApoE compared activity in medium from in naïve CHO cell (Figure 3.5)

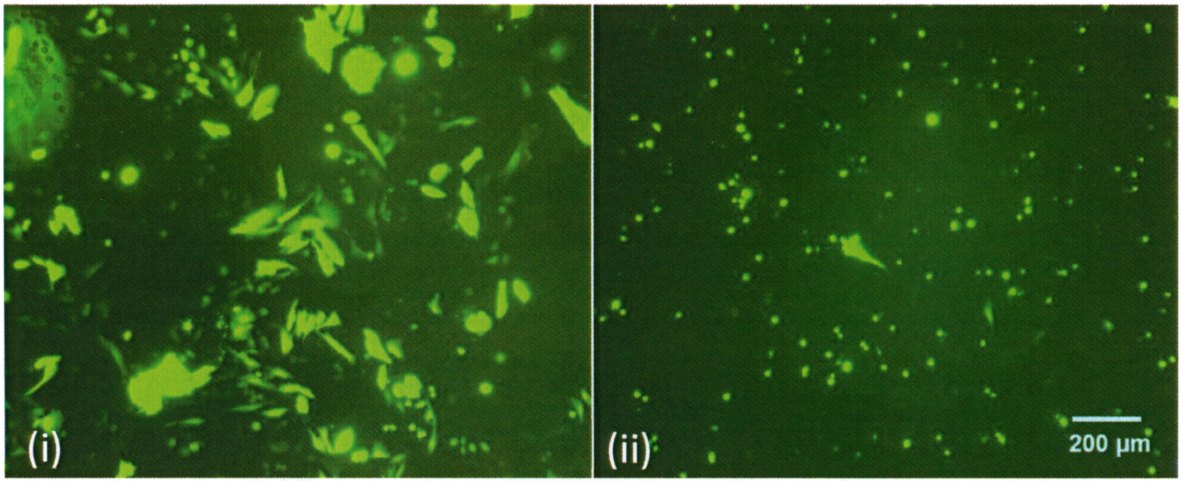


**Figure 3.4** Fluorescence in transient transfectants. CHO cells were assessed 48 hours after transfection for expression of GFP and GFPApoE. Images were taken at 200X magnification with a Leica DMIRB fluorescence microscope with a QImaging Retiga 1300 camera using appropriate filters. CHO cells were transfected with control plasmid, pLvGFP (i) and the expression clone, pGFPApoE(ii).

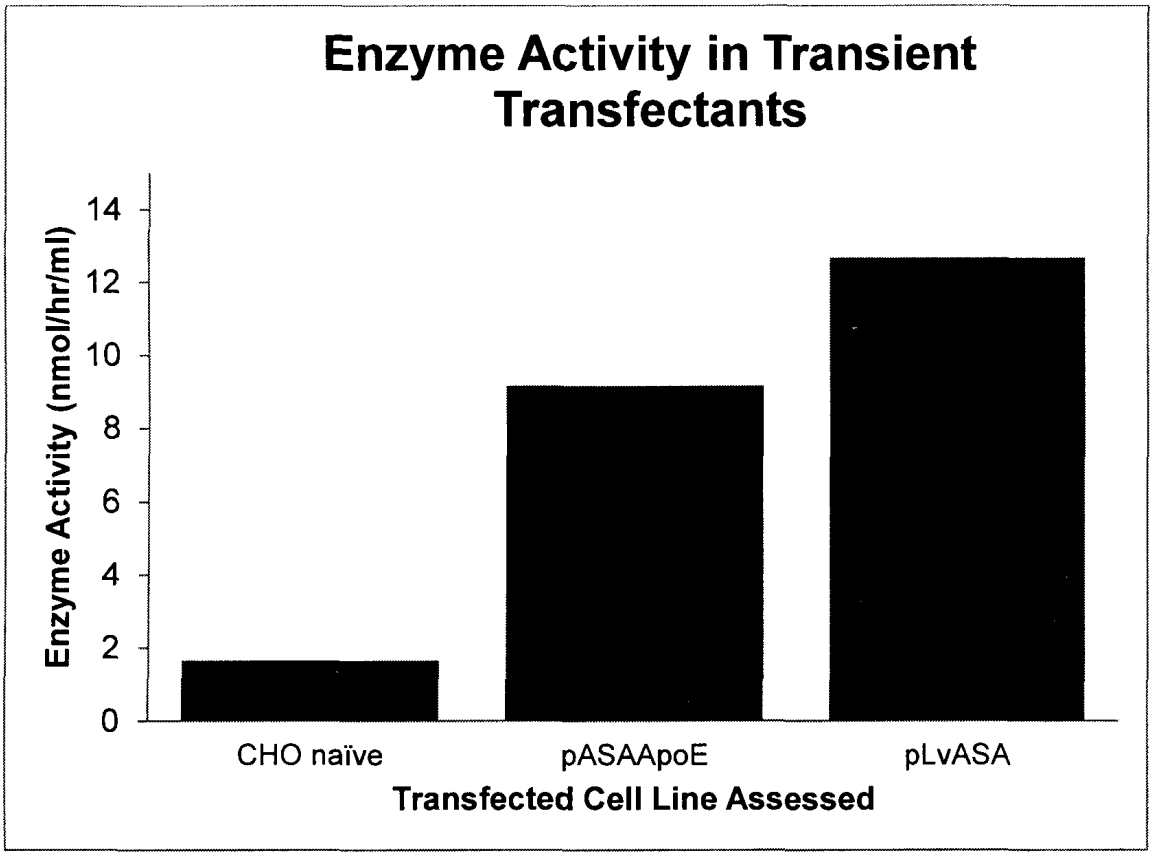


**Figure 3.5** Enzyme activity in transient transfectants. Medium from non-transfected (naïve) cells and cells transiently transfected with control plasmid, pLvASA and the expression clone, pASAApoE was assessed 48 hours after transfection for enzyme activity. Each cell culture was grown to similar levels of confluence prior to the assessment and assays were performed at 4°C for 48 hr. Samples were analyzed spectrophotometrically using a multimode microplate reader (Varioskan™, Thermo Electron Corp.) and absorbance values (516 nm) converted nmol/hr/ml activity.

### 3.1.5.2 Stable transfectants

Once stable transfectants were established, medium was collected and assayed for enzyme activity and cells expressing fluorescent proteins were assessed using fluorescence microscopy.

Under fluorescence microscopy, stable transfected CHO cells expressing either GFP or GFPApoE could be visualized. The number of cells expressing protein was significantly lower in the GFPApoE cell line. These cells appeared smaller and typically had a more rounded morphology similar to that seen in the transiently transfected cells (Figure 3.6).

Enzyme activity in stable transfected CHO cells was assessed as described in the subsection above with some minor changes: assays were done in quadruplicate over 72 hr at 4°C. The enzyme activity was 1.94 nmol/hr/ml in medium from cells transfected with pASAApoE and 477.43 nmol/hr/ml in medium collected from cells transfected with pLvASAV5 compared to enzyme activity of 0.31 nmol/hr/ml in medium collected from CHO cells not expressing ASAV5 (Figure 3.7).

### 3.1.6 Generating lentiviral expression plasmid

To increase the stability and expression levels of fusion proteins, lentiviral expression plasmids were generated using the entry clones created previously in section 3.2. pLvASAApoE and pLvGFPApoE expression clones were isolated from transformed cells and sequenced to verify each DNA element was inserted accurately (Figure 3.8).

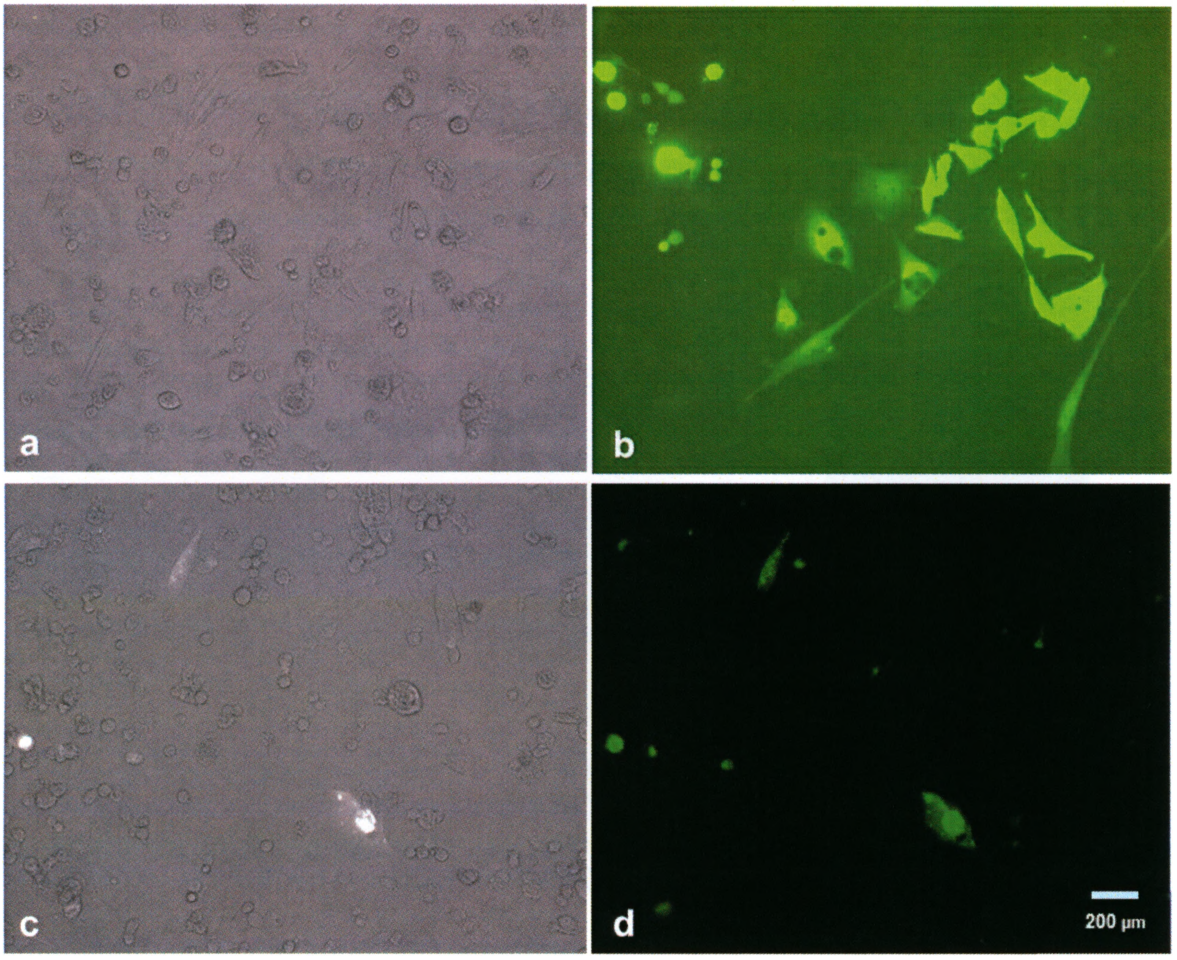


**Figure 3.6** Fluorescence in stable transfected cells. Cells were transfected with plasmids encoding either GFP(a,b) or GFPApoE (c,d). Fluorescence appears well distributed in GFP-expressing cells (b) but is expressed in discrete areas in cells expressing GFPApoE (d). Phase contrasts (a,c) and fluorescence images (b,d) were taken at 200X magnification with a Leica DMIRB fluorescence microscope equipped with a QImaging Retiga 1300.

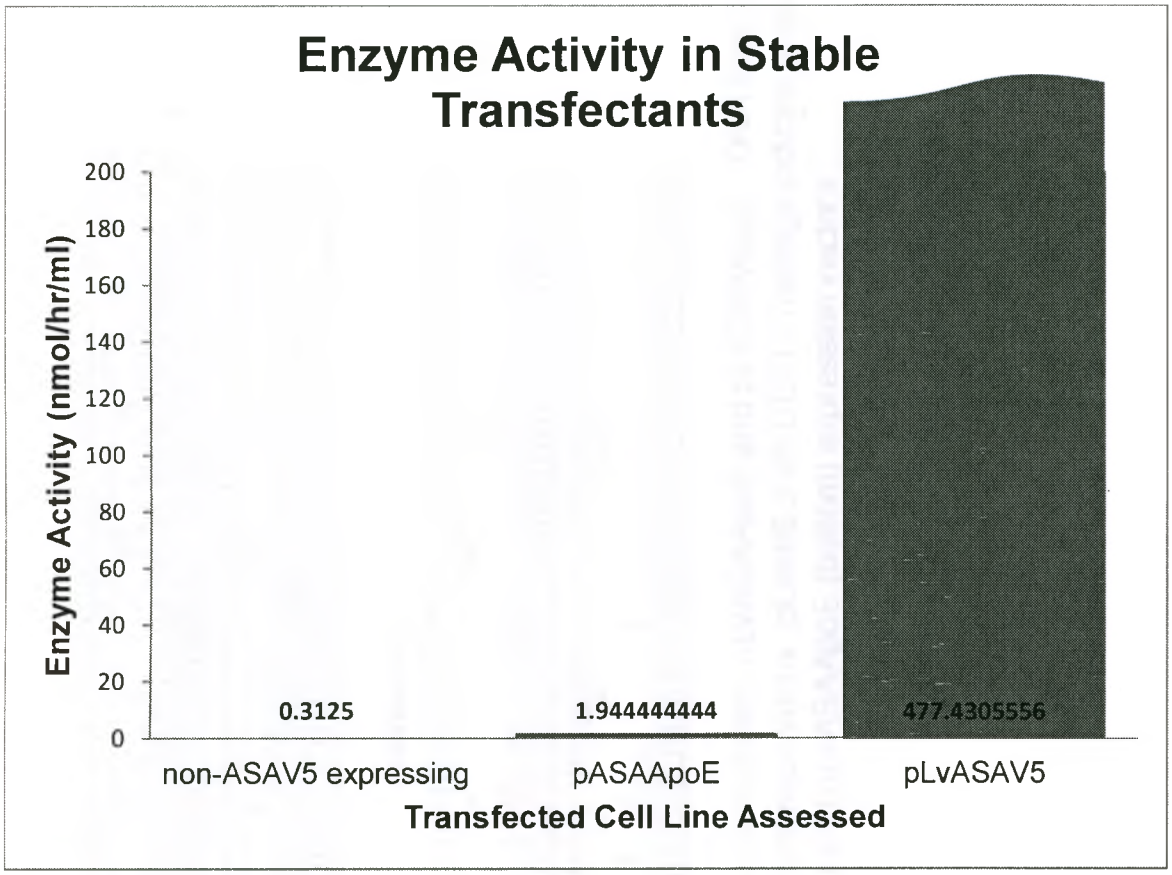


**Figure 3.7** Enzyme activity in stable transfectants. Medium from CHO cells without ASA expression, stable transfected cells transfected with control plasmid, pLvASAV5 and the expression clone, pASAApoE was assessed for enzyme activity. Assays were performed at 4°C for 72 hr. Samples were analyzed spectrophotometrically using a multimode microplate reader (Varioskan™, Thermo Electron Corp.) and absorbance values (516 nm) converted to nmol/hr/ml activity.

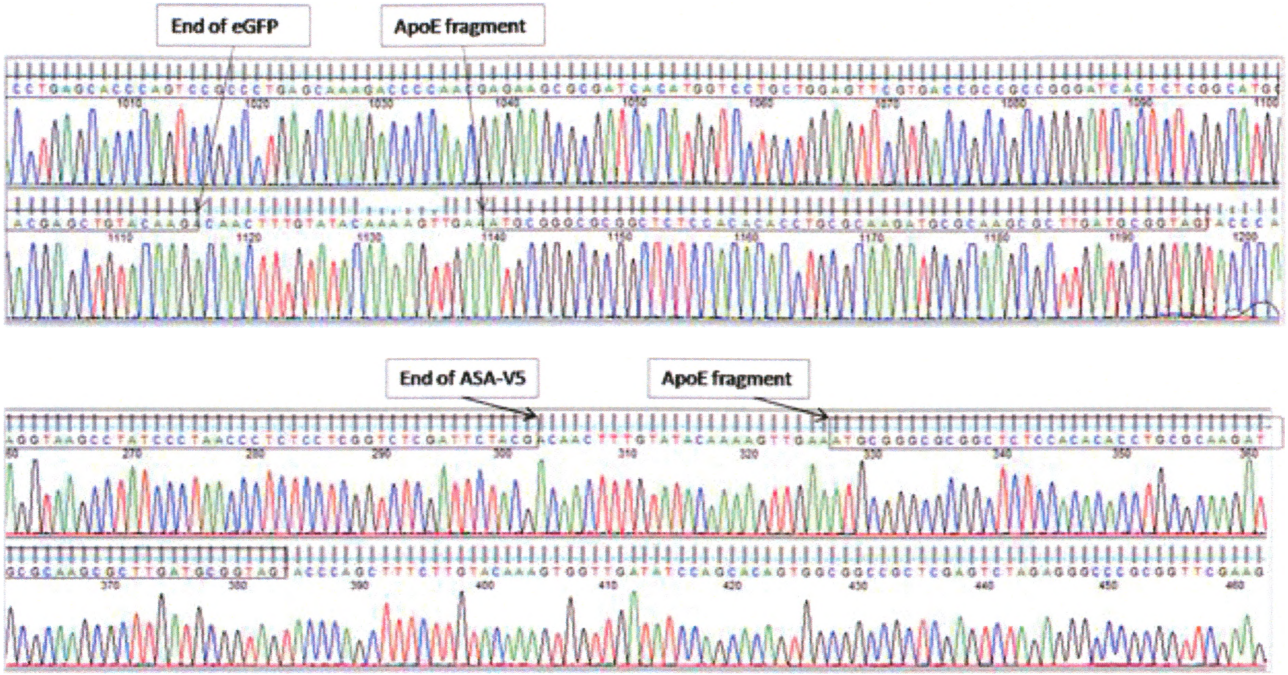


**Figure 3.8** DNA sequences of lentiviral-based expression clones, pLvASAApoE and pLvGFPApoE. DNA from two entry clones was simultaneously inserted into the destination vector, pLenti6.3/V5-DEST. Tracings indicate proper insertion of DNA elements in the pLvGFPApoE (top) and pLvASAApoE (bottom) expression vectors.

### 3.1.7 Restriction enzyme analysis of pLenti

Analysis of pLenti DNA digested by *AflII* and *XhoI* appeared to yield the expected fragments of 3600 bp, 3175 bp, and 1725 bp for pLvGFPApoE and 3750 bp, 3625 bp, 1725 bp, and 198 bp for LvASAApoE (Figure 3.9). The quality and quantity of the expression clones were analyzed by spectrophotometry. The absorbance ratio 260/280 was 1.92 for both clones and the absorbance ratio 260/230 was 2.28-2.30. The concentration of expression clones was determined to be 835 ng/µl for pLvASAApoE and 761 ng/µl for pLvGFPApoE.

### 3.1.8 Lentivirus production

pLvASAApoE and pLvGFPApoE were each cotransfected with a viral packaging mix into the 293FT producer line, producing replication incompetent lentiviral stocks. The titer of each lentivirus was determined and the titer was determined to be $5.5 \times 10^5$ TU/ml for LvASAApoE and $3.4 \times 10^5$ TU/ml for LvGFPApoE (Figure 3.10).

### 3.1.9 Transducing CHO cells with lentivirus

CHO cells were transduced with either LvASAApoE or LvGFPApoE with a multiplicity of infection (MOI) of ~1 and a mock transfected set of cells was included. Cells were placed under selective pressure using 3 µg/ml blasticidin and after 13 days no mock transfected cells were viable.

The medium from confluent ASAApoE-transduced cells was collected 24 hr after transduction and exhibited enzyme activity of 169 nmol/hr/ml. Compared to the activity in stable transfectants (1.9 nmol/hr/ml), transduced cells demonstrated an 80-fold increase in enzyme activity (Figure 3.11).

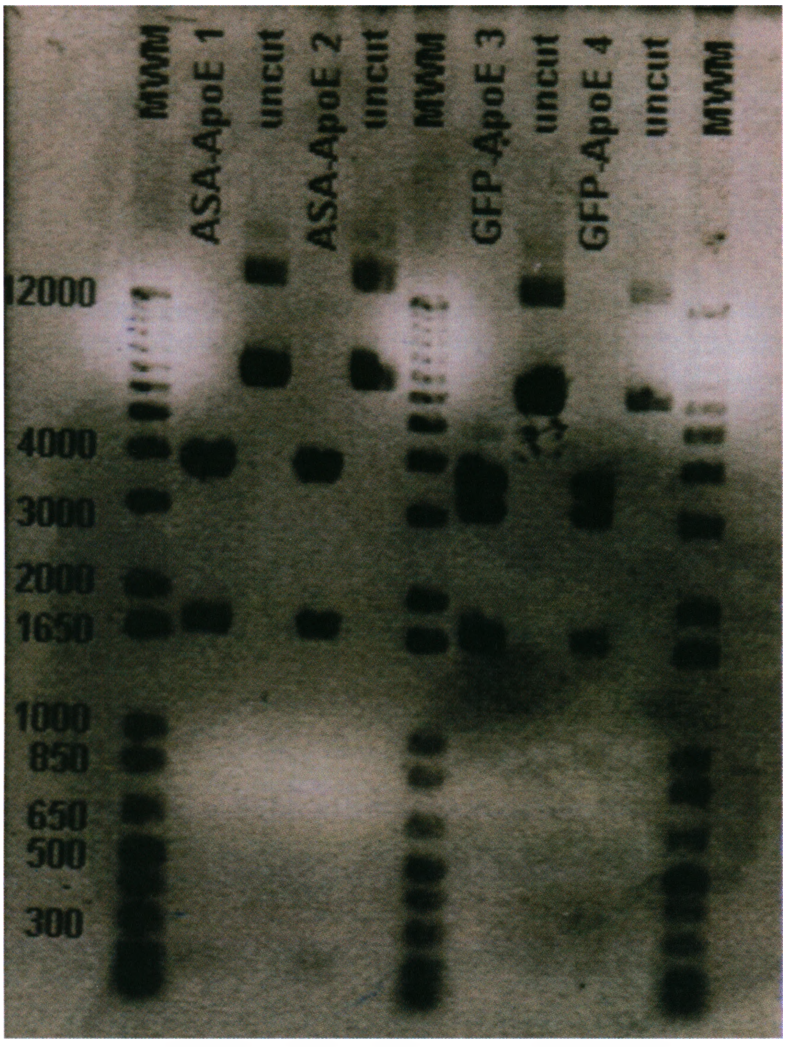


**Figure 3.9** Restriction digestions of lentiviral-based plasmids (pLvDNA). To verify that no rearrangement had occurred in the LTR regions of plasmid, pLvASAApoE and pLvGFPApoE were digested with endonucleases *Xho*I and *Afl*II. Digestion of pLvASAApoE (lanes 2, 4) indicates expected bands at ~3750 bp, ~3635 bp, ~1725 bp, and ~198 bp. Undigested plasmid is shown in lanes 3 and 5. Digestion of pLvGFPApoE (lanes 7, 9) indicates expected bands of ~3600 bp, ~3175 bp, and ~1725 bp. Undigested pLvGFpApoE plasmid is shown in lanes 8, 10. Lanes 1, 6, and 11 represent molecular weight markers. Aliquots of digested pLvDNA were electrophoresed on 0.8% agarose gel and visualized with ethidium bromide.

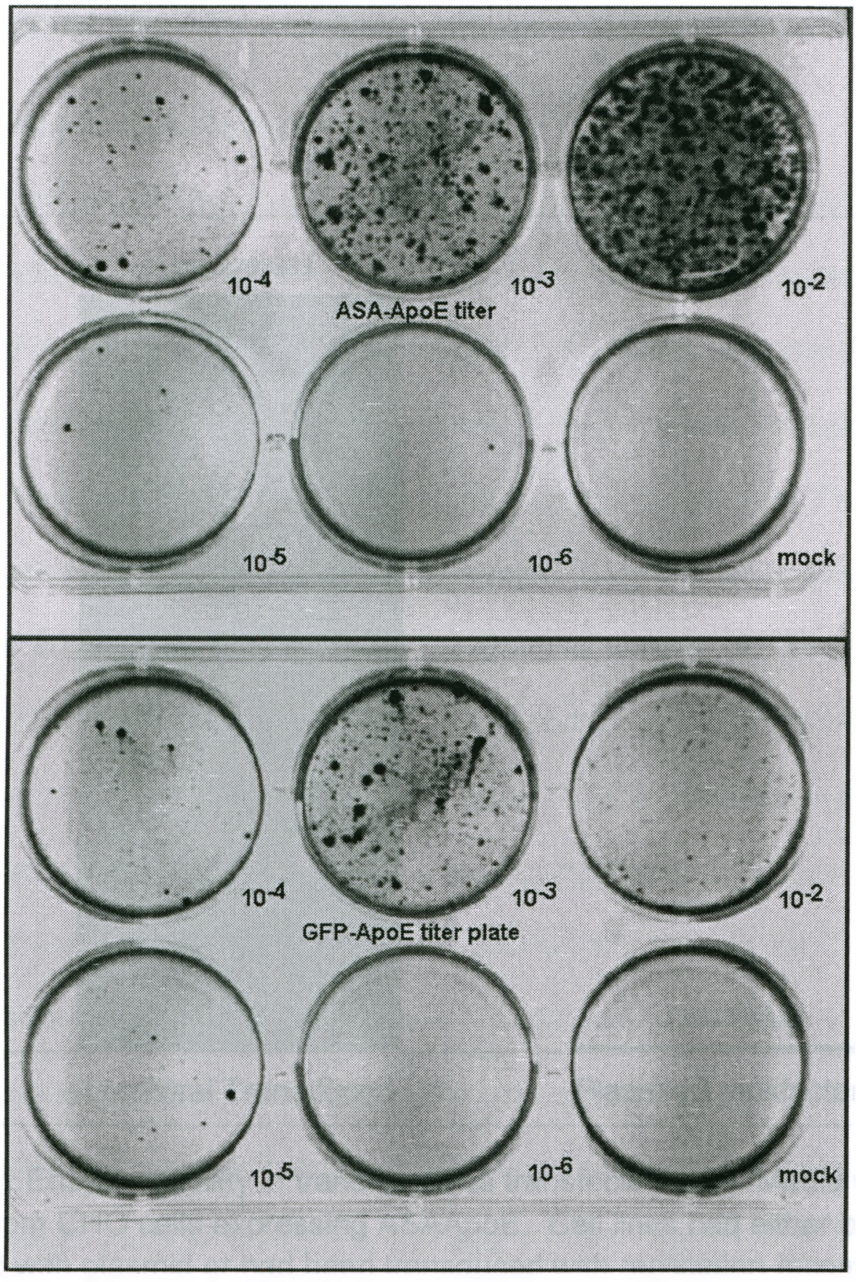


**Figure 3.10** Titer of lentiviral stocks. Titers were determined using CHO cells transduced with 10-fold serial dilutions of lentiviral supernatant ($10^{-2}$ to $10^{-6}$ dilutions) or untransduced (mock) cells. Cells were placed under Blasticidin selection (3 µg/ml) 48 hr after the transduction (day 2). On day 15, cells were fixed with 4% PFA and stained with crystal violet. Titer was determined to be 5.5 x $10^5$ TU/ml for LvASAApoE (top) and 3.4 x $10^5$ TU/ml for LvGFPApoE (bottom).

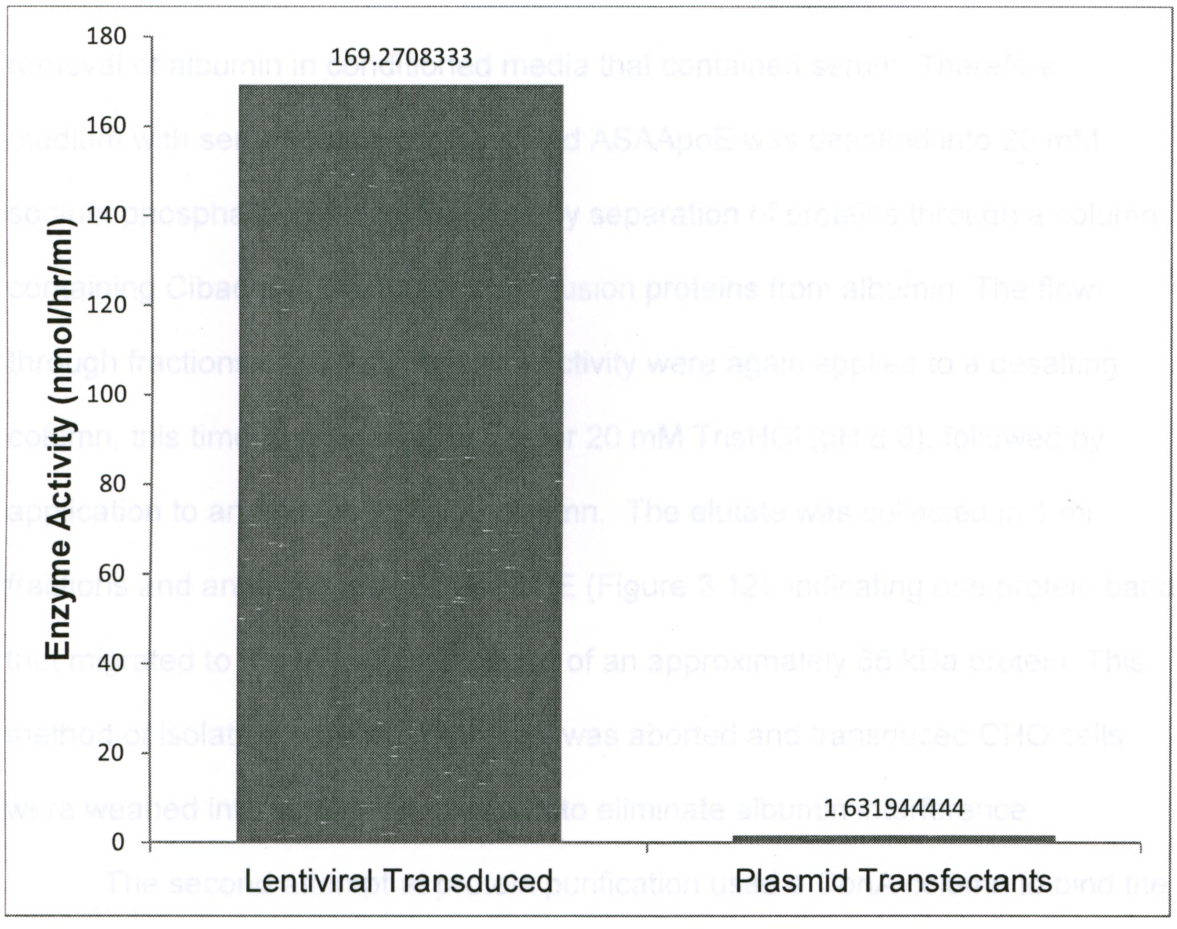


**Figure 3.11** Enzyme activity in transduced vs transfected cells. Media was collected from CHO cells expressing ASAApoE. Cell lines had either been transfected with plasmid or had been transduced with replication-incompetent lentivirus. Cell lines were at similar levels of confluence at the time of harvest and media was analyzed for enzyme activity using an absorbance wavelength of 516 nm and converted to nmol/hr/ml enzyme activity.

## PART 2 FUSION PROTEIN PURIFICATION AND CHARACTERIZATION

### 3.2.1 Collection of fusion proteins

The first set of steps in the collection of fusion proteins included the removal of albumin in conditioned media that contained serum. Therefore, medium with serum containing secreted ASAApoE was desalted into 20 mM sodium phosphate (pH 8.0), followed by separation of proteins through a column containing Cibacron Blue to separate fusion proteins from albumin. The flow-through fractions containing enzyme activity were again applied to a desalting column, this time to exchange buffer for 20 mM TrisHCl (pH 8,0), followed by application to an anion-exchange column. The elutate was collected in 1 ml fractions and analyzed with SDS-PAGE (Figure 3.12), indicating one protein band that migrated to the expected distance of an approximately 65 kDa protein. This method of isolating proteins, however, was aborted and transduced CHO cells were weaned into serum-free medium to eliminate albumin interference.

The second attempt at protein purification used a ConA column to bind the fusion proteins and separate them from albumin in the condition media that contained serum. Medium containing secreted ASAV5, TfASAV5, or ASAApoE was desalted into 20 mM TrisHCl as noted previously and applied to a ConA column. Under the conditions used, the enzyme-containing proteins were difficult to elute, stripping the column with 15 CV of 0.1 M borate buffer showed protein was still trapped in the column. This method was deemed impractical for the purpose at hand.

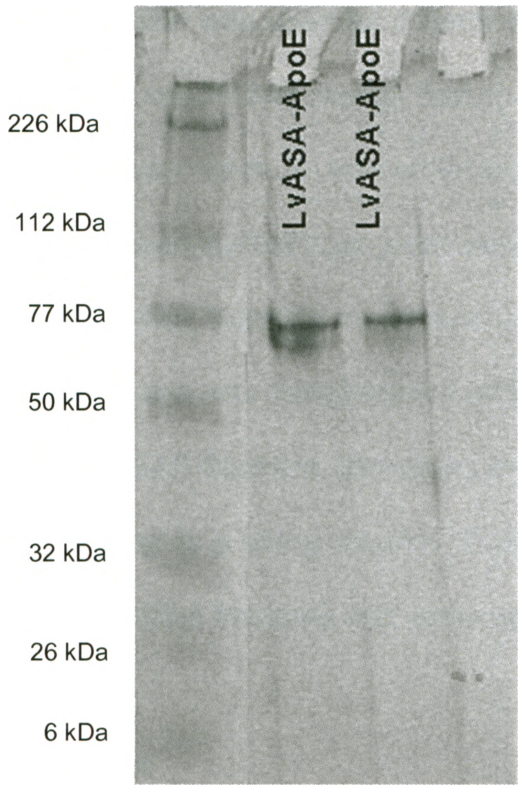


**Figure 3.12** Purification of ASAApoE using Cibacron blue F3G-A. Purifying the fusion proteins was complicated by the presence of albumin, a protein that is similar in size to ASA. To remove albumin, samples from cells expressing ASAApoE were applied to a HiTrap™ Blue HP column (GE Healthcare Life Sciences). The flow-through fractions containing enzyme activity were applied to a DEAE column. DEAE fractions having enzyme activity were pooled and analyzed using SDS-PAGE under reducing conditions with 12% polyacrylamide gel and silver-stained for visualization. Under these conditions, there is one clear band, indicating that the protein is ~65 kDa, the expected size of ASAApoE.

The third protocol for purification was used for collection of fusion proteins after the cells were weaned into serum-free media. Serum-free medium containing secreted proteins (crude medium) was collected and concentrated ~ 20-fold. Concentrated medium was loaded onto a desalting column to exchange medium for 20 mM TrisHCl (pH 8.0), followed by separation of proteins in an anion-exchange column. The eluate was collected in 1 ml fractions. To further purify ASAV5 and ASAApoE, DEAE fractions containing enzyme activity were pooled, concentrated, and applied to a sizing column. Eluted fractions were collected in 0.48 ml fractions and the fractions with enzyme activity were pooled (Figures 3.13, 3.14, 3.15).

### 3.2.2 Analyzing fusion proteins

#### 3.2.2.1 Enzyme activity

All fractions collected from Part 2, section 3.2.1 were measured for ASA activity, absorbance (280 nm) and total protein content. The specific activity (S.A.) in nmol/hr/µg protein was calculated for each step in the purification process and the purification index assessed. An increase in S.A. was noted for each step in the purification process with the exception of DEAE fractions collected from the purification of ASAApoE. These fractions indicated a decrease in S.A. when compared to the calculated S.A. of the fractions collected from desalted media. TfASAV5 fractions collected following elution from the DEAE column indicated a 3.50-fold increase in specific activity purification from the crude medium prior, with a S.A. of 58.69 nmol/hr/µg protein. The S.A. of ASAV5 and ASAApoE fractions collected from the gel filtration column was 59.24 nmol/hr/µg protein and 26.34 nmol/hr/µg protein, respectively. There was a 7.30-

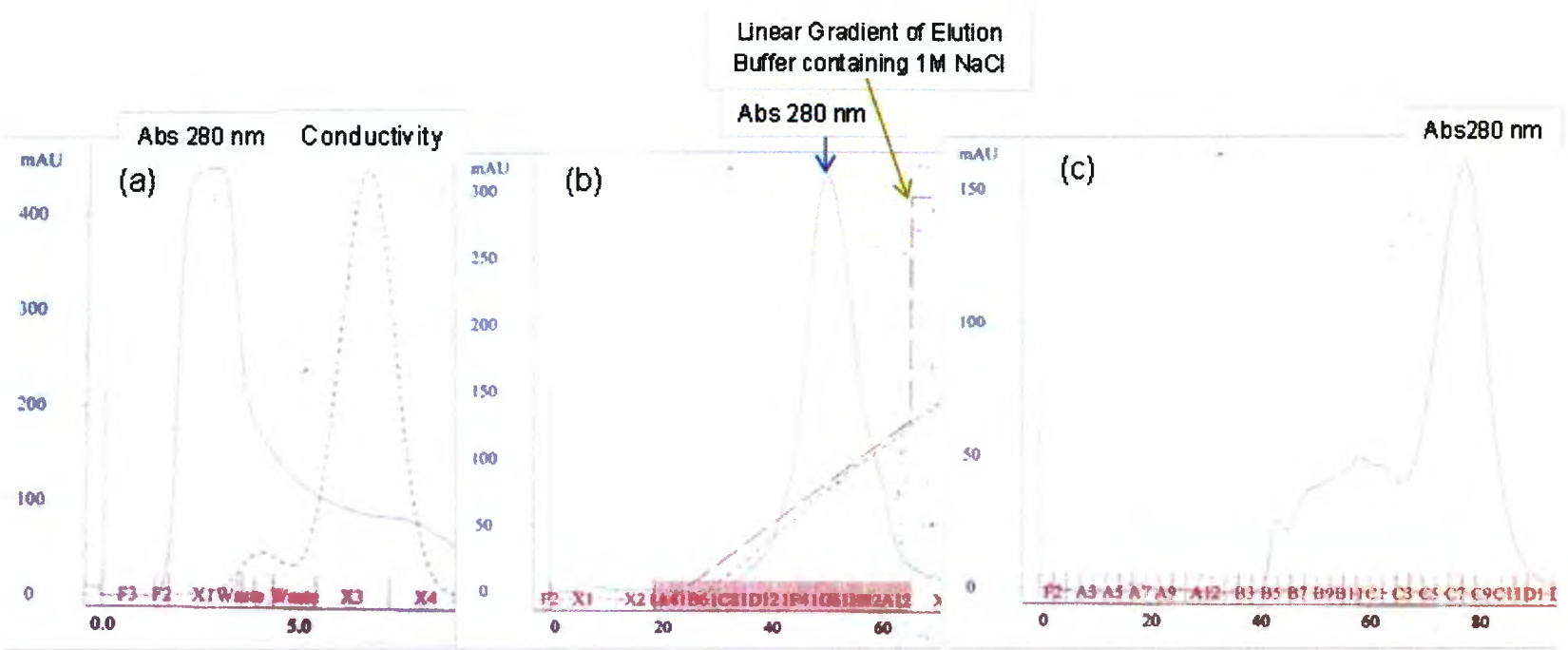


**Figure 3.13** Chromatograms from ASAApoE purification. Fast performance liquid chromatography (FPLC) with the ÄKTApurifier™ system (GE Healthcare) was used for purification. Fractions were monitored for absorbance (280 nm) and recorded in mAu. Media from transduced CHO cells expressing ASAApoE was collected from 75 cm2 flasks every 48-72 hr, filter-sterilized, and pooled. These pooled contents were concentrated and applied to a desalting column for buffer exchange into 20 mM TrisHCl, pH 8.0 (a). Desalted contents were applied to an anion-exchange column and proteins eluted using a linear gradient of elution buffer (20 mM TrisHCl, 1 M NaCl, pH 8.0) (b). Collected fractions having enzyme activity were pooled, concentrated, and applied to a sizing column. Collected fractions from the sizing columns that were positive for enzyme activity were pooled and stored at -20°C.

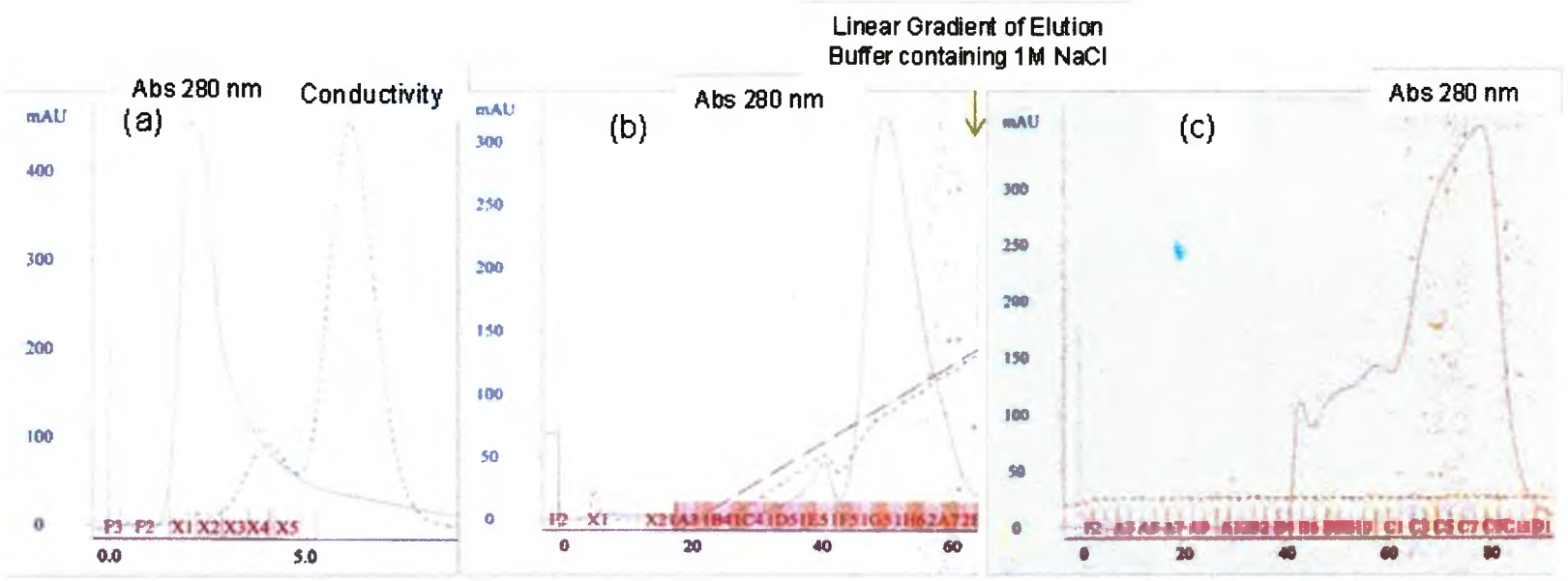


**Figure 3.14** Chromatograms from ASAV5 purification. Fast performance liquid chromatography (FPLC) with the ÄKTApurifier™ system (GE Healthcare) was used for purification of protein. Fractions were monitored for absorbance (280 nm) and recorded in mAu. Media from transduced CHO cells expressing ASAV5 was collected from 75 cm2 flasks every 48-72 hr, filter-sterilized, and pooled. These pooled contents were concentrated and applied to a desalting column for buffer exchange into 20 mM TrisHCl, pH 8.0 (a). Desalted contents were applied to an anion-exchange column and proteins eluted using a linear gradient of elution buffer (20 mM TrisHCl, 1 M NaCl, pH 8.0) (b). Collected fractions having enzyme activity were pooled, concentrated and applied to a sizing column. Collected fractions from the sizing columns that were positive for enzyme activity were pooled and stored at -20°C.

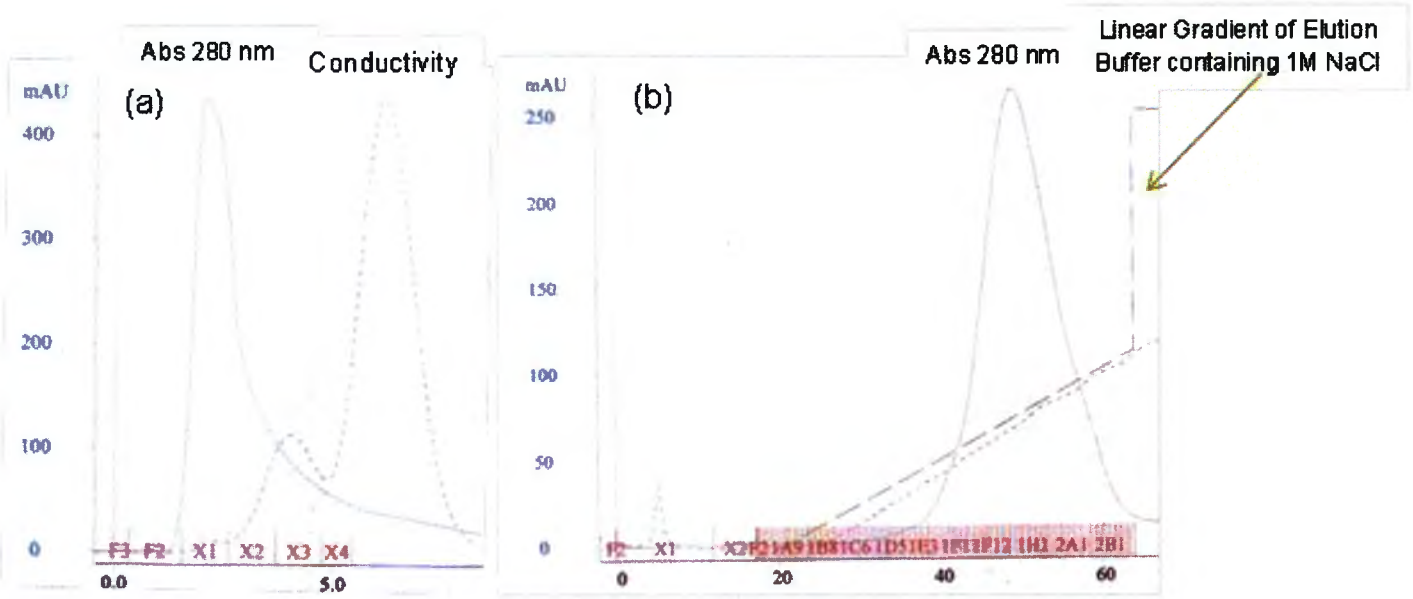


**Figure 3.15** Chromatograms from TfASAV5 purification. Fast performance liquid chromatography (FPLC) with the ÄKTApurifier™ system (GE Healthcare) was used for purification process. Fractions were monitored for absorbance (280 nm) and recorded in mAu. Media from transduced CHO cells expressing TfASAV5 was collected from 75 cm2 flasks every 48-72 hr, filter-sterilized, and pooled. These pooled contents were concentrated and applied to a desalting column for buffer exchange into 20 mM TrisHCl, pH 8.0 (a). Desalted contents were applied to an anion-exchange column and proteins eluted using a linear gradient of elution buffer (20 mM TrisHCl, 1 M NaCl, pH 8.0) (b). Collected fractions having enzyme activity were pooled and stored at -20°C

fold increase in purification for ASAV5 and 4.89-fold increase in purification for ASAApoE. (Table III)

### 3.2.2.2 Gel electrophoresis

Aliquots of ASAV5, ASAApoE, and TfASAV5 from fractions collected during the purification steps were analyzed by SDS-PAGE and silver stained for relative size of the protein and for relative purity. The sizing fractions collected from ASAApoE did not resolve into discrete bands but present as a smear between 47.7-77.6 kDa. Repeated attempts to resolve the sizing fractions into discrete bands were unsuccessful. The DEAE fractions collected and pooled from TfASAV5 resolved as a large, single band with the expected size of 140 kDa. Assessing the sizing fractions collected from ASAV5, there is one large band corresponding to the expected 62 kDa band expected and a second, smaller band resolves at ~ 40 kDa. (Figure 3.16)

### 3.2.2.3 Analyzing fluorescence

Live transduced CHO cells were analyzed using fluorescence microscopy to detect the expression of GFP and GFPApoE (Figure 3.17). Transduced CHO cells expressing GFP-ApoE and GFP were assessed using fluorescence microscopy to determine the intensity and location of GFP fluorescence. Whereas GFP appeared to be expressed evenly throughout the cell, GFPApoE appeared to be more localized within the cell body.

### 3.2.2.4 Glycosylation

TfASAV5, ASAApoE, ASAV5, and a control protein apo-transferrin (ApoTf) were incubated with (+) or without (-) PNGase F. Samples of each protein were loaded on 12% polyacrylamide gels, electrophoresed, and silver-stained. A

**Table III** Purification of Recombinant Proteins

| Protein | Step | Total volume in sample (ml) | Total Enzyme Activity (µmol/hr) | Specific Activity (µmol/hr/mg) | Yield[1] | Purification Factor[2] |
|---|---|---|---|---|---|---|
| ASAV5 | Enriched media | 8.20 | 186 | 8.32 | 100% | 1.0 |
| | Desalting column chromatography | 4.15 | 178 | 12.36 | 95% | 1.5 |
| | Ion exchange chromatography | 0.55 | 135 | 31.46 | 72% | 3.8 |
| | Gel Filtration | 1.92 | 117 | 59.94 | 63% | 7.2 |
| TfASAV5 | Enriched media | 10 | 363 | 16.79 | 100% | 1.0 |
| | Desalting column chromatography | 8.50 | 340 | 18.00 | 94% | 1.1 |
| | Ion exchange chromatography | 4.80 | 315 | 59.38 | 87% | 3.5 |
| ASAApoE | Enriched | 16.00 | 391 | 5.37 | 100% | 1.0 |
| | Desalting column chromatography | 9.50 | 362 | 5.98 | 93% | 1.1 |
| | Ion exchange chromatography | 1.20 | 332 | 6.26 | 85% | 1.2 |
| | Gel Filtration | 7.68 | 289 | 26.65 | 74% | 5.0 |

[1] Percent yield compares total enzyme activity resulting from each purification step to total enzyme activity in the starting material
[2] Purification factor compares specific activity of solution from each purification step to specific activity in the starting material

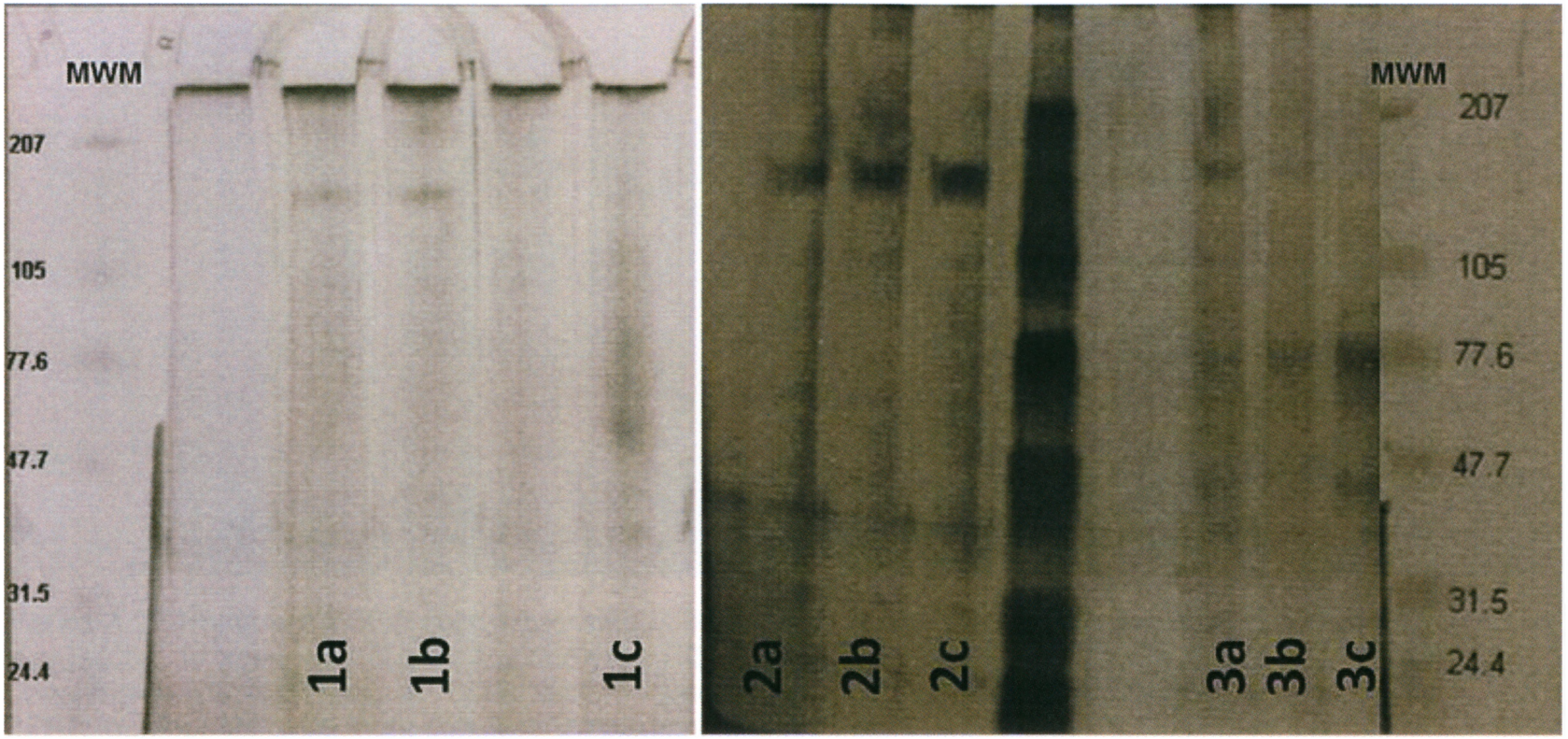


**Figure 3.16** SDS-PAGE analysis of proteins. Aliquots from each step of the purification schema were electrophoresed in a 12% polyacrylamide gel under reducing conditions and silver stained for visualization. Samples of ASAApoE in lanes 1a, 1b, 1c represent aliquots from crude media, pooled desalted fractions, and pooled sizing fractions (respectively). Lanes 2a, 2b, 2c represent aliquots from TfASAV5 crude media, desalted fractions, and DEAE pooled fractions, respectively. Samples of ASAV5 in lanes 3a, 3b, 3c represent samples from desalted fractions, DEAE pooled fractions, and pooled sizing fractions, respectively. The expected size of ASAApoE is ~ 65 kDa, ASAV5 is ~ 62 kDa, and TfASAV5 is expected to be ~ 140 kDa. No clear resolution of ASAApoE from sizing columns was obtained.

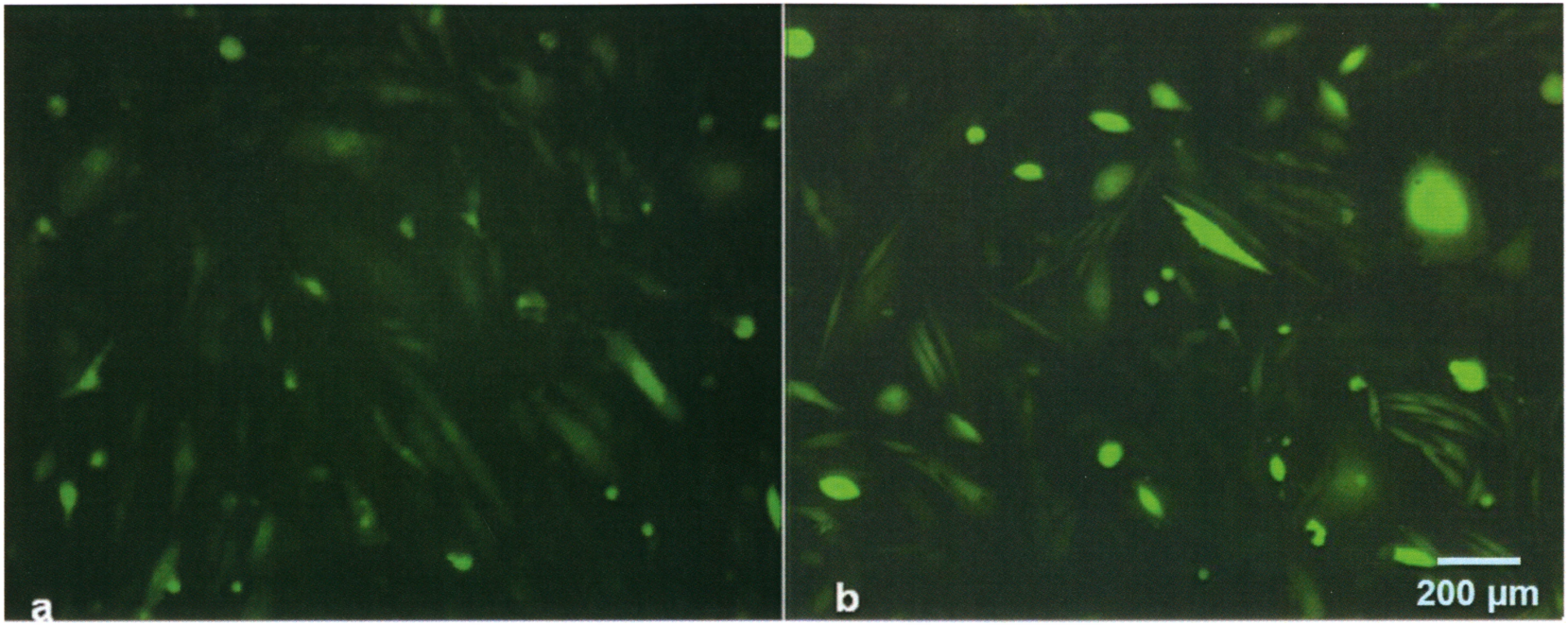


**Figure 3.17** Transduced CHO cells expressing GFPApoE (a) and GFP (b) were assessed using fluorescence microscopy. Images were obtained at 200X magnification using a Leica DMIRB fluorescence microscope with a QImaging Retiga 1300 camera. Whereas GFP appears to be expressed evenly throughout the cytosol (b), GFPApoE appears to be more compartmentalized within the cells.

downward shift in mobility was visible in samples of ApoTf, TfASAV5, and ASAV5 that had been incubated with PNGase F compared to the same proteins not incubated with PNGase F, indicating the removal of N-linked carbohydrate. Samples of ASAApoE resolved as a smear, with no discrete bands observed regardless of the presence or absence of PNGase F. (Figure 3.18)

## PART 3 BLOOD BRAIN BARRIER MODEL EXPERIMENTS

### 3.3.1 Generating an *in vitro* BBB

bEND3 cells grew on collagen-coated cell culture inserts in the presence of modified DMEM. After approximately 48 hr of incubation, cells were of suitable confluence to assess both the electrical resistance of the monolayer as well as the ability of proteins to cross the layer.

### 3.3.2 Measuring transendothelial electrical resistance (TEER) across the monolayer

To assess resistance across the monolayer over time, measurements were taken prior to starting any experimentation ($T_0$) and upon completion of experimentation ($T_{16}$). Readings were corrected for the background resistance encountered by the cell culture insert (11 Ω) and standard deviations calculated. No significant change in TEER was observed and the average TEER at $T_0$ was 53.96 +/- 3.77 Ω and at $T_{16}$ was 52.71 +/- 5.58 Ω (Figure 3.19).

### 3.3.3 Assessing paracellular transport of BSA488

A standard curve was produced comparing the concentration of BSA488 to relative fluorescence units and the slope of the curve was calculated to be

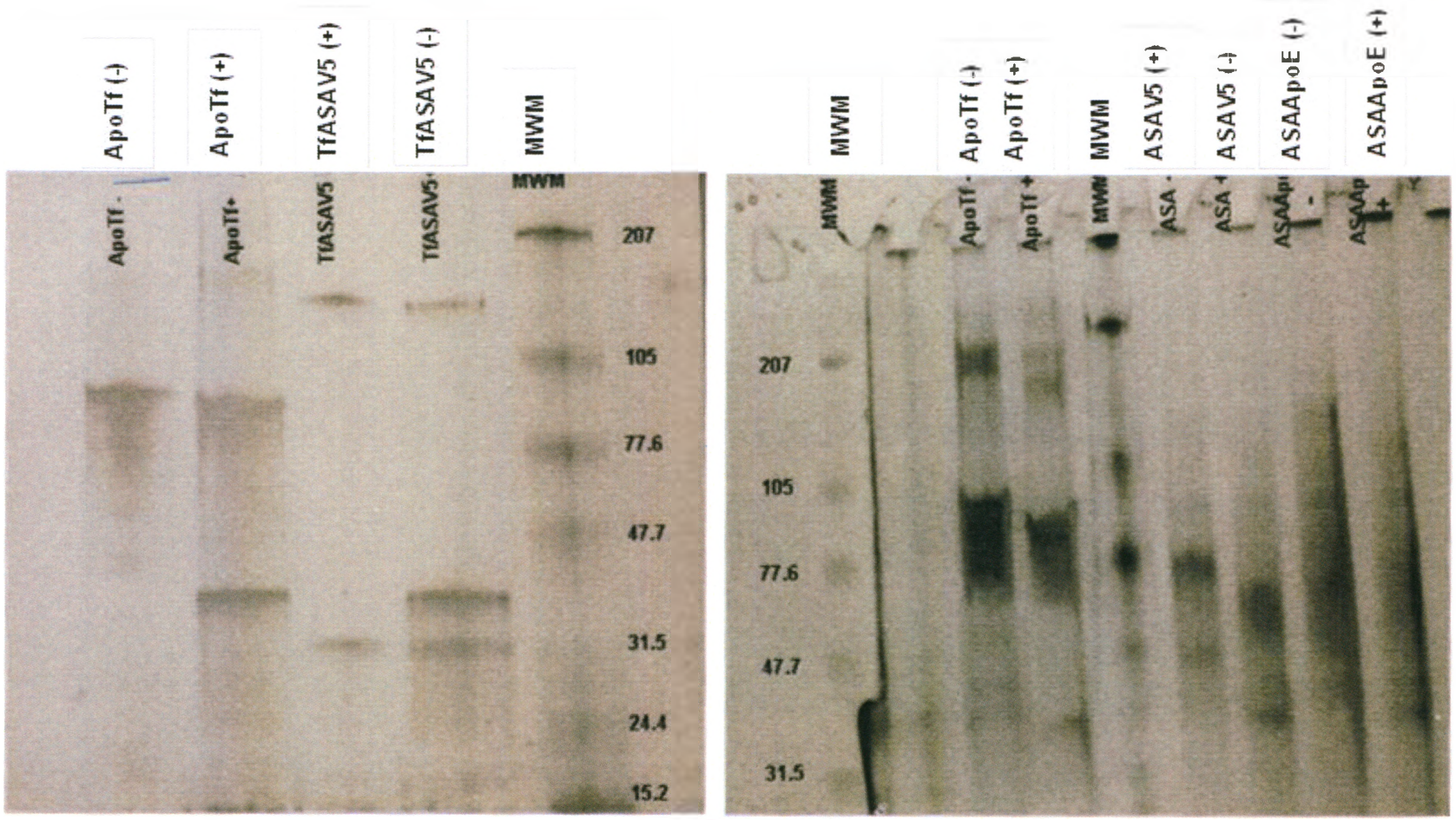


**Figure 3.18** Release of N-linked oligosaccharides by PNGase F. Fusion proteins and a control glycoprotein, apo-transferrin (ApoTf), were incubated with (+) or without (-) PNGase F for 1hr at 37°C. Samples were subjected to 12% SDS-polyacrylamide gel electrophoresis and silver-stained for visualization. The control protein displayed a downward shift in protein mobility after treatment with PNGase F. A similar shift is also seen in PNGase F-treated TfASAv5 and ASAV5. Samples of ASAApoE did not resolve into discrete bands.

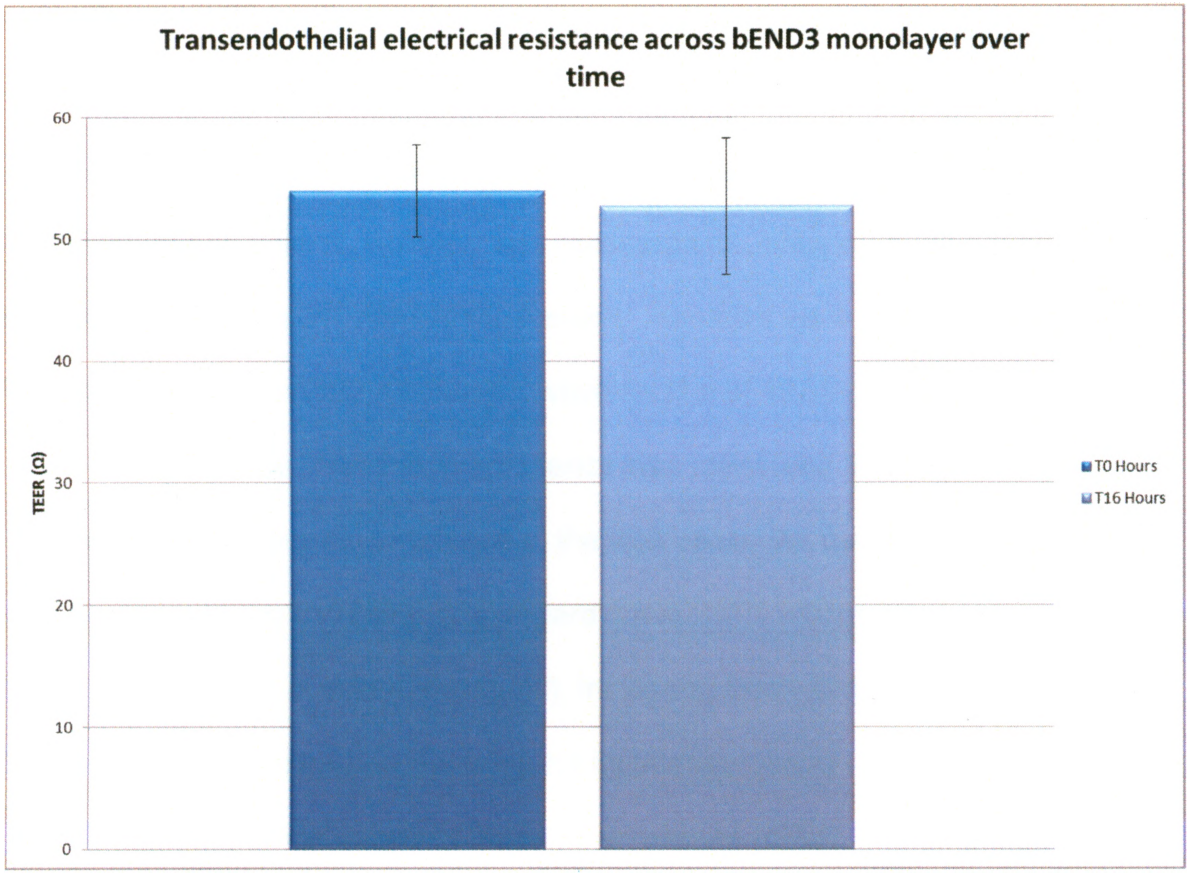


**Figure 3.19** TEER readings across bEND3 monolayers. After 16 hr of exposure to proteins, there was no significant decrease in TEER readings across bEND3 monolayers. Transendothelial electrical resistance across the monolayer was measured prior to any manipulation ($T_0$, left) and measured again after 16 hr ($T_{16}$, right) of exposure to ASAV5, ASAApoE, and TfASAV5. Numbers were corrected for background resistance and standard deviation calculated. (n=24)

y = 0.8606x + 28.694. Concentrations between 25-750 µg/ml were measurable within the curve (Figure 3.20, top).

To ensure that proteins were capable of diffusing through the membrane of the cell culture inserts, BSA488 was measured for diffusion across the membrane without a cell monolayer present. Samples were scanned for fluorescence with excitation/emission wavelengths of 497/520 nm. Over the period of 6.5 hr, a decrease in fluorescence was measured in the cell culture insert with a corresponding increase in the well below the membrane (Figure 3.20, bottom). Using the slope of standard curve, RFU readings were converted to the concentration of BSA488 (mg/ml), indicating that ~20% of the BSA488 diffused across the membrane during the incubation period.

To assess the passage of BSA488 across the bEND3 monolayer, samples of 50 µg of BSA488 were diluted in modified DMEM and applied to the apical sides of bEND3 monolayers (n=8). After 16 hr of incubation, the medium was removed from both the apical and basolateral sides of the membrane and the passage of protein was calculated. The average RFU/ml on the apical side after 16 hr was 1201.61 +/- 83.48 and on the basolateral side was 39.18 +/- 3.30. Under these conditions, 3.16% of the BSA488 translocated across the monolayer (Figure 3.21).

### 3.3.4 Uptake of LDLR-binding fragment of ApoE

To assess the ability of the ApoE peptide to facilitate uptake of protein into bEND3 cells, lysate from GFP-expressing CHO cells and lysate and medium from GFPApoE-expressing CHO cells were applied to bEND3 cells and incubated for 23 hr. Fluorescence was seen in discrete areas of cells incubated

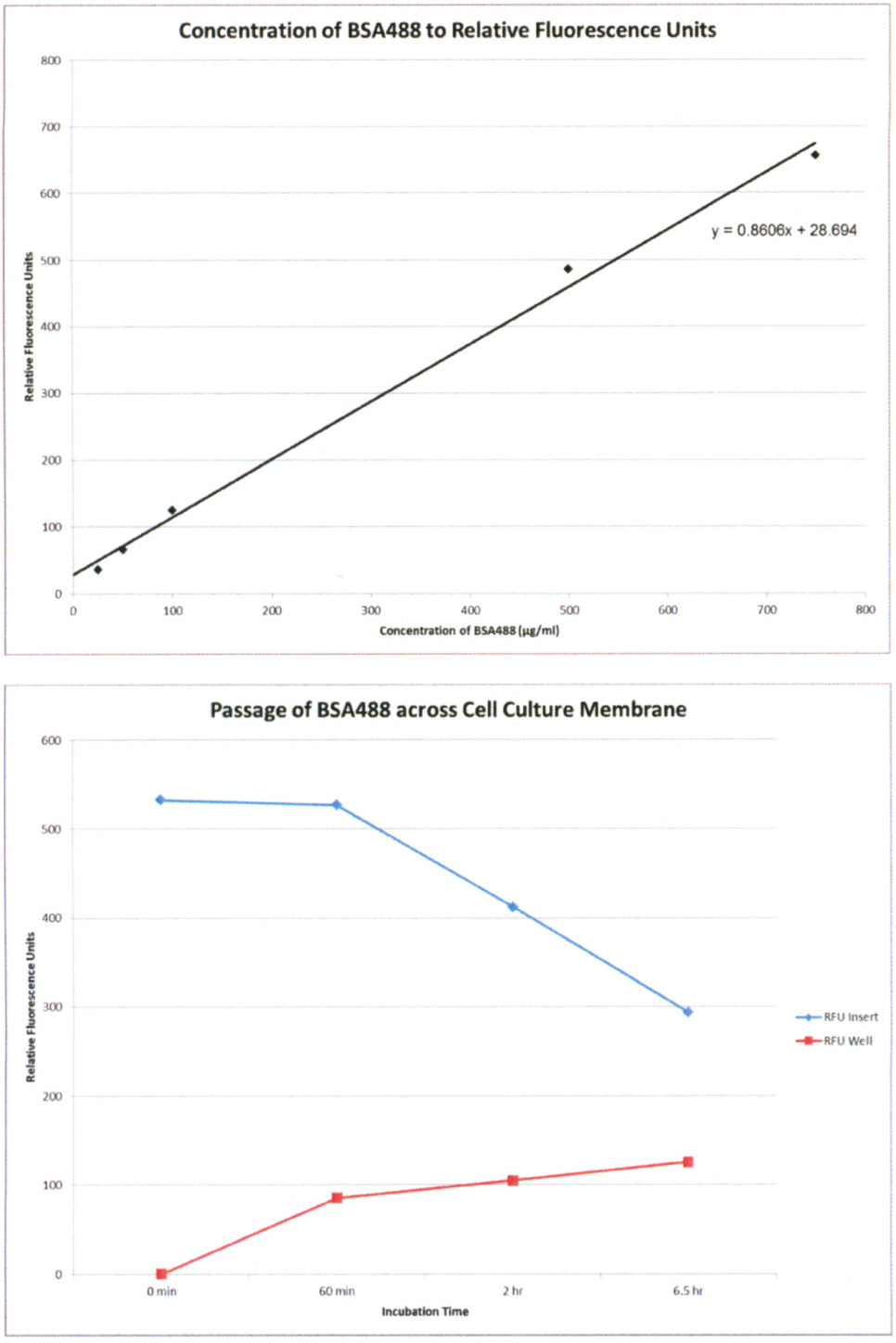


**Figure 3.20** Bovine serum albumin conjugated to AlexFluor488 (BSA488) was measured for fluorescence at known concentrations to generate a standard curve (top). To determine the ability of BSA488 to diffuse through 3.0 µm pores in cell culture inserts, BSA488 was added to the insert and assessed for changes in fluorescence in both the insert and the well below the membrane (bottom). Fluorescence was measured at excitation/emission wavelengths of 497/520 nm.

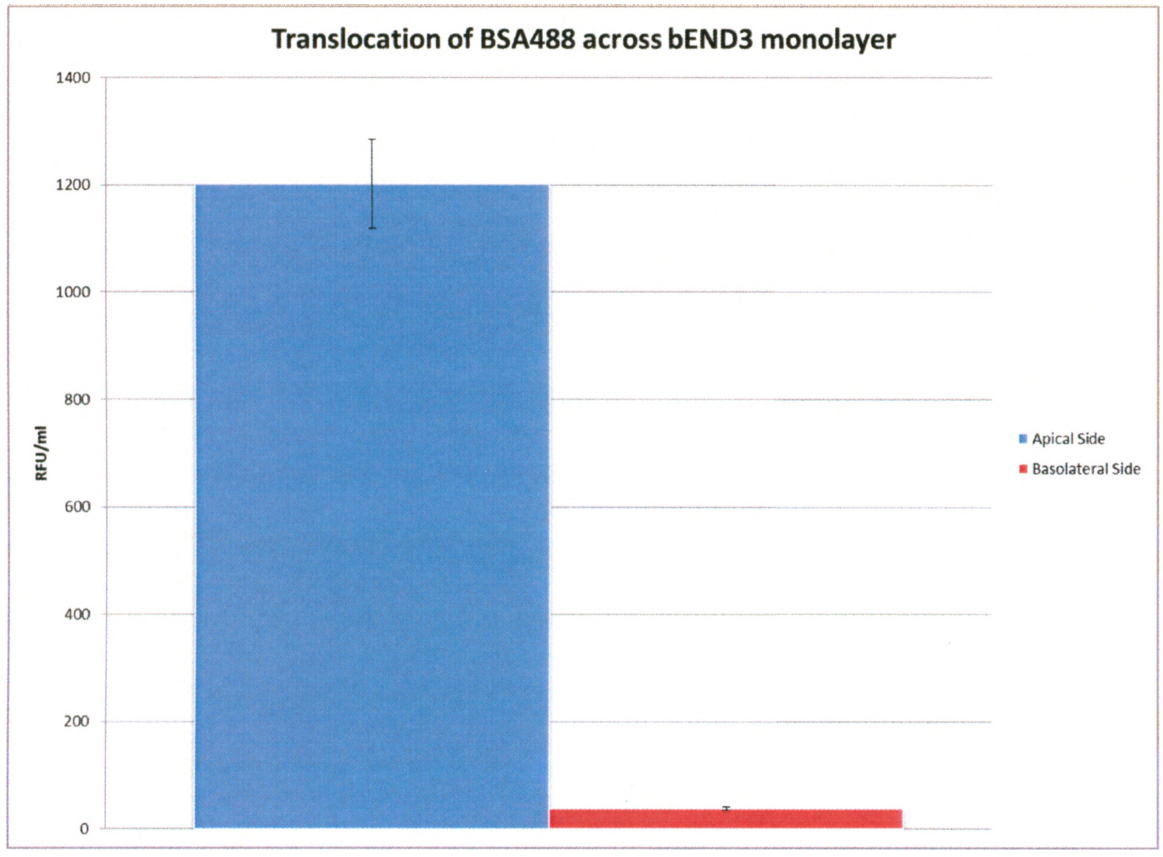


**Figure 3.21** The passage of BSA488 was assessed with application of 50 µg of the protein to the apical side of a bEND3 monolayer. After 16 hr, samples were taken and assessed for fluorescence from both the apical (left) and basolateral side (right) of the monolayer. Fluorescence was measured with excitation/emission wavelengths of 497/520 and was corrected for background fluorescence. (n=8)

with GFPApoE. There was no significant uptake in cells incubated with GFP and no fluorescence was seen in naïve bEND3 cells (Figure 3.22).

### 3.3.5 Passage of fusion proteins through *in vitro* blood brain barrier

To assess the passage of the fusion proteins, ASAApoE and TfASAV5, as well as ASAV5 across the bEND3 monolayer, between 2000-2800 nmol/hr of each protein was diluted in modified DMEM and applied to the apical side of a bEND3 monolayers followed by incubation for 16 hr. TEER readings were taken across each monolayer before the proteins were applied and after the 16 hr incubation period and were consistent at both time points (Figure 3.23 a). Medium was removed from both the apical and basolateral sides of the monolayer and assessed for enzyme activity. The total enzyme activity in media from the apical side of the monolayers were: TfASAV5, 388.0 nmol/hr; ASAApoE, 214.5 nmol/hr, and ASAV5, 77.2 nmol/hr. For total enzyme activity in medium from the basolateral side of the monolayers were: TfASAV5, 2.9 nmol/hr ; ASAApoE, 3.5 nmol/hr; ASAV5, 2.0 nmol/hr. The percentage of enzyme activity that passed through the bEND3 monolayer was 0.74 % (+/-0.02) for TfASAV5, 1.59 % (+/-0.09) for ASAApoE, and 2.58 % (+/-0.11) for ASAV5 (Figure 3.23 b).

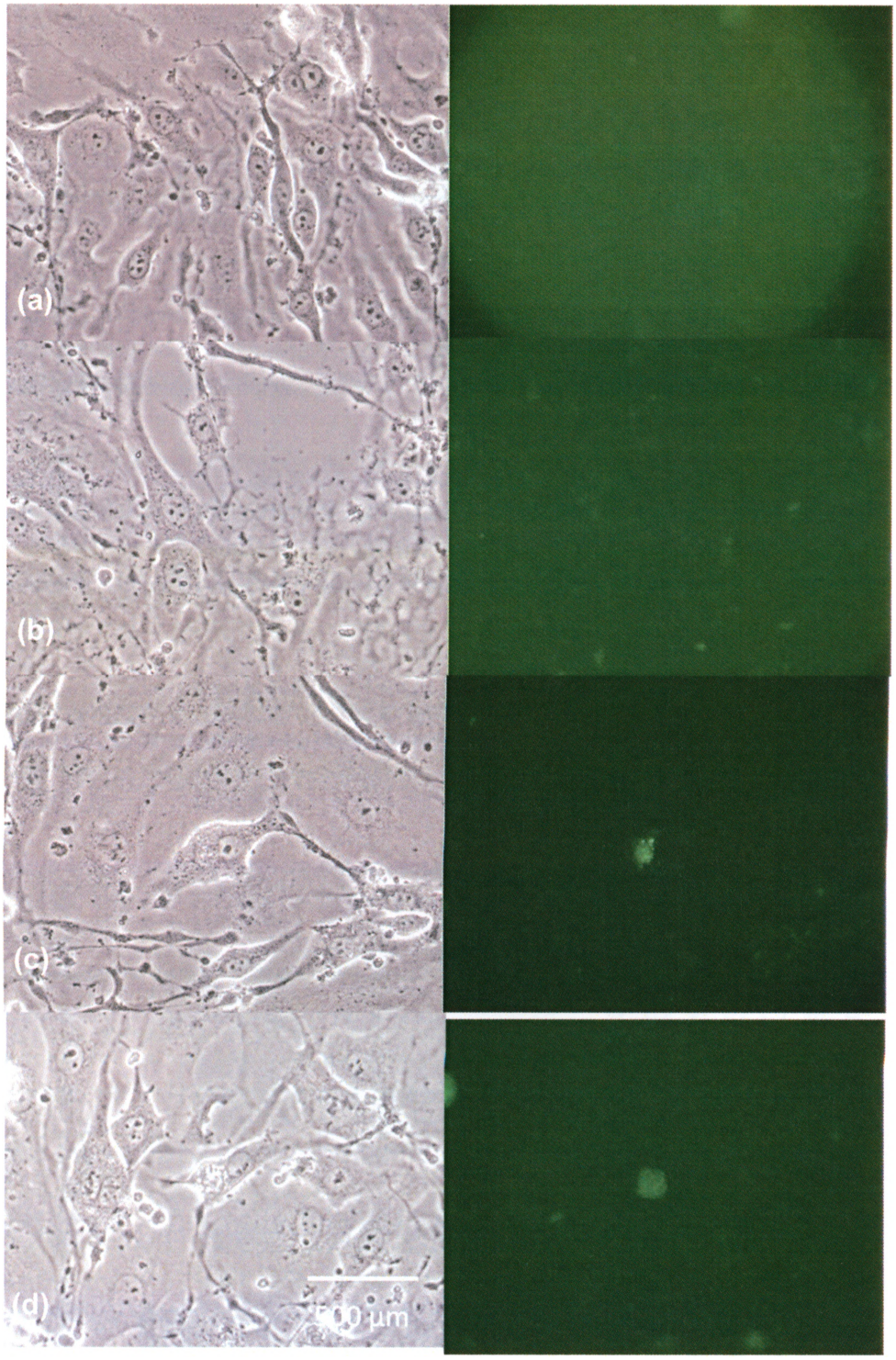


**Figure 3.22** Uptake of fluorescent proteins in bEND3 cells. bEND3 cells were incubated for 23 hr without protein (a), with GFP cell lysate (b), and medium collected from GFPApoE-transduced CHO cells (c,d) and assessed for uptake of fluorescence. Each image on the left (phase contrast) is from the same field as the fluorescent image on the right and was visualized using a Zeiss Axiovert 200M fluorescence microscope at 400 X magnification.

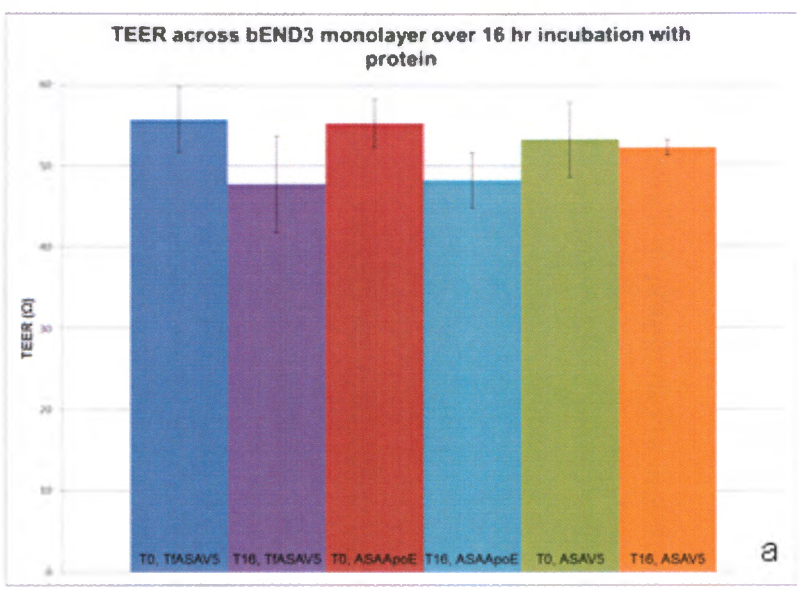


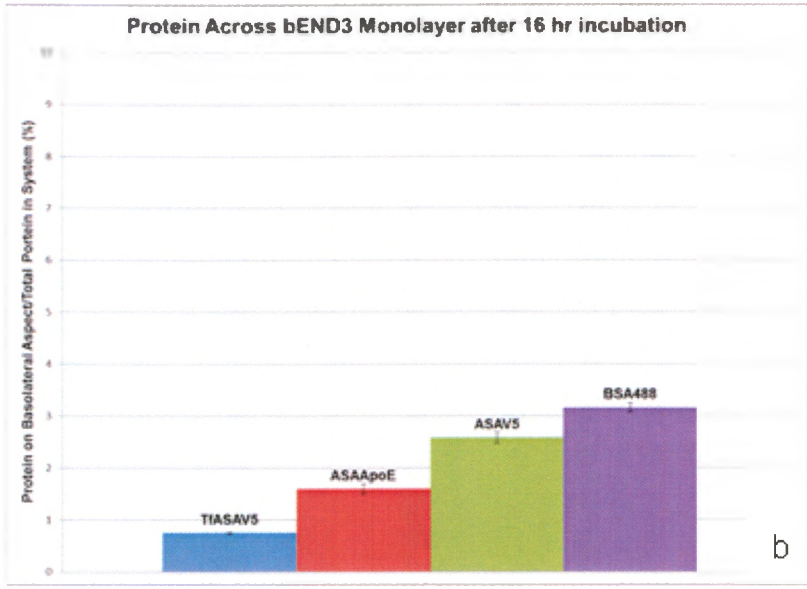


**Figure 3.23** Passage of fusion proteins across bEND3 monolayers (n=4). (a) Prior to application of proteins to the apical side of the bEND3 monolayer, TEER readings were taken ($T_0$). Following 16 hr of incubation, these readings were once again measured ($T_{16}$). (b) Fusion proteins, TfASAV5 and ASAApoE, as well as ASAV5 and BSA488 were applied to the apical side of bEND3 monolayers. After 16 hr, samples were collected from both the basolateral and apical sides of the bEND3 monolayer. The enzyme activity (nmol/hr/total volume) was calculated for medium collected from cells incubated with TfASAV5, ASAApoE, and ASAV5. Relative fluorescence units were measured from samples collected from cells incubated with BSA488. The percentage of proteins located on the basolateral side was calculated.

# Chapter 4 – Discussion and Conclusions

## 4.1 Summary of project

This project consisted of three main objectives:

1. Construction of ASAApoE and GFPApoE fusion proteins
2. Assessing the expression of ASAApoE, TfASAV5, and ASAV5 in a eukaryotic expression system
3. Delivery of fusion proteins having ASA activity through an *in vitro* blood-brain barrier

### 4.1.1 Successful construction of ASAApoE and GFPApoE

In this thesis, two different fusion proteins, ASAApoE and GFPApoE were generated. The LDLR-binding domain of apoE was fused to the C-terminus of the gene sequence for ASAV5 to preserve the signal sequence in the ASAV5 pre-protein for targeting to the mannose-6 phosphate pathway. The proteins were expressed by CHO cells transduced with lentiviral-based expression vectors. This observation is based on the following facts:

a) Lentiviral expression vectors were digested using restriction enzymes and displayed the expected digestion patterns, indicating that proper recombination into the vector had occurred (Figure 3.9).
b) The vectors were sequenced and the sequences were analyzed (Figure 3.8). The vectors contained either the full-length ASA-V5 gene or the full-length

eGFP gene fused with a 21 nucleotide linker to the 17 amino acid fragment of ApoE at the C-terminus with the correct orientation (Figure 3.8)

c) After using the expression vectors to generate lentiviral stock, CHO cells were transduced and analyzed for fusion protein expression. GFPApoE-expressing CHO cells displayed fluorescence (Figure 3.17) and ASAApoE-expressing CHO cells had a specific activity of 26 μmol/hr/mg protein (Table III)

### 4.1.2 Expression of ASA-fusion proteins in eukaryotic expression systems

The characteristics of proteins ASAApoE, ASAV5, and TfASAV5 (previously generated by Danielle Croucher) were assessed for size, enzyme activity, and glycosylation state.

**a) Sizing and enzyme activity**

While isolating an enzyme, each purification step should result in an increase in enzyme S.A. with a corresponding decrease in the amount of total protein. Aliquots of fractions collected at each step were electrophoresed under denaturing conditions to assess purity.

The proteins recovered had: S.A. of 26 and 74% yield for ASAApoE; S.A. of 59 and 63% yield for ASAV5; and S.A. of 59 and 87% yield for TfASAV5 (Table III). SDS-PAGE analysis of each fraction shows protein bands resolved on the gel to distances corresponding to the expected size of the fusion proteins (Figure 3.16). The smearing pattern seen in the ASAApoE sizing fractions is discussed in Chapter 4.2.

**b) Glycosylation state**

ASA is normally glycosylated and carries high mannose oligosaccharides. Both ASAV5 and the fusion protein, TfASAV5 appear to be N-glycosylated based

on a shift in mobility on SDS-PAGE following deglycosylation by PNGase F (Figure 3.16). Repeated attempts to assess the glycosylation state of ASAApoE were unsuccessful; however it is important to note that ASAApoE retained enzyme activity. In order to be active, this protein requires modification of the amino acid, cysteine-69, to a formylglycine residue (6). This modification occurs post-translationally and has been shown to likely occur after N-glycosylation (71). Based on these previous studies, it is likely that ASAApoE is N-glycosylated. Other experiments could be used to confirm the presence of glycoproteins for example, treatment with endoglycosidase such as Endo H, performance of SDS-PAGE of the protein could be followed by either staining with periodic acid-Schiff reaction or by lectin blotting using concanavalin A .(72-74)

**c) Development of an *in vitro* blood-brain barrier**

For the purpose of these experiments, bEND3 cell monolayers formed effective blood brain barriers based on the following: the integrity of the membrane was maintained according to the stability of transendothelial electrical resistance across the monolayer over a 16-hr period (Figure 3.19); and approximately 3% of BSA488 applied to the apical side of the monolayer passed into the basolateral compartment (Figure 3.20). Because the blood brain barrier does not appear to express any specific transport mechanism for albumin (75), passage of BSA488 can be assumed to be through leakage between bEND3 cells of the *in vitro* BBB barrier.

### 4.1.3 Delivery of active enzyme through an in vitro blood-brain barrier

Under the conditions used, neither ASAApoE nor TfASAV5 passed through the bEND3 monolayer at levels higher than the BSA488 baseline (Figure 3.23b). Possible explanations for these results are discussed in Chapter 4.3.

Despite the apparent lack of passage of the fusion proteins, the ApoE-fragment did appear to facilitate the uptake of GFP. Fluorescent assessment of bEND3 cells incubated with either GFP or GFPApoE indicated that those cells incubated with GFPApoE had taken up the fluorescent protein in a perinuclear-like distribution (Figure 3.22). No fluorescence was seen in cells incubated with GFP, indicating that the ApoE-fragment may be necessary for uptake.

## 4.2 Unexpected results and challenges

### a) Plasmid transfection of CHO led to low-level expression of proteins

Plasmid transfectants had insufficient levels of expression based on enzyme activity. To increase expression, lentiviral expression vectors were generated. This resulted in an over 80-fold increase in enzyme activity (Figure 3.11).

### b) Albumin interfered with purification process

10% FBS was used as a component of the CHO culture medium (Chapter 2.4.1). FBS contains albumin, a 66 kDa protein approximately the same size as both ASAV5 and ASAApoE and the presence of albumin in harvested media resulted in interference during the purification process. Initially, media was desalted and applied to a column containing Cibacron Blue F3G-A which binds albumin. The flow through collected from this column contained ASAApoE and the enzyme-containing fractions were desalted and applied to a DEAE column.

Fractions having enzyme activity were pooled and analyzed using SDS-PAGE under reducing conditions with 12% polyacrylamide gel and silver-stained for visualization. Under these conditions, there is one clear band, indicating that the protein is ~65 kDa, the expected size of ASAApoE (Figure 3.12).

Another approach used to isolate the enzyme away from albumin was the use of ConA-Sepharose chromatography. The column used contains concanavalin A (Con A), a protein isolated from the jack bean that binds molecules containing α-D-mannopyranosyl, α-D-glucopyranosyl and sterically related residues. After applying the proteins to this column, however, the ASA-fused proteins were so strongly bound that elution of enzyme became impractical. Similar difficulties in eluting ASAV5 from ConA columns have been encountered by other researchers in this laboratory.

Due to the complications and number of steps required to remove albumin from the media, a decision was made to wean the CHO cells into a serum-free medium. The cells were successfully weaned into this medium, retaining enzyme activity, however the cells became less adherent and more than 70% of cells were in suspension.

**c) ASAApoE resolved in a smear following SDS-PAGE**

Several attempts were made to demonstrate that ASAApoE collected from DEAE-column chromatography and the sizing column were the expected size of ~65 kDa. The resolution of the sizing fractions under reducing conditions was poor and resulted in smearing (Figure 3.16). It should be noted, however, that

with the use of cibacron blue column chromatography, the isolated protein was clearly illustrated to be the correct size (Figure 3.12).

One possible reason for the lack of a discrete protein band could be the presence of multiple species with different glycosylation states. This is unlikely to be the problem, however, because the banding did not become tighter following treatment with PNGase F, which should have removed any existing sugar moieties and resulted in a single deglycosylated form as seen for TfASAV5 and ASAV5 (Figure 3.18).

Another reason for the smearing could have been the conditions used for SDS-PAGE. To address this possibility, different periods of heat-denaturation were used, fresh DTT was used, and the proteins were rapidly cooled in an ice and ethanol bath following heat-denaturation. None of these steps resolved this problem.

Because ASAV5 was purified under the same conditions as ASAApoE and resolved to a clean band, it is unlikely that the buffers or columns used for FPLC resulted in smearing. However, elution of ASAV5 and ASAApoE from the DEAE column requires slightly different concentrations of NaCl (Figures 3.13, 3.14). It is possible, then, that proteolytic lysosomal enzymes could co-purify with and cause partial degradation of ASAApoE, resulting in smearing seen on the gels. Due to time constraints and the fact that active enzyme was collected, attempts were not made to inhibit proteases present.

It is possible that the protein formed aggregates during the purification process or in the presence of the SDS. Due to time constraints, different methods to ensure that the protein was fully denatured were not examined.

**d) Molecular Trojan horses fused to ASA did not transcytose**

Under the experimental conditions used, there was no apparent transcytosis of fusion proteins. However, the fact remains that GFPApoE but not GFP was taken up by bEND3 cells (Figure 3.22) indicating that the ApoE-fragments facilitated uptake of fusion proteins. Several suggestions regarding the lack of transcytosis of ASAApoE and TfASAV5 are discussed in the next section.

**4.3 Possible reasons for lack of successful transcytosis**

**a) Different rates of transcytosis**

In reduced form, BSA488 is approximately 66 kDa, TfASAV5 is approximately 140 kDa, while ASAV5 and ASAApoE are approximately 62 kDa and 65 kDa, respectively. Although there is some evidence that the rate of receptor-mediated transcytosis is not dependant on the size of the protein(76), the increasing size of proteins correlate to the percentage of the proteins found on the basolateral side of the bEND3 monolayer after 16 hr incubation (Figure 3.23).

It should be noted that at pH 7.5, ASA exists as a homodimer with a molecular weight of ~110 kDa (77) with possible exposure of both N- and C-terminal portions (78). Assuming that the other ASA-fusion proteins also form homodimers, ASAApoE would be ~120 kDa and TfASAV5 would be ~280 kDa. Interestingly, if the sizes of the protein dimers are compared to the percentage of total protein that entered the basolateral compartment, there is a clear decrease in passage as proteins increase in size (Figure 4.1). It is possible then, that the size of the proteins have an inverse relationship with the rate of transcytosis.

**b) Endocytosis without transcytosis**

TfASAV5 and ASAApoE were designed to express a V5 epitope tag to enable detection of the proteins in bEND3 cells using antibody detection. Unfortunately, V5 antibodies cross-reacted with the bEND3 cells and the presence of ASAApoE, ASAV5, and TfASAV5 in these cells could not be determined (data not shown). As well, bEND3 cells have endogenous levels of transferrin and ASA, such that antibodies to these proteins are unlikely to discriminate between native and fusion proteins. It was therefore not possible to determine the presence of the fusion proteins within the cells and endocytosis of the fusion proteins could not be ascertained.

**c) Competition for binding sites**

bEND3 cells were grown in complete DMEM medium containing 10% FBS. Attempts to grow these cells with a lower concentration of FBS resulted in cells that appeared less adherent and less likely to form appropriate monolayers (results not shown). For transcytosis experiments, ASAV5, ASAApoE, TfASAV5, and BSA488 proteins were diluted in bEND3 complete medium and the final amount of FBS in the diluted samples ranged from 2.5-7.5% (TfASAV5, 2.5%; ASAApoE, 6.25%; ASAV5 and BSA488, 7.5%). The medium on the basolateral side of the monolayer contained 10% FBS.

FBS contains both transferrin and LDL and these proteins would likely have high affinity for binding to available receptors on bEND3 cells and, therefore, very strong potential to compete with the Trojan horses for binding sites. To determine the concentration of these proteins in FBS, the average concentration of LDL and transferrin in 10 different lots of qualified FBS were

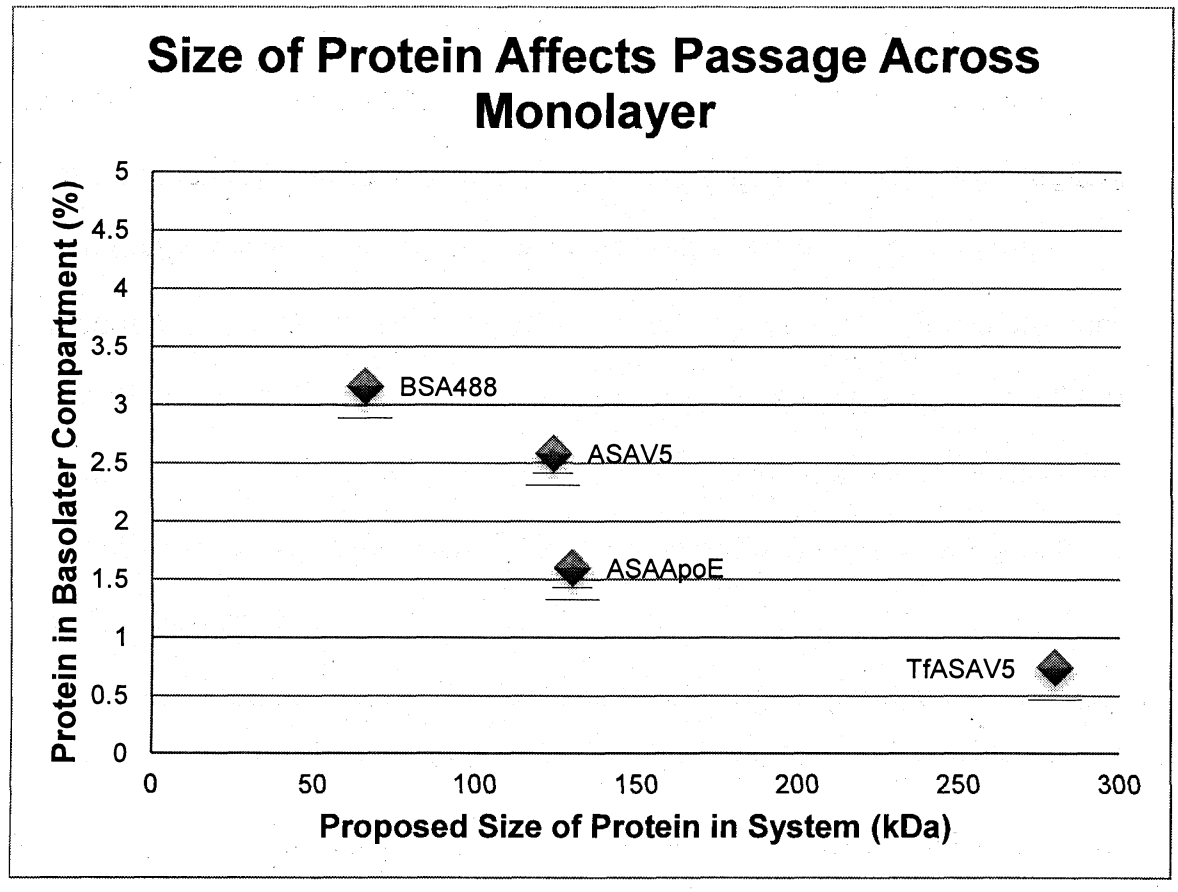


**Figure 4.1** Effect of protein size on transcytosis. A comparison of the proposed size of the proteins that are applied to the *in vitro* blood brain barrier to the percentage of that protein entering the basolateral compartment of the barrier appears to indicate a connection between the size of the protein and the ability to translocate to the basolateral compartment. This chart assumes that ASAV5, ASAApoE, and TfASAV5 exist in a dimerized form in solution.

calculated from published Certificates of Analysis by Invitrogen (79) and determined to be ~17.06 ± 1.73 mg/dL and 226.82 ± 45.69 mg/dL, respectively. These concentrations can be roughly converted into nanomolar concentrations based on the following: bovine transferrin is ~ 76 kDa (80); and the main component of calf serum LDL is ApoB, a 3 million Da particle. Therefore, the concentration of TfASAV5 applied to the apical side of the system was ~ 8100 pmol/L and this would be competing with ~ 750 pmol/L serum transferrin. The concentration of ASAApoE was ~ 8 µmol/L and it would be competing with ~ 3.5 nmol/L of serum LDL.

To out-compete the fusion proteins for binding to ligand, this would require that the affinity of the TfR for binding to serum transferrin and of LDLR for binding to serum LDL would remarkably have to be 10-fold and 2000-fold higher than the affinity for TfASAV5 and ASAApoE, respectively.

**d) Reduction in Number of Receptors Available**

There are studies available documenting the uptake of transferrin and LDL by bEND3 cells (82, 83). Although there is little data available to quantity the number of Tf or LDL receptors available on these cells, the evidence indicates that receptors are up-regulated when the basolateral compartment of the *in vitro* blood brain barrier contains lipoprotein-deficient serum or serum-free medium. The receptors have also been shown to be up-regulated in *in vitro* blood barriers generated from co-cultures of cerebrovascular endothelial cells and astrocytes (84-86).

The inference from these studies is that the number of receptors available for the experiments described in this thesis may be reduced due to the presence

of serum in the basolateral compartment as well as the absence of astrocytes in a co-culture. Therefore once the available receptors have been fully occupied by their ligand, increasing the concentration of fusion proteins applied to the system would not likely increase their rate of uptake (76).

**4.4 Future Considerations**

Future considerations for uptake experiments across the bEND3 monolayer include the following:

a) In order to isolate the fusion proteins, protease inhibitors should be included in harvested cell culture medium.
b) To better resolve ASAApoE on SDS-PAGE, the protein samples could be heated in loading buffer at 60°C for 20 minutes and different denaturants could be used such as urea. As well, the addition of mild detergents such as CHAPS or NP-40 to the purification processes may reduce the risk of aggregation.
c) Cultivation of bEND3 into serum-free medium would reduce the interference of serum proteins to uptake experiments. This may also result in up-regulation of receptors on the cell surface.
d) A co-culture of bEND3 cells with astrocytes may also result in a better *in vitro* BBB as well as up-regulation of receptors on bEND3 cells.
e) Competition experiments may aid the interpretation of the methods by which fusion proteins are taken up by bEND3 cells. Quantifiable competition with either ligand or antibodies specific to receptors should be considered to optimize the concentration of fusion protein to be applied to an in vitro blood

brain barrier system. It should also be noted that ASA-containing fusion proteins may be taken up by M6PR and therefore mannose-6-phosphate can be used for competition studies as well.

f) In order to study the uptake of fusion proteins in bEND3 cells, fusion proteins could be generated that incorporate a different epitope tag could be used for visualization of the fusion proteins in fixed cells.

g) Studies could be undertaken to determine the rate of transcytosis of the proteins in different time trials.

h) Further studies could determine the effect of the fusion proteins on sulfatide storage in arylsulfatase A deficient cells.

**4.5 Conclusion**

In this study, fusion proteins were generated using the LDLR-binding region of apoE as a molecular Trojan horse bound to full-length ASA. As well, an *in vitro* blood brain barrier was produced using an immortalized murine cerebrovascular endothelial cell line. Under the initial experimental conditions, transcytosis of fusion proteins was not observed. However, there was evidence indicating that the apoE peptide was capable facilitating the uptake of fusion proteins into the BBB cells based on intracellular fluorescence in the cells exposed to GFPApoE fusion proteins.

The optimal experimental conditions for the use of these fusion proteins require much more investigation before any conclusions are made regarding their ability to transcytose the blood brain barrier. Ultimately, the goal of these experiments is to find an effective treatment for MLD.

## Chapter 5 – References

1. Gieselmann V, Krageloh-Mann I. Metachromatic leukodystrophy--an update. Neuropediatrics. 2010 Feb;41(1):1-6.

2. Gieselmann V. Metachromatic leukodystrophy: Recent research developments. J Child Neurol. 2003 Sep;18(9):591-4.

3. Hess B, Saftig P, Hartmann D, Coenen R, Lullmann-Rauch R, Goebel HH, et al. Phenotype of arylsulfatase A-deficient mice: Relationship to human metachromatic leukodystrophy. Proc Natl Acad Sci U S A. 1996 Dec 10;93(25):14821-6.

4. Sevin C, Aubourg P, Cartier N. Enzyme, cell and gene-based therapies for metachromatic leukodystrophy. J Inherit Metab Dis. 2007 Apr;30(2):175-83.

5. Gustavson KH, Hagberg B. The incidence and genetics of meta chromatic leuko dystrophy in northern sweden. Acta Paediatr Scand. 1971;60(5):585-90.

6. von Figura K, Gieselmann V, Jaeken J. Metachromatic leukodystrophy. In: Scriver CR, Beaudet AL, Sly WS, Valle D, editors. The Metabolic & Molecular Bases of Inherited Disease. 8th ed. New York: McGraw Hill; 2001. p. 3695.

7. Kreysing J, von Figura K, Gieselmann V. The structure of the arylsulfatase A gene. Eur J Biochem. 1990;191:627-31.

8. Gieselmann V, Polten A, Kreysing J, von Figura K. Molecular genetics of metachromatic leukodystrophy. J Inherit Metab Dis. 1994;17(4):500-9.

9. von Bulow R, Schmidt B, Dierks T, Schwabauer N, Schilling K, Weber E, et al. Defective oligomerization of arylsulfatase a as a cause of its instability in lysosomes and metachromatic leukodystrophy. J Biol Chem. 2002 Mar 15;277(11):9455-61.

10. Kornfeld S. Structure and function of the mannose 6-Phosphate/Insulinlike growth factor II receptors. Annu Rev Biochem. 1992 07/01;61(1):307-30.

11. Sands MS, Davidson BL. Gene therapy for lysosomal storage diseases. Mol Ther. 2006 May;13(5):839-49.

12. Eckhardt M. The role and metabolism of sulfatide in the nervous system. Mol Neurobiol. 2008 Apr-Jun;37(2-3):93-103.

13. Saher G, Simons M. Cholesterol and myelin biogenesis. Subcell Biochem. 2010;51:489-508.

14. Poduslo SE, Miller K, Jang Y. Biochemical studies of the late infantile form of metachromatic leukodystrophy. Acta Neuropathol. 1982;57(1):13-22.

15. Ginsberg L, Gershfeld NL. Membrane bilayer instability and the pathogenesis of disorders of myelin. Neurosci Lett. 1991 Sep 2;130(1):133-6.

16. Eto Y, Wiesmann U, Herschkowitz NN. Sulfogalactosylsphingosine sulfatase. characteristics of the enzyme and its deficiency in metachromatic leukodystrophy in human cultured skin fibroblasts. J Biol Chem. 1974 Aug 10;249(15):4955-60.

17. Toda K, Kobayashi T, Goto I, Kurokawa T, Ogomori K. Accumulation of lysosulfatide (sulfogalactosylsphingosine) in tissues of a boy with metachromatic leukodystrophy. Biochem Biophys Res Commun. 1989 Mar 15;159(2):605-11.

18. Biffi A, Lucchini G, Rovelli A, Sessa M. Metachromatic leukodystrophy: An overview of current and prospective treatments. Bone Marrow Transplant. 2008 Oct;42 Suppl 2:S2-6.

19. Kurlemann G, Palm DG. Vigabatrin in metachromatic leucodystrophy; positive influence on spasticity. Dev Med Child Neurol. 1991 Feb;33(2):182.

20. Pardridge WM. Biopharmaceutical drug targeting to the brain. J Drug Target. 2010 Apr;18(3):157-67.

21. Leinekugel P, Michel S, Conzelmann E, Sandhoff K. Quantitative correlation between the residual activity of beta-hexosaminidase A and arylsulfatase A and the severity of the resulting lysosomal storage disease. Hum Genet. 1992 Mar;88(5):513-23.

22. Hsu J, Serrano D, Bhowmick T, Kumar K, Shen Y, Kuo YC, et al. Enhanced endothelial delivery and biochemical effects of alpha-galactosidase by ICAM-1-targeted nanocarriers for fabry disease. J Control Release. 2011 Feb 10;149(3):323-31.

23. SanRaffaele-GeneTherapyTrialUpdate-2010-07 [Internet].; 2010 [updated 07/24/2010. Available from: http://mldfoundation.org/pdfs/SanRaffaele-GeneTherapyTrialUpdate-2010-07.pdf.

24. Gieselmann V, Matzner U, Hess B, Lullmann-Rauch R, Coenen R, Hartmann D, et al. Metachromatic leukodystrophy: Molecular genetics and an animal model. J Inherit Metab Dis. 1998 Aug;21(5):564-74.

25. Stroobants S, Leroy T, Eckhardt M, Aerts JM, Berckmans D, D'Hooge R. Early signs of neurolipidosis-related behavioural alterations in a murine model of metachromatic leukodystrophy. Behav Brain Res. 2008 Jun 3;189(2):306-16.

26. Gieselmann V. Metachromatic leukodystrophy: Genetics, pathogenesis and therapeutic options. Acta Paediatr Suppl. 2008 Apr;97(457):15-21.

27. Matzner U, Habetha M, Gieselmann V. Retrovirally expressed human arylsulfatase A corrects the metabolic defect of arylsulfatase A-deficient mouse cells. Gene Ther. 2000 May;7(9):805-12.

28. Matzner U, Harzer K, Learish RD, Barranger JA, Gieselmann V. Long-term expression and transfer of arylsulfatase A into brain of arylsulfatase A-deficient mice transplanted with bone marrow expressing the arylsulfatase A cDNA from a retroviral vector. Gene Ther. 2000 Jul;7(14):1250-7.

29. Biffi A, Capotondo A, Fasano S, del Carro U, Marchesini S, Azuma H, et al. Gene therapy of metachromatic leukodystrophy reverses neurological damage and deficits in mice. J Clin Invest. 2006 Nov;116(11):3070-82.

30. Biffi A, De Palma M, Quattrini A, Del Carro U, Amadio S, Visigalli I, et al. Correction of metachromatic leukodystrophy in the mouse model by transplantation of genetically modified hematopoietic stem cells. J Clin Invest. 2004 Apr;113(8):1118-29.

31. Matzner U, Herbst E, Hedayati KK, Lullmann-Rauch R, Wessig C, Schroder S, et al. Enzyme replacement improves nervous system pathology and function in a mouse model for metachromatic leukodystrophy. Hum Mol Genet. 2005 May 1;14(9):1139-52.

32. Matzner U, Matthes F, Herbst E, Lullmann-Rauch R, Callaerts-Vegh Z, D'Hooge R, et al. Induction of tolerance to human arylsulfatase A in a mouse model of metachromatic leukodystrophy. Mol Med. 2007 Sep-Oct;13(9-10):471-9.

33. Matzner U, Lullmann-Rauch R, Stroobants S, Andersson C, Weigelt C, Eistrup C, et al. Enzyme replacement improves ataxic gait and central nervous system histopathology in a mouse model of metachromatic leukodystrophy. Mol Ther. 2009 Apr;17(4):600-6.

34. Consiglio A, Quattrini A, Martino S, Bensadoun JC, Dolcetta D, Trojani A, et al. In vivo gene therapy of metachromatic leukodystrophy by lentiviral vectors: Correction of neuropathology and protection against learning impairments in affected mice. Nat Med. 2001 Mar;7(3):310-6.

35. Sevin C, Verot L, Benraiss A, Van Dam D, Bonnin D, Nagels G, et al. Partial cure of established disease in an animal model of metachromatic leukodystrophy after intracerebral adeno-associated virus-mediated gene transfer. Gene Ther. 2007 Mar;14(5):405-14.

36. Sevin C, Benraiss A, Van Dam D, Bonnin D, Nagels G, Verot L, et al. Intracerebral adeno-associated virus-mediated gene transfer in rapidly progressive forms of metachromatic leukodystrophy. Hum Mol Genet. 2006 Jan 1;15(1):53-64.

37. Spencer BJ, Verma IM. Targeted delivery of proteins across the blood-brain barrier. Proc Natl Acad Sci U S A. 2007 May 1;104(18):7594-9.

38. Vite CH, McGowan JC, Niogi SN, Passini MA, Drobatz KJ, Haskins ME, et al. Effective gene therapy for an inherited CNS disease in a large animal model. Ann Neurol. 2005 Mar;57(3):355-64.

39. Colle MA, Piguet F, Bertrand L, Raoul S, Bieche I, Dubreil L, et al. Efficient intracerebral delivery of AAV5 vector encoding human ARSA in non-human primate. Hum Mol Genet. 2010 Jan 1;19(1):147-58.

40. Pardridge WM, Oldendorf WH, Cancilla P, Frank HJ. Blood-brain barrier: Interface between internal medicine and the brain. Ann Intern Med. 1986 Jul;105(1):82-95.

41. Pardridge WM, Oldendorf WH, Cancilla P, Frank HJL. Blood-brain barrier: Interface between internal medicine and the brain. Ann Intern Med. 1986 07;105(1):82.

42. Davson H. Review lecture. the blood-brain barrier. J Physiol (Lond ). 1976 February 1, 1976;255(1):1-28.

43. Pardridge WM. Blood-brain barrier biology and methodology. J Neurovirol. 1999 Dec;5(6):556-69.

44. Pardridge WM. Drug and gene targeting to the brain with molecular trojan horses. Nat Rev Drug Discov. 2002 02//print;1(2):131-9.

45. Ballabh P, Braun A, Nedergaard M. The blood-brain barrier: An overview: Structure, regulation, and clinical implications. Neurobiol Dis. 2004 Jun;16(1):1-13.

46. Levin VA. Relationship of octanol/water partition coefficient and molecular weight to rat brain capillary permeability. J Med Chem. 1980 Jun;23(6):682-4.

47. Pardridge WM. Re-engineering biopharmaceuticals for delivery to brain with molecular trojan horses. Bioconjug Chem. 2008 Jul;19(7):1327-38.

48. Abbott NJ, Patabendige AA, Dolman DE, Yusof SR, Begley DJ. Structure and function of the blood-brain barrier. Neurobiol Dis. 2010 Jan;37(1):13-25.

49. Patel MM, Goyal BR, Bhadada SV, Bhatt JS, Amin AF. Getting into the brain: Approaches to enhance brain drug delivery. CNS Drugs. 2009;23(1):35-58.

50. Begley ,D.J. Understanding and circumventing the blood-brain barrier.

51. Zlokovic BV. The blood-brain barrier in health and chronic neurodegenerative disorders. Neuron. 2008 Jan 24;57(2):178-201.

52. Boado RJ. A new generation of neurobiological drugs engineered to overcome the challenges of brain drug delivery. Drug News Perspect. 2008 Nov;21(9):489-503.

53. Boado RJ, Zhang Y, Zhang Y, Wang Y, Pardridge WM. GDNF fusion protein for targeted-drug delivery across the human blood-brain barrier. Biotechnol Bioeng. 2008 Jun 1;100(2):387-96.

54. Boado RJ, Zhang Y, Zhang Y, Pardridge WM. Genetic engineering, expression, and activity of a fusion protein of a human neurotrophin and a molecular trojan horse for delivery across the human blood-brain barrier. Biotechnol Bioeng. 2007 Aug 15;97(6):1376-86.

55. Xia CF, Boado RJ, Zhang Y, Chu C, Pardridge WM. Intravenous glial-derived neurotrophic factor gene therapy of experimental parkinson's disease with trojan horse liposomes and a tyrosine hydroxylase promoter. J Gene Med. 2008 Mar;10(3):306-15.

56. Zhang Y, Wang Y, Boado RJ, Pardridge WM. Lysosomal enzyme replacement of the brain with intravenous non-viral gene transfer. Pharm Res. 2008 Feb;25(2):400-6.

57. Boado RJ, Zhang Y, Zhang Y, Wang Y, Pardridge WM. IgG-paraoxonase-1 fusion protein for targeted drug delivery across the human blood-brain barrier. Mol Pharm. 2008 Oct 16.

58. Boado RJ, Zhang Y, Zhang Y, Xia CF, Wang Y, Pardridge WM. Genetic engineering, expression, and activity of a chimeric monoclonal antibody-avidin fusion protein for receptor-mediated delivery of biotinylated drugs in humans. Bioconjug Chem. 2008 Mar;19(3):731-9.

59. Boado RJ, Zhang Y, Zhang Y, Xia CF, Wang Y, Pardridge WM. Genetic engineering of a lysosomal enzyme fusion protein for targeted delivery across the human blood-brain barrier. Biotechnol Bioeng. 2008 Feb 1;99(2):475-84.

60. Hussain MM, Strickland DK, Bakillah A. The mammalian low-density lipoprotein receptor family. Annu Rev Nutr. 1999;19:141-72.

61. Zensi A, Begley D, Pontikis C, Legros C, Mihoreanu L, Wagner S, et al. Albumin nanoparticles targeted with apo E enter the CNS by transcytosis and are delivered to neurones. J Control Release. 2009 Jul 1;137(1):78-86.

62. Birnboim HC, Doly J. A rapid alkaline extraction procedure for screening recombinant plasmid DNA. Nucleic Acids Res. 1979 Nov 24;7(6):1513-23.

63. Rip JW, Gordon BA. A simple spectrophotometric enzyme assay with absolute specificity for arylsulfatase A. Clin Biochem. 1998 Feb;31(1):29-31.

64. Dekroon RM, Armati PJ. ENDOCYTOSIS OF apoE-EGFP BY PRIMARY HUMAN BRAIN CULTURES. Cell Biol Int. 2002;26(9):761-70.

65. Ye SQ, Reardon CA, Getz GS. Inhibition of apolipoprotein E degradation in a post-golgi compartment by a cysteine protease inhibitor. J Biol Chem. 1993 04/25;268(12):8497-502.

66. Grant KI, Casciola LA, Coetzee GA, Sanan DA, Gevers W, van der Westhuyzen DR. Ammonium chloride causes reversible inhibition of low density lipoprotein receptor recycling and accelerates receptor degradation. J Biol Chem. 1990 03/05;265(7):4041-7.

67. Bradford MM. A rapid and sensitive method for the quantitation of microgram quantities of protein utilizing the principle of protein-dye binding. Analytical Biochemistry. 1976;72:248-54.

68. Laemmli UK. Cleavage of structural proteins during the assembly of the head of bacteriophage T4. Nature. 1970 Aug 15;227(5259):680-5.

69. Brown RC, Morris AP, O'Neil RG. Tight junction protein expression and barrier properties of immortalized mouse brain microvessel endothelial cells. Brain Res. 2007 Jan 26;1130(1):17-30.

70. Schneeberger EE, Lynch RD. Structure, function, and regulation of cellular tight junctions. Am J Physiol. 1992 Jun;262(6 Pt 1):L647-61.

71. Dierks T, Schmidt B, von Figura K. Conversion of cysteine to formylglycine: A protein modification in the endoplasmic reticulum. Proc Natl Acad Sci U S A. 1997 Oct 28;94(22):11963-8.

72. Marino K, Bones J, Kattla JJ, Rudd PM. A systematic approach to protein glycosylation analysis: A path through the maze. Nat Chem Biol. 2010 Oct;6(10):713-23.

73. Haselbeck A, Hosel W. Immunological detection of glycoproteins on blots based on labeling with digoxigenin. Methods Mol Biol. 1993;14:161-73.

74. Breidenbach MA, Gallagher JE, King DS, Smart BP, Wu P, Bertozzi CR. Targeted metabolic labeling of yeast N-glycans with unnatural sugars. Proc Natl Acad Sci U S A. 2010 Mar 2;107(9):3988-93.

75. Pardridge WM, Eisenberg J, Cefalu WT. Absence of albumin receptor on brain capillaries in vivo or in vitro. Am J Physiol. 1985 Sep;249(3 Pt 1):E264-7.

76. Hastings RH, Folkesson HG, Matthay MA. Mechanisms of alveolar protein clearance in the intact lung. Am J Physiol Lung Cell Mol Physiol. 2004 Apr;286(4):L679-89.

77. Lewinski K, Chruszcz M, Ksiazek D, Laidler P. Crystallization and preliminary crystallographic analysis of a new crystal form of arylsulfatase A isolated from human placenta. Acta Crystallogr D Biol Crystallogr. 2000 May;56(Pt 5):650-2.

78. Lukatela G, Krauss N, Theis K, Selmer T, Gieselmann V, von Figura K, et al. Crystal structure of human arylsulfatase A: The aldehyde function and the metal ion at the active site suggest a novel mechanism for sulfate ester hydrolysis. Biochemistry. 1998 Mar 17;37(11):3654-64.

79. Certificates of analysis for fetal bovine serum, qualified [Internet]. Available from: http://products.invitrogen.com/ivgn/product/10099133?ICID=search-product#coa.

80. Tsuji S, Kato H, Matsuoka Y, Fukushima T. Molecular weight heterogeneity of bovine serum transferrin. Biochem Genet. 1984 Dec;22(11-12):1145-59.

81. Bauchart D, Durand D, Laplaud PM, Forgez P, Goulinet S, Chapman MJ. Plasma lipoproteins and apolipoproteins in the preruminant calf, bos spp: Density distribution, physicochemical properties, and the in vivo evaluation of the contribution of the liver to lipoprotein homeostasis. J Lipid Res. 1989 Oct;30(10):1499-514.

82. Hallmann R, Savigni DL, Morgan EH, Baker E. Characterization of iron uptake from transferrin by murine endothelial cells. Endothelium. 2000;7(2):135-47.

83. Montesano R, Pepper MS, Mohle-Steinlein U, Risau W, Wagner EF, Orci L. Increased proteolytic activity is responsible for the aberrant morphogenetic behavior of endothelial cells expressing the middle T oncogene. Cell. 1990 Aug 10;62(3):435-45.

84. Dehouck B, Fenart L, Dehouck MP, Pierce A, Torpier G, Cecchelli R. A new function for the LDL receptor: Transcytosis of LDL across the blood-brain barrier. J Cell Biol. 1997 Aug 25;138(4):877-89.

85. Dehouck B, Dehouck MP, Fruchart JC, Cecchelli R. Upregulation of the low density lipoprotein receptor at the blood-brain barrier: Intercommunications between brain capillary endothelial cells and astrocytes. J Cell Biol. 1994 Jul;126(2):465-73.

86. Descamps L, Dehouck MP, Torpier G, Cecchelli R. Receptor-mediated transcytosis of transferrin through blood-brain barrier endothelial cells. Am J Physiol. 1996 Apr;270(4 Pt 2):H1149-58.

87. Weisgraber K, Innerarity T, Harder K, Mahley R, Milne R, Marcel Y, Sparrow J. The Recepter-binding domain of human apolipoprotein E. J Biol Chem. 1983 Oct; 258(20):12348-12354.

88. Mahley R, Rall Jr. S. Apolipoprotein E: far more than a lipid transport protein. Annu Rev Genomics Hum Genet 2000; 1:507-537